1-1-2015

Intrathecal Adeno-Associated Virus Vector Delivery for Mucopolysaccharidosis Type I

Christian Hinderer
University of Pennsylvania, hinderer@mail.med.upenn.edu

Intrathecal Adeno-Associated Virus Vector Delivery for Mucopolysaccharidosis Type I

Abstract
Mucopolysaccharidosis type I (MPS I) is a lysosomal storage disease resulting from deficiency of the enzyme α-L-iduronidase (IDUA). Accumulation of the IDUA substrates heparan and dermatan sulfate causes widespread organ pathology. While many of the somatic manifestations of MPS I can be treated with intravenous enzyme replacement, the devastating CNS sequelae—cognitive impairment, spinal cord compression, and hydrocephalus—do not respond to treatment. Partial preservation of cognitive function is possible with early hematopoietic stem cell transplantation, although transplant is associated with substantial morbidity and mortality. Gene transfer using adeno-associated virus (AAV) vectors offers a potential alternative approach to deliver the IDUA enzyme to the CNS. Introducing a functional IDUA gene to a subset of quiescent cells could provide a permanent source of secreted enzyme beyond the blood-brain barrier. However, preclinical studies evaluating direct injection of AAV vectors into the brain have shown that transduction is limited to small regions surrounding the injection site, and that injection can be associated with a localized inflammatory response and immune-mediated killing of transduced cells. In order to overcome these limitations, we evaluated delivery of an AAV serotype 9 vector into the cerebrospinal fluid as a less invasive method to achieve widespread brain transduction. Studies in nonhuman primates demonstrated that intrathecal AAV9 delivery results in transduction of cells throughout the brain and spinal cord without eliciting destructive immune responses to the transgene product. Intrathecal injection of AAV9 vectors expressing IDUA in canine and feline models of MPS I replicated the widespread transduction observed in primate studies, and demonstrated resolution of storage lesions throughout the CNS. Antibodies against the enzyme were detected in the CSF of some animals, which coincided with lower CSF IDUA activity and less efficient correction of storage lesions. We found that immunological tolerance could be induced to IDUA by exposing newborn MPS I dogs to the enzyme, which enhanced the efficacy of subsequent gene transfer. These results were replicated in rhesus macaques, supporting the potential to translate neonatal tolerance induction to clinical applications. Intrathecal AAV delivery offers the potential for widespread gene transfer in the CNS with a single minimally invasive vector injection, which could prove transformative for the field of gene therapy for inherited neurological disorders.

Degree Type
Dissertation

Degree Name
Doctor of Philosophy (PhD)

Graduate Group
Cell & Molecular Biology

First Advisor
James M. Wilson

Keywords
gene therapy, mucopolysaccharidosis

Subject Categories
Genetics | Medicine and Health Sciences | Molecular Biology

INTRATHECAL ADENO-ASSOCIATED VIRUS VECTOR DELIVERY FOR MUCOPOLYSACCHARIDOSIS TYPE I

Christian Hinderer

A DISSERTATION

in

Cell and Molecular Biology

Presented to the Faculties of the University of Pennsylvania

in

Partial Fulfillment of the Requirements for the

Degree of Doctor of Philosophy

2015

Supervisor of Dissertation

_____

James M Wilson, MD PhD

Professor, Pathology and Laboratory Medicine

Graduate Group Chairperson

_____

Daniel S Kessler, PhD

Associate Professor, Cell and Developmental Biology

Dissertation Committee:

Philip R Johnson, MD, Professor of Pediatrics

Jean Bennett, MD PhD, Professor of Ophthalmology

Jean Boyer, PhD, Research Associate Professor of Pathology and Laboratory Medicine

Virginia Lee, PhD, Professor of Pathology and Laboratory Medicine

INTRATHECAL ADENO-ASSOCIATED VIRUS VECTOR DELIVERY FOR MUCOPOLYSACCHARIDOSIS TYPE I

ABSTRACT

INTRATHECAL ADENO-ASSOCIATED VIRUS VECTOR DELIVERY FOR MUCOPOLYSACCHARIDOSIS TYPE I

Christian Hinderer

James M Wilson, MD PhD

Mucopolysaccharidosis type I (MPS I) is a lysosomal storage disease resulting from deficiency of the enzyme α-L-iduronidase (IDUA). Accumulation of the IDUA substrates heparan and dermatan sulfate causes widespread organ pathology. While many of the somatic manifestations of MPS I can be treated with intravenous enzyme replacement, the devastating CNS sequelae—cognitive impairment, spinal cord compression, and hydrocephalus—do not respond to treatment. Partial preservation of cognitive function is possible with early hematopoietic stem cell transplantation, although transplant is associated with substantial morbidity and mortality. Gene transfer using adeno-associated virus (AAV) vectors offers a potential alternative approach to deliver the IDUA enzyme to the CNS. Introducing a functional IDUA gene to a subset of quiescent cells could provide a permanent source of secreted enzyme beyond the blood-brain barrier. However, preclinical studies evaluating direct injection of AAV vectors into the brain have shown that transduction is limited to small regions surrounding the injection site, and that injection can be associated with a localized inflammatory response and immune-mediated killing of transduced cells. In order to overcome these limitations, we evaluated delivery of an AAV serotype 9 vector into the cerebrospinal fluid as a less invasive method to achieve widespread brain transduction. Studies in nonhuman primates demonstrated that intrathecal AAV9 delivery results in transduction of cells throughout the brain and spinal cord without eliciting destructive immune responses to the transgene product. Intrathecal injection of AAV9 vectors expressing IDUA in canine and feline models of MPS I replicated the widespread transduction observed in primate studies, and demonstrated resolution of storage lesions throughout the CNS. Antibodies against the enzyme were detected in the CSF of some animals, which coincided with lower CSF IDUA activity and less efficient correction of storage lesions. We found that immunological tolerance could be induced to IDUA by exposing newborn MPS I dogs to the enzyme, which enhanced the efficacy of subsequent gene transfer. These results were replicated in rhesus macaques, supporting the potential to translate neonatal tolerance induction to clinical applications. Intrathecal AAV delivery offers the potential for widespread gene transfer in the CNS with a single minimally invasive vector injection, which could prove transformative for the field of gene therapy for inherited neurological disorders.

TABLE OF CONTENTS

ABSTRACT III

LIST OF TABLES VI

LIST OF ILLUSTRATIONS VII

CHAPTER 1: INTRODUCTION 1

Mucopolysaccharidosis type I 1

Adeno-associated virus mediated gene therapy for MPS I 5

Intrathecal AAV Delivery 7

Large animal models of MPS I 10

Goals of this dissertation 11

CHAPTER 2: WIDESPREAD GENE TRANSFER IN THE CENTRAL NERVOUS SYSTEM OF CYNOMOLGUS MACAQUES FOLLOWING DELIVERY OF AAV9 INTO THE CISTERNA MAGNA 13

Abstract 14

Introduction 14

Materials and Methods 17

Results 20

Discussion 24

CHAPTER 3: INTRATHECAL GENE THERAPY CORRECTS CNS PATHOLOGY IN A FELINE MODEL OF MUCOPOLYSACCHARIDOSIS I 42

Abstract 43

Introduction 43

Materials and Methods 47

Results 51

Discussion 58

CHAPTER 4: NEONATAL SYSTEMIC AAV INDUCES TOLERANCE TO CNS GENE THERAPY IN MPS I DOGS AND NONHUMAN PRIMATES 76

Abstract 77

Introduction 77

Materials and Methods 80

Results 84

Discussion 90

CHAPTER 5: INDUCTION OF TRANSGENE-SPECIFIC IMMUNE TOLERANCE ENABLES EVALUATION OF A HUMAN GENE THERAPY FOR MUCOPOLYSACCHARIDOSIS TYPE I IN AN AUTHENTIC DOG MODEL ... 105

Abstract: 106

Introduction 106

Materials and Methods 109

Results 110

Discussion 114

CHAPTER 6: GENERAL DISCUSSION 126

BIBLIOGRAPHY 136

LIST OF TABLES

Table 2-1. Summary of study subjects 38

Table 2-2. Quantification of transduced motor neurons throughout the spinal cord 39

Table 2-3. Quantification of GFAP and Iba1 positive cells in brain 40

Table 2-4. CSF analysis 41

Table 3-1. Summary of study subjects 73

Table 3-2. CSF analysis in treated MPS I cats 74

Table 3-3. Quantification of histopathology 75

Table 4-1. Summary of study subjects 102

Table 4-2. CSF nucleated cell count in MPS I dogs following vector injection 103

Table 4-3. Vector biodistribution 104

Table 5-1. Vector biodistribution 125

LIST OF ILLUSTRATIONS

Figure 2-1. AAV9 biodistribution following intrathecal delivery in nonhuman primates 29

Figure 2-2. Transduction throughout the brain following intracisternal AAV9 delivery 30

Figure 2-3. Predominantly neuronal transduction of intrathecal AAV9 31

Figure 2-4. Spinal cord transduction following intrathecal AAV9 32

Figure 2-5. Limited CNS transduction following intravascular AAV9 delivery 33

Figure 2-6. Evaluation of anatomic landmarks for suboccipital puncture 34

Figure 2-7. Detection of false positive GFP expressing cells by immunohistochemistry 35

Figure 2-8. Differentiating GFP fluorescence from autofluorescence in spinal cord 36

Figure 2-9. Absence of an inflammatory response following intrathecal delivery of AAV9 expressing GFP 37

Figure 3-1. IDUA expression in CSF and serum following IT AAV9 delivery 61

Figure 3-2. Normalization of CSF hexosaminidase activity 62

Figure 3-3. Global CNS transduction and biochemical correction following IT gene transfer 64 65

Figure 3-4. Reversal of brain ganglioside storage 66

Figure 3-5. Correction of neuronal storage lesions 67

Figure 3-6. Reduced GAG storage in the cerebral vasculature and meninges 68

Figure 3-7. Correction of somatic lesions 69

Figure 3-8. Peripheral GAG clearance following intrathecal AAV9 delivery 70

Figure 3-9. Reduced serum heparin cofactor II-thrombin complex 71

Figure 3-10. Absence of inflammation or cellular infiltration in treated animals 72

Figure 3-11. Absence of astrocyte activation in treated animals 95

Figure 4-1. Neonatal systemic IDUA gene transfer induces tolerance to subsequent CNS gene therapy in MPS I dogs 96

Figure 4-2. Biochemical markers are normalized following intrathecal gene therapy in MPS I dogs 98

Figure 4-3. CNS storage lesions are more effectively cleared by intrathecal gene therapy in MPS I dogs tolerized to IDUA as neonates 99

Figure 4-4. Neonatal gene transfer induces tolerance in nonhuman primates 100

Figure 4-5: Serum IDUA activity in MPS I dogs 101

Figure 4-6. Serum IDUA activity in rhesus monkeys. 118

Figure 5-1. CSF IDUA activity in MPS I dogs 119

Figure 5-2. CSF antibody titer against human IDUA 120

Figure 5-3. CSF nucleated cell counts following intrathecal AAV9 injection 121

Figure 5-4. Lymphocyte infiltration of the lumbar spinal cord 121

Figure 5-5. Normalization of brain hexosaminidase activity in human IDUA tolerant MPS I dogs treated with intrathecal AAV9 122

Figure 5-6. Dose-dependent correction of brain storage lesions 123

Figure 5-7. Partial correction of brain storage lesions 124

Figure 5-8. Normalization of CSF hexosaminidase activity after IT AAV9 treatment 124

CHAPTER 1: Introduction

Mucopolysaccharidosis type I

Mucopolysaccharidosis type I (MPS I) is a rare genetic disease affecting approximately 1 in 100,000 newborns worldwide (Moore et al. 2008). Children with MPS I typically appear normal at birth, although umbilical hernias or spinal deformities are sometimes present (Beck et al. 2014). Often after one to two years of normal development, patients rapidly develop a constellation of devastating disease manifestations—chronic upper respiratory infections, joint pain and immobility, bone deformities, coarsened facial features, hepatomegaly, carpal tunnel syndrome, communicating hydrocephalus, spinal cord compression, hearing impairment, corneal clouding, obstructive sleep apnea, and cardiac disease (Beck et al. 2014, Aldenboven, Boelens, and de Koning 2008, Boelens et al. 2007, Souillet et al. 2003, Whitley et al. 1993). Most patients also begin to show signs of developmental delay by 2 years of age, which progresses to profound intellectual impairment in early childhood. Without treatment most patients do not survive beyond the first decade (Aldenboven, Boelens, and de Koning 2008, Boelens et al. 2007, Fleming et al. 1998, Souillet et al. 2003, Staba et al. 2004, Whitley et al. 1993).

MPS I is caused by mutations in the *IDUA* gene encoding the lysosomal enzyme α-L-iduronidase (IDUA). IDUA catalyzes the hydrolysis of iduronic acid linkages in heparan and dermatan sulfate, two ubiquitous glycosaminoglycans (GAG). In the setting of deficient IDUA activity, undegraded GAGs accumulate in nearly every tissue, leading to diverse clinical manifestations. GAG storage in the cornea causes characteristic clouding and visual impairment, airway abnormalities caused by GAG infiltration

contribute to obstructive sleep apnea and chronic upper respiratory infections, and storage lesions in the cardiac valves cause the valves to thicken and shorten, leading to mitral and aortic regurgitation. Both spinal cord compression and communicating hydrocephalus have been linked to GAG storage in the meninges—the thickened dura mater directly compresses the spinal cord, and leptomeningeal GAG storage is thought to block perivascular channels and arachnoid granulations through which CSF is resorbed, leading to increased CSF pressure (Dickson, Hanson, et al. 2010, Kakkis, McEntee, et al. 2004, Munoz-Rojas et al. 2008, Kachur and Del Maestro 2000, Taccone et al. 1993). The mechanism by which IDUA deficiency leads to cognitive dysfunction is less clear; neurons exhibit GAG storage, but this does not appear to correlate with disease onset or severity. Neurons do, however, exhibit marked abnormalities. Ectopic neurite growth, axonal spheroids, and storage of gangliosides are pronounced in cortical neurons, and these features correlate with cognitive phenotype in MPS I as well as in related lysosomal storage disorders (Constantopoulos, Iqbal, and Dekaban 1980, Shull et al. 1984, Walkley and Vanier 2009). It is not clear how the primary biochemical defect leads to these downstream consequences in the brain.

MPS I patients present across a spectrum of severity, ranging from the most common and severe presentation of early somatic involvement and rapid cognitive decline, to onset after the first decade of life with attenuated somatic disease and normal intelligence (Beck et al. 2014). The disease phenotype is related to residual enzyme activity—patients with the attenuated form of MPS I typically have missense mutations, whereas patients with severe disease have nonsense mutations, deletions or insertions (Terlato and Cox 2003). In the US the most frequent mutations are W402X and Q70X, both of which cause the severe form of the disease in homozygotes or compound

heterozygotes. The disease causing mutations that result in an attenuated phenotype produce less than 1% of normal IDUA activity, demonstrating that very low levels of enzyme can modify the course of the disease (Terlato and Cox 2003).

The first therapy developed for MPS I was hematopoietic stem cell transplantation (HSCT). HSCT can impact systemic storage pathology through the principle of cross correction: upon successful engraftment of HSCs, donor derived cells secrete small amounts of IDUA, which is taken up by host cells from the systemic circulation through receptor-mediated binding of terminal mannose-6 phosphate residues present on glycosylated IDUA (Dahms, Lobel, and Kornfeld 1989, Sando and Neufeld 1977, Aldenboven, Boelens, and de Koning 2008). Uptake of IDUA through this pathway results in trafficking to the lysosome, where the enzyme catalyzes the degradation of stored polysaccharides. HSCT has demonstrated improvements in survival, growth, cardiac and respiratory function, mobility, and intellect. The effect of HSCT on the CNS is attributed to migration of bone marrow derived precursors across the blood-brain barrier, where they differentiate into microglia and serve as a source of secreted IDUA in the brain (Aldenboven, Boelens, and de Koning 2008).

Despite the impact of HSCT on the clinical course of MPS I, there are important limitations of the procedure. HSCT for MPS I is associated with substantial morbidity and up to 20% mortality (Aldenboven, Boelens, and de Koning 2008). Accordingly, the procedure is now reserved only for patients with severe disease. HSCT is also generally only performed in patients identified before two years of age, as the risk-benefit ratio is thought to be more favorable in younger patients who are more likely to derive greater cognitive benefit (de Ru et al. 2011). A second critical limitation of HSCT is the incomplete treatment of CNS symptoms. Among successfully engrafted patients,

cognitive decline continues for up to a year after transplant before stabilizing, leaving permanent developmental deficits (Fleming et al. 1998, Staba et al. 2004). This delayed effect of HSCT is believed to be due to the time required for bone marrow-derived microglia to migrate into the CNS. Studies in animal models suggest that only 30% of microglial engraftment occurs by one year after transplant, with most of these engrafted cells occupying perivascular spaces rather than the brain parenchyma (Kennedy and Abkowitz 1997). There is therefore little improvement in neuronal storage lesions within the first year after transplantation (Ellinwood et al. 2007).

More recently, a recombinant form of human IDUA has been approved for the treatment of MPS I. Given as a weekly intravenous infusion, enzyme replacement therapy (ERT) has demonstrated many of the same benefits as HSCT, including improvement in hepatomegaly, growth, mobility and respiratory function (de Ru et al. 2011, Sifuentes et al. 2007, Wraith et al. 2007, Wraith et al. 2004). However, as the enzyme cannot cross the blood-brain barrier, ERT does not treat the CNS manifestations of MPS I. Several studies have investigated the direct delivery of recombinant IDUA to the CNS by intrathecal (IT) injection (Dickson, Naylor, Mlikotic, Victoroff, Chen, Passage, and Le 2008, Dickson, Naylor, Mlikotic, Victoroff, Chen, Passage, Le, et al. 2008, Munoz-Rojas et al. 2008, Vera et al. 2013). Monthly IT infusions of IDUA demonstrated minimal adverse effects, and have shown evidence for improvement in spinal cord compression. However, IT ERT has limited potential for the treatment of CNS disease in MPS I due to the need for repeated access to the cerebrospinal fluid (CSF) for the life of the patient. Further, the efficacy of this approach is likely limited by the extremely short half-life of the enzyme in the CSF and the long intervals between injections (Vite et al. 2011).

Adeno-associated virus mediated gene therapy for MPS I

The limitations of HSCT and ERT leave a significant unmet need for a method to safely achieve long term IDUA reconstitution in the CNS. Delivery of the gene encoding the enzyme to cells within the CNS could provide a permanent source of secreted IDUA beyond the blood-brain barrier, allowing for long term cross-correction of cells throughout the CNS. This strategy could also provide rapid IDUA delivery to the brain, potentially preventing the progression of developmental deficits that otherwise occurs in Hurler patients during the slow process of donor cell migration into the CNS following HSCT.

Adeno-associated virus (AAV) vectors have demonstrated the potential for safe, long term transgene expression *in vivo*. The wild type AAV from which these vectors are derived is a small non-enveloped parvovirus that is ubiquitous in humans and other species (Samulski and Muzyczka 2014). AAV is nonpathogenic and has limited replicative capacity in the absence of a helper virus. AAV is composed of a 20 nm icosahedral capsid containing a 4.7 kb single-stranded DNA genome. The genome contains three protein coding genes—*Rep, Cap, and AAP*—flanked by short double-stranded inverted terminal repeats. The *Rep* gene encodes four proteins required for the replication and packaging of the genome. *Cap* encodes three proteins—VP1, VP2 and VP3—that form the viral capsid. AAP (assembly activator protein) is expressed from an alternate reading frame overlapping *Cap,* and appears to have a role in capsid assembly (Sonntag, Schmidt, and Kleinschmidt 2010). Only the inverted repeats are essential for DNA packaging in AAV; the other essential proteins can be provided in *trans* (Samulski, Chang, and Shenk 1989, 1987). Completely replacing the viral coding sequences of AAV has yielded vectors capable of *in vivo* gene transfer. Upon entering a

host cell, the vector genome persists as an episome, allowing for stable expression for at least ten years in quiescent tissues (Buchlis et al. 2012). However, early clinical trials utilizing AAV vectors showed limited gene transfer and poor efficacy. Over the past decade, a second generation of AAV vectors discovered as latent viruses in human and macaque tissues has demonstrated vastly improved gene transfer efficiency over that achieved with the original vectors based on AAV serotype 2 (AAV2) (Gao et al. 2004, Gao et al. 2002, Xiao et al. 1999). Using these new vectors, clinical trials of gene transfer to both liver and muscle have demonstrated efficacy in diseases such as hemophilia B and lipoprotein lipase deficiency, the latter leading to the first approved gene therapy product in Europe (Nathwani et al. 2011, Bryant et al. 2013).

AAV vectors have been tested extensively for gene transfer to the brain. One of the most heavily pursued CNS targets for early AAV trials was Parkinson's disease (PD). Preclinical studies in a nonhuman a primate model of drug induced degeneration of the substantia nigra demonstrated the efficacy of several gene therapy strategies (Bankiewicz et al. 2006, Bartus et al. 2011, Björklund et al. 2000, Bohn et al. 1999, Burns et al. 1983, Emborg et al. 2007, Hadaczek et al. 2010, Jarraya et al. 2009, Muramatsu et al. 2002, Nagahara et al. 2009). Some were based on expression of enzymes involved in neurotransmitter synthesis, aiming to augment dopamine production in the substantia nigra in order to increase responsiveness to the dopamine precursor L-dopa, or to increase GABA production in the subthalamic nucleus to restore inhibitory signals to the basal ganglia that are disrupted in PD. Other strategies were based on delivery of genes encoding neurotrophic factors, aiming to preserve remaining dopaminergic neurons. The efficacy of these approaches in the primate model led to a series of human trials. However, after more than 100 patients have been treated, there

has been little evidence of efficacy (Bartus, Weinberg, and Samulski 2014). While these studies called into question the relevance of the drug-induced primate model of PD, these early human studies provided important evidence for the safety of AAV delivery to the brain. Further, PET imaging studies carried out in a trial for a vector expressing aromatic amino acid decarboxylase (AADC) demonstrated transgene expression in the brain for several years after treatment (Mittermeyer et al. 2012). Thus while gene therapy has not shown promise for the treatment of PD, the failed PD trials paved the way for a variety of CNS gene therapy studies. Many of these were for rare genetic diseases, and to date these are some of the only indications for which there has been evidence of efficacy. In trials for Canavan disease and aromatic amino acid decarboxylase deficiency, treated patients have shown evidence of modestly attenuated disease progression after intracranial AAV delivery (Janson et al. 2002, Leone et al. 2012, Hwu et al. 2012).

Intrathecal AAV Delivery

All trials of AAV-mediated CNS gene transfer to date have utilized multiple intraparenchymal brain injections. While this delivery method demonstrated efficacy in mouse models of many genetic disorders, there are two potential problems with translating this approach to humans—scaling to the larger human brain (for diseases that require whole-brain targeting), and the potential inflammatory response caused by localized brain damage at the injection site. The issue of scaling is derived from the distribution of transduction after intraparenchymal brain injection. Transgene expression is generally limited to the cells immediately surrounding the injection site, although some transduction can occur at more distal sites due to vector transport along axonal projections (Vite et al. 2005, Castle et al. 2014). Some investigators have attempted to

increase vector distribution using convection-enhanced delivery, which employs pressure gradients to drive the vector deeper into the brain parenchyma, although improvements have been modest (Bankiewicz et al. 2000). In mouse models, even the limited distribution that occurs after intraparenchymal injection results in transduction of a significant portion of the brain. The problem with applying this approach to diseases in which the entire CNS is affected has become apparent in studies of canine and feline models of lysosomal storage diseases. Even with the potential cross correction of neighboring cells due to transgene secretion, these studies typically required at least 6 injections to correct storage pathology in a significant portion of the brain (Vite et al. 2005, Ciron et al. 2006). Scaling this method from the 30-70 g brain of a cat or dog to a 1.4 kg human brain would require more than 100 injections for equivalent distribution. Since this is not feasible in humans, trials have instead pursued much more limited injection strategies that cannot replicate the extent of brain transduction that has been required for efficacy in animal models.

A second obstacle to translation of intraparenchymal vector injection to humans is the potential local inflammation caused by the injection, and the resulting impact on immune responses to the transgene product. Initiation of an adaptive immune response requires an inflammatory “danger” signal to activate antigen presenting cells and recruit lymphocytes, including CD8 T cells that can kill host cells presenting the target antigen, as well as CD4 T cells which can activate B cells to produce antibodies against the antigen. In the absence of inflammatory signals, reactive lymphocytes enter a default pathway of anergy or tolerance to the foreign antigen. In the setting of gene therapy, it is critical to avoid inflammatory signals at the time of vector delivery, as the newly expressed non-self antigen could be a target for circulating B and T cells, and providing

a danger signal can initiate this response. This has been demonstrated in studies with adenoviral vectors, in which the vector capsid provides an inflammatory signal so that immunity is elicited against the transgene (Liu and Muruve 2003). With AAV vectors, tolerance typically develops to the transgene product, apparently due to expression in the absence of an inflammatory signal from the viral capsid or genome. However, providing the inflammatory signal by other means—such as local tissue destruction at the time of injection—could result in transgene-specific immunity. This seems to have occurred in early preclinical studies of AAV-mediated CNS gene therapy for two lysosomal storage diseases. In dog models of these diseases, direct brain injection of AAV vectors resulted in localized tissue damage followed by lymphocyte recruitment and elimination of transduced cells (Ciron et al. 2006, Ellinwood et al. 2011).

Intrathecal injection presents a clear alternative to multiple direct brain injections. CSF is produced by the choroid plexus in the ventricles and flows through the ventricular system to the cisterna magna, then around the length of the spinal cord and the surface of the brain. Thus vector injection into CSF could allow for widespread distribution in the CNS with a single injection. However, intrathecal injection has not been widely pursued as a method for delivery of biologics to the brain due to the belief that CSF is primarily confined between the pia and arachnoid membranes, with little interaction with the brain parenchyma (Papisov, Belov, and Gannon 2013). More recent studies have revealed that in fact CSF flows deep into the brain via perivascular channels, and that even large molecules can directly diffuse from these channels into the brain interstitial fluid (Iliff et al. 2013, Iliff et al. 2012). This new view of CSF flow is supported by studies of intrathecal enzyme replacement therapy in animal models, which demonstrate that enzyme delivered into CSF is readily taken up by the brain (Dickson, Ellinwood, et al.

2010, Dickson et al. 2009, Dickson, Hanson, et al. 2010, Dickson, Naylor, Mlikotic, Victoroff, Chen, Passage, Le, et al. 2008, Kakkis, McEntee, et al. 2004, Vite et al. 2011). These findings opened up the possibility of widespread delivery of proteins, or even viral vectors, to the entire CNS with a single injection. This approach could potentially solve the issue of scaling intraparenchymal injections to the human brain, and could have a more favorable immunological profile by avoiding tissue damage and inflammation at the time of injection.

Large animal models of MPS I

Evaluating intrathecal AAV delivery for MPS I requires animal models that accurately reflect disease pathophysiology while also having the necessary size and CNS anatomy to reasonably replicate intrathecal vector delivery and distribution in humans. Mutations in the gene encoding IDUA resulting in a phenotype mimicking MPS I have been described in transgenic mice, the Plott Hound dog, and the domestic shorthair cat (Menon, Tieu, and Neufeld 1992, Shull et al. 1984, Haskins, Desnick, et al. 1979, Haskins, Jezyk, et al. 1979, He et al. 1999). MPS I mice have been generated both as traditional knockouts and by targeting a common human mutation (W402X) to the endogenous gene. The MPS I cat carries a 3 base pair in-frame deletion in the IDUA gene, resulting in production of a protein missing a single aspartate residue that is critical for substrate binding (He et al. 1999, Maita et al. 2013). The MPS I dog carries a splice site mutation that results in the inclusion of the first intron in the mature mRNA, creating an immediate stop codon (Menon, Tieu, and Neufeld 1992). All three animal models exhibit the biochemical and histological abnormalities characteristic of MPS I, including extensive storage lesions in the CNS. The neuropathology in the dog has been the best characterized, and shows remarkably similarity to humans, with ectopic neurite

growth, axonal spheroids, and extensive ganglioside storage, providing strong evidence for similar pathophysiology to the human disease.

The canine and feline models were used for all studies, as these species appeared to much more closely recapitulate critical characteristics of MPS I patients. Foremost among these is the sheer scale of the brain and CSF compartment. Delivery of enzyme to cells throughout the brain is an essential obstacle for CNS directed gene therapy for MPS I, which is dependent on both the diffusion of the vector in the CSF and penetration into the brain parenchyma, as well as diffusion of the secreted enzyme from transduced cells. In the small mouse brain (0.4 g) even very limited enzyme diffusion from transduced cells near the injection site could result in significant correction of storage lesions; however, in the 80 to 200-fold larger feline or canine brain, widespread correction would depend on the same process of distribution through CSF that would be essential for efficacy in humans. These considerations of vector distribution and similarities in brain pathology made the MPS I dog and cat appealing models for evaluation of intrathecal AAV delivery for MPS I.

Goals of this dissertation

The following studies were carried out based on the central hypothesis that IT AAV could achieve widespread targeting of cells in the CNS, and through cross-correction, globally resolve storage pathology. Chapter 2 outlines the development of the intrathecal approach for AAV delivery in nonhuman primates and initial findings supporting the capacity of this method to achieve widespread transduction and evade immune activation. These studies also delineate the critical importance of the site of intrathecal injection for the distribution of vector in the CNS. Chapter 3 describes the

application of this approach to MPS I in the feline model, including the impact on brain pathology and the importance of humoral immune responses to the transgene. In Chapter 4 intrathecal AAV delivery was evaluated in MPS I dogs, which resulted in strong antibody responses to IDUA. To circumvent the antibody response, a method was developed to induce persistent antigen specific tolerance to IDUA. Subsequent studies helped to define the impact of antibodies on CSF enzyme levels and disease correction. This study also presented a potential method for preventing immune responses to gene and protein therapies for recessive diseases, an approach that was confirmed in nonhuman primates. Finally in Chapter 5 this approach was utilized to induce tolerance to the human IDUA enzyme in MPS I dogs to allow for evaluation of intrathecal injection of a clinical candidate vector as a prelude to first in human trials.

Chapter 2: Widespread Gene Transfer in the Central Nervous System of Cynomolgus Macaques Following Delivery of AAV9 into the Cisterna Magna

---

Chapter 2 is adapted from: C. Hinderer, P. Bell, C. H. Vite, J.-P. Louboutin, R. Grant, E. Bote, H. Yu, B. Pukenas, R. Hurst, J. M. Wilson, *Molecular Therapy — Methods & Clinical Development* (2014).

Abstract

Adeno-associated virus serotype 9 (AAV9) vectors have recently been shown to transduce cells throughout the central nervous system of nonhuman primates when injected into the cerebrospinal fluid (CSF), a finding which could lead to a minimally invasive approach to treat genetic and acquired diseases affecting the entire CNS. We characterized the transduction efficiency of two routes of vector administration into the CSF of cynomolgus macaques— lumbar puncture, which is typically used in clinical practice, and suboccipital puncture, which is more commonly used in veterinary medicine. We found that delivery of vector into the cisterna magna via suboccipital puncture is up to 100-fold more efficient for achieving gene transfer to the brain. In addition, we evaluated the inflammatory response to AAV9-mediated GFP expression in the nonhuman primate CNS. We found that while CSF lymphocyte counts increased following gene transfer, there were no clinical or histological signs of immune toxicity. Together these data indicate that delivery of AAV9 into the cisterna magna is an effective method for achieving gene transfer in the CNS, and suggest that adapting this uncommon injection method for human trials could vastly increase the efficiency of gene delivery.

Introduction

Gene therapy using AAV vectors has enormous potential to treat acquired and congenital diseases affecting the central nervous system (CNS). Numerous studies in murine disease models have demonstrated the efficacy of AAV-mediated gene transfer in the brain, and initial human studies have shown an excellent safety profile (Haurigot et

al. 2013, Wolf et al. 2011, Tardieu et al. 2013, Kaplitt et al. 2007, McPhee et al. 2006). These pioneering clinical trials were carried out using multiple direct injections of the vector into the brain parenchyma, a strategy which has been shown in preclinical studies to achieve efficient gene transfer to cells surrounding the injection site (Vite et al. 2005). However, treatment of diseases affecting cells throughout the CNS will ultimately necessitate a delivery strategy capable of widespread transduction. Simply increasing the number of intra-parenchymal injections is not feasible, as even the most promising large animal studies have required at least 4 injection sites, which would translate to more than 100 injections in an adult human (Vite et al. 2005, McCurdy et al. 2014). Intravascular (IV) delivery of AAV serotype 9, which can traverse the blood-brain barrier, has been proposed as an alternative approach to achieve widespread transduction in the CNS (Bevan et al. 2011). While IV delivery is extremely effective in mice, in larger animals transduction in the CNS has been much more restricted (Gray et al. 2011, Samaranch et al. 2012). This approach is further limited by the extremely large doses required to achieve transduction in the brain and the resulting high off-target transduction of peripheral organs (Bevan et al. 2011, Gray et al. 2011).

Several groups have recently reported that delivery of AAV serotypes 7 and 9 into the cerebrospinal fluid (CSF) of nonhuman primates can effect transduction of both neurons and glia throughout the brain and spinal cord (Samaranch et al. 2012, Samaranch, Salegio, et al. 2013, Gray et al. 2013). This represents a critical advance in the field of CNS gene therapy. It may now be possible not only to achieve gene transfer throughout the CNS in humans, but to do so with a single minimally invasive injection. Access to the subarachnoid CSF is routinely achieved by lumbar puncture in clinical practice for diagnostic purposes and for administration of medications. Although less

common, access can also be achieved at the level of the cisterna magna by sub-occipital puncture. Intrathecal AAV delivery therefore represents a relatively low-risk delivery strategy that could be readily translated to the clinic.

In order to advance this approach toward clinical trials, we performed nonhuman primate studies to evaluate the efficiency of two minimally invasive delivery approaches—lumbar puncture and suboccipital puncture—for achieving vector distribution throughout the brain and spinal cord. One previous study reported that both strategies result in transgene expression in the brain, but did not quantitatively compare vector distribution (Gray et al. 2013). Based on our findings we estimate that sub-occipital puncture is 10 to 100-fold more efficient for brain transduction, making this approach far more promising for clinical use.

In addition, we performed detailed evaluation of histological markers of inflammation in the CNS of treated animals. Several studies have found intrathecal delivery of AAV9 to be safe in nonhuman primates and other species, although one group has reported that macaques treated with a vector carrying a GFP transgene experienced neurological deficits associated with histological evidence of an inflammatory response (Samaranch et al. 2014). We found that treated animals exhibited no clinical or histological abnormalities, although CSF lymphocytes were elevated in some animals. Overall our data suggest that intrathecal AAV injection by suboccipital puncture could serve as a useful gene transfer method for the treatment of neurological disease.

Materials and Methods

Animals: All study protocols were approved by the institutional animal care and use committee of the University of Pennsylvania. Six adult female cynomolgus macaques were used in this study. These animals were not pre-screened for AAV9 neutralizing antibodies. An additional female rhesus macaque was used for the intravenous delivery experiment. This animal was prescreened for AAV9 neutralizing antibodies as previously described(Wang et al. 2011).

Lumbar vector injection: Animals were anesthetized using IM ketamine/dexmedetomidine. The hair over the lumbar spine was shaved and the skin sterilely prepped. To widen the intervertebral space the spine is flexed slightly, drawing the animal's hind limbs forward toward the umbilicus. A spinal needle was inserted into the center of the L3-L4 intervertebral space just behind the anterior vertebral spinous process. Needle placement was confirmed by CSF return. CSF (1 mL) was collected, then a syringe containing vector (1 mL diluted in PBS) was attached to the spinal needle through a flexible linker. Vector was slowly injected by hand over one minute. After injection placement was again confirmed by CSF return. The needle was removed and direct pressure applied to the puncture site.

Intracisternal vector injection: Animals were anesthetized using IM ketamine/dexmedetomidine. The hair over the back of the head and neck was shaved and the skin sterilely prepped. The occipital protuberance at the back of the skull and the wings of the atlas (C1) were palpated, and a needle was inserted midway between them. Needle placement was confirmed by CSF return. CSF (1 mL) was collected, then a syringe containing vector (1 mL diluted in PBS) was attached to the needle through a flexible linker. Vector was slowly injected by hand over one minute. After injection

placement was again confirmed by CSF return. The needle was removed and direct pressure applied to the puncture site.

Vector Production: Single-stranded AAV9 vectors were produced by triple transfection of 293 cells and purified by iodixanol gradient centrifugation as previously described(Wang et al. 2011).

Quantitative PCR: Vector genomes were quantified in tissue samples by Taqman PCR as previously described(Wang et al. 2011).

Histology: Brains were divided into left and right hemisphere. The right half was sliced, fixed in formalin overnight, and embedded in paraffin for the preparation of H&E stained sections and for immunostaining. Slices from the left half were formalin-fixed and processed for GFP detection as described below. PCR samples for vector biodistribution studies were also retrieved from the left brain half prior to fixation. Tissues from spinal cord was collected from cervical, thoracic, and lumbar regions and processed for paraffin and cryosections as described for the brain.

Hematoxylin and eosin staining (H&E): H&E staining was performed on 6 μm paraffin sections according to standard protocols.

GFP fluorescence: Brain slices were fixed overnight in formalin, equilibrated sequentially in 15% and 30% sucrose in PBS, and frozen in OCT embedding medium for the preparation of cryosections for visualization of direct GFP fluorescence. Sections were mounted in Vectashield containing DAPI (Vector Laboratories, Burlingame, CA) as nuclear counterstain.

Immunohistochemistry for GFP: Sections were deparaffinized through an ethanol and xylene series, boiled in a microwave for 6 min in 10mM citrate buffer (pH 6.0) for antigen retrieval, treated sequentially with 2% H_2O_2 (15 min), avidin/biotin blocking reagents (15

min each; Vector Laboratories), and blocking buffer (1% donkey serum in PBS + 0.2% Triton for 10 min) followed by incubation with primary (1h) and biotinylated secondary antibodies (45 min; Jackson Immunoresearch, West Grove, PA) diluted in blocking buffer. As primary antibodies served a rabbit serum or a chicken antibody against GFP (both from Abcam, Cambridge, MA; diluted 1:1000) which both yielded similar results. A Vectastain Elite ABC kit (Vector Laboratories) was used according to the manufacturer's instructions with DAB as substrate to visualize bound antibodies as brown precipitate. Sections were slightly counterstained with hematoxylin to show nuclei. In some experiments hematoxylin counterstaining or antibodies were omitted as described in the text.

Immunofluorescence: Immunostaining was performed on sections from formalin-fixed paraffin-embedded tissue samples. Sections were deparaffinized and treated for antigen retrieval as described above, then blocked with 1% donkey serum in PBS + 0.2% Triton for 15 min followed by sequential incubation with primary (1 h) and fluorescence-labeled secondary antibodies (45 min) diluted in blocking buffer. Primary antibodies used were goat antibodies against GFAP (Novus Biologicals, Littleton, CO; 5µg/ml working concentration) and Iba1 (Abcam, 1:200), and TRITC-labeled donkey anti-goat (Jackson Immunoresearch, 1:100) served as secondary antibody.

Morphometric analyses: To quantify astrocytes (GFAP-positive cells) and microglia (Iba1-positive cells), 15 images were taken from immunostained brain sections per animal with a 20x objective showing the area directly below the cerebral cortex surface. Positive cells were counted manually and averaged for each animal. Brain tissues from two cynomolgus macaques from an unrelated study that had received AAV2.TGB.EPO intravenously and showed negligible vector genome copy numbers in the brain (below $1x10^{-4}$ gc/cell) served as controls (Gao et al. 2006).

For the quantification of transduced motor neurons, spinal cord sections were stained with Neurotrace red fluorescent Nissl stain (Life Technologies, Grand Island, NY) according to the manufacturer's instructions and images were taken at low magnification (4x objective) showing GFP expression and Neurotrace staining. Between three to five images were taken from the ventral area of each spinal cord region (cervical, thoracic, lumbar) to cover several sections per animal. ImageJ software (Rasband W. S., National Institutes of Health, USA; http://rsb.info.nih.gov/ij/) was used to first threshold and then select all Neurotrace-positive cells with a minimum pixel number of 175 reflecting a threshold diameter of approximately 25 μm. To determine the percentage of size-selected neurons that were GFP-positive, all selected neurons and those that were GFP-positive were counted for each image.

Results

Intracisternal delivery achieves broader vector distribution in the CNS

We treated six cynomolgus macaques with an intrathecal injection of a single-stranded AAV9 vector expressing GFP from either the cytomegalovirus (CMV) or chicken beta-actin (CB) promoter (Table 2-1). Four of the animals were injected via sub-occipital puncture; two were treated via lumbar puncture. There were no adverse clinical events during the course of the study. All animals were sacrificed 14 days after injection for histological analysis.

Vector distribution was evaluated in CNS and peripheral tissues by quantitative PCR (Figure 2-1). All animals treated by sub-occipital puncture exhibited substantial vector deposition in the brain and spinal cord, with up to one vector genome per cell in

most regions. Animals treated by lumbar puncture had approximately 10-fold lower gene transfer throughout the spinal cord, and up to 100-fold less in the brain. In contrast, both groups had similar distribution to peripheral organs. Vector copy numbers were quite high in liver and spleen, indicating significant vector escape to the peripheral circulation.

As previous studies have demonstrated the ability of AAV9 to transduce cells within the CNS following intravascular injection, we treated one rhesus macaque intravenously to compare the efficiency of this approach to intrathecal injection (Figure 2-1). Despite the use of a high vector dose (2×10^{13} GC/kg) and the absence of detectable neutralizing antibodies to AAV9 in this animal, vector distribution to the CNS was substantially lower than that achieved at 4-8 fold lower doses via cisternal injection. Due to the low CNS gene transfer efficiency observed in this animal we did not explore this route of administration further.

GFP false positives complicate assessment of transgene expression in the CNS

We initially attempted to quantify GFP expressing cells in the CNS by immunohistochemistry (IHC), as other groups have previously utilized this method to measure GFP expression in the nonhuman primate CNS (Gray et al. 2013, Samaranch, Salegio, et al. 2013). We identified what appeared to be a large number of GFP positive cells throughout the CNS of treated macaques (Figure 2-7, A and C). However, we also detected a similar staining pattern in some negative control brain tissues from animals that had not received a GFP expressing vector (Figure 2-7, B and D). The false-positive neurons appeared dark on H&E sections, a property consistent with the “dark neuron” artifact that has long been described in brain tissue, particularly when prepared by

immersion fixation (Jortner 2006). The high affinity of these cells for H&E did not explain their dark color in IHC sections, as the cells still appeared to stain positive when the hematoxylin counterstain was omitted from IHC sections (Figure 2-7 E, G). Omission of the primary antibody and both primary and secondary antibodies in combination demonstrated that the false-positive neurons did not exhibit endogenous peroxidase activity, but instead nonspecifically bound antibodies used for IHC (Figure 2-7 F, H). Because these false positive neurons were detected sporadically in various negative control tissues, we determined that IHC could not be used to reliably detect GFP expression in brain samples.

In order to overcome the problem of GFP false positive cells, we instead used direct GFP fluorescence to measure expression. We initially avoided this method because many cells in the CNS exhibit auto-fluorescence. We found that we could account for these fluorescence false positives by overlaying images captured in a red fluorescence channel, as GFP is detectable only in the green channel whereas auto-fluorescent material appears across several channels (Figure 2-8). We therefore used direct GFP fluorescence verified by overlay with a red channel image to identify GFP positive cells. Using this method, GFP expressing cells were detected in treated animals but not in any control tissues. All subsequent analyses were carried out using this approach, and red channel images are shown for all cases in which auto-fluorescence was observed.

Intracisternal AAV9 transduces cells throughout the brain and spinal cord

Consistent with the high vector distribution to the brain in animals treated by intra-cisternal injection, GFP expression was observed in clusters of cells throughout

most regions of the brain, which were interspersed with untransduced regions (Figure 2-3). Costaining with a fluorescent Nissl stain (NeuroTrace) and antibodies against astrocyte and microglial markers (GFAP and Iba1) revealed that virtually all GFP positive cells were neurons (Figure 2-3) although rare transduced astrocytes were also detected (Figure 2-3, l). Virtually no GFP positive cells were detected in the cerebrum of animals treated by lumbar puncture. In the spinal cord, GFP expression was prominent in the ventral horns of animals treated by intracisternal injection (Figure 2-4a). High magnification images show that these transduced cells were primarily the large lower motor neurons (Figure 2-4b). These cells were heavily transduced in the thoracic and lumbar segments of animals treated by intracisternal injection (Figure 2-4, Table 2-2). There were also a small number of transduced motor neurons in the cervical spinal cord of these animals. Transduced spinal cord cells were rare in the animals treated by lumbar administration (Table 2-2). The macaque treated with a high dose of intravenous AAV9 exhibited no GFP expression in the cerebrum or cerebellum, although several transduced neurons were observed in the thoracic and lumbar spinal cord (Figure 2-5, Table 2-2).

Intrathecal AAV9 does not induce an inflammatory response in the nonhuman primate brain

As one previous study reported evidence of inflammation in the cerebrum of nonhuman primates following intrathecal delivery of an AAV9 vector expressing GFP, we analyzed the brains of all treated animals for signs of inflammation (Samaranch et al. 2014). No untreated animal tissues were available for histology controls, so we analyzed brains from two cynomolgus macaques that were treated with an intravenous injection of an AAV serotype 2 vector expressing erythropoietin from a liver specific

promoter; these animals were previously found to have virtually no vector deposition in the brain (Gao et al. 2006). Histopathology showed no evidence of cellular infiltrates in the brain parenchyma or in the meninges or perivascular spaces in any of the treated animals (Figure 2-9). We quantified cells expressing GFAP, an intermediate filament protein that is upregulated in astrocytes in the setting of inflammation. There were no differences in the frequency of GFAP positive cells in the brains of treated animals and controls (Figure 2-9, Table 2-3). We also quantified microglia by Iba1 staining. The frequency of microglia was normal in all animals, and microglia exhibited morphology characteristic of a resting rather than an activated state (Figure 2-9, Table 2-3). Although there was no evidence of inflammation in brain tissue, we did observe a moderate lymphocytic pleocytosis in the CSF of two of the animals that were treated with intracisternal injection, which correlates with the higher CNS transduction in these animals (Table 2-4).

Discussion

As the first gene transfer strategy capable of achieving high levels of transduction throughout the CNS in large animals, intrathecal AAV delivery could greatly expand the applications of gene therapy in neurological disease. Intrathecal AAV injection is a particularly attractive strategy because of the relative ease of accessing the intrathecal space compared to the invasive neurosurgical procedure required for intraparenchymal injection. We found that vector delivery into the CSF at the level of the cisterna magna is far more efficient than lumbar intrathecal injection for gene transfer to the brain and spinal cord. It is interesting that the level of CSF access had such a profound effect on vector distribution, as previous work has shown that a protein infused into the lumbar CSF is distributed throughout the CNS (Calias et al. 2012). This may therefore

represent a property of the viral particle, and not reflect the behavior of other substances delivered into the intrathecal space. One potential explanation is that the vector quickly binds to cell surfaces, which would allow for wide distribution from the rapidly dispersing cisternal CSF, but not from the slower moving CSF lying inferior to the spinal cord in the lumbar cistern. Vector distribution in the CSF could be influenced by additional factors—such as the volume and formulation of the injection—which should be evaluated in future studies. Translation of this approach to humans may also benefit from further investigation of the impact of total CSF volume and cisternal volume on vector distribution, as these factors vary between species and among humans (Whitney et al. 2013).

Given the superior transduction efficiency achieved by vector delivery into the cisterna magna, it will be critical to develop a safe means of performing this procedure in patients. Though cisternal injection is commonly performed in nonhuman primates and other animals, it is infrequently utilized in clinical practice. Suboccipital puncture of the cisterna magna was first described in humans in 1920 as a technique for introduction of air or contrast material for diagnostic studies (Ayer 1920). Traditional indications for cisternal puncture have also included CSF sampling. The suboccipital puncture has largely been supplanted by noninvasive diagnostic studies including CT and MRI and by CSF sampling from lower levels of the spinal canal, such as between the first and second cervical vertebrae or between lumbar vertebrae below the level of the spinal cord, techniques which are associated with lower rates of complications. The most serious complications associated with cisternal puncture include inadvertent injury to vascular structures with resultant hemorrhage as well as brainstem injury. A 1929 review of the literature identified 6 reported deaths in 2019 reported procedures in 535

patients (Ayer 1920). These authors also identified 9 additional cases of medullary injury, noting however that in skilled hands the procedure should not be considered dangerous (Saunders and Riordan 1929). In 1973, Keane again reviewed the literature finding that subarachnoid hemorrhage was the most common major complication of cisternal puncture, with at least 30 reported fatalities (Keane 1973). He noted that other serious complications resulted from direct puncture of brain substance. In 1989, Ward et al. evaluated cisternal puncture in cadavers, finding that "tenting" of the dura at the site of needle penetration could result in deeper than expected penetration prior to entry into the subarachnoid space (Ward, Orrison, and Watridge 1989).

The few more recent publications available on suboccipital puncture suggest that modern day imaging equipment may improve safety by enhancing visualization of critical structures during the procedure. A recent report described better visualization of critical structures during a cisternal puncture by performing a contrast enhanced CT immediately prior to needle insertion (Pomerantz 2005). Axial and sagittal contrast enhanced CT images (Figure 2-6) would allow for visualization of the entire needle path, which courses in the midline between the base of the occiput and the first vertebra to the cisterna magna. Contrast enhanced CT allows for visualization of the local vascular structures, particularly the posterior inferior cerebellar artery (PICA), which has historically been the source of bleeding in reported cases of subarachnoid hemorrhage following suboccipital puncture. Employing imaging with suboccipital puncture could also be useful for preventing damage to the medulla, a previously reported complication resulting from advancing the needle beyond the cisterna magna. The use of more sophisticated integrated navigation systems, like the Philips PercuNav system, may also provide an additional layer of safety by allowing real time needle visualization during the

procedure. We therefore believe that suboccipital puncture, though uncommonly utilized, could represent a safe and feasible vector delivery approach for clinical use.

Consistent with previous studies, we observed efficient transduction of motor neurons in the thoracic and lumbar spinal cord following intrathecal AAV9 delivery. We found that transduction in the cerebrum, however, was much more diffuse, consisting of patches of GFP expressing cells. The transduction efficiency we observed in the brain was much lower than that reported by others, particularly following lumbar intrathecal delivery (Gray et al. 2013). Given the potential for immunohistochemistry to produce GFP false positive cells in the CNS, it is likely that this artifact may have contributed to exaggerated transduction efficiencies in some reports. This possibility is supported by quantitive PCR data, which in one previous study show approximately one vector genome present per 100 cells in the brain—similar to our results for lumbar delivery—which would preclude transduction of the nearly 50 percent of cells identified as GFP positive by immunohistochemistry in that study (Gray et al. 2013). Other studies of intrathecal AAV9 injection have demonstrated a pattern of brain transduction more similar to that described here (Samaranch et al. 2012, Samaranch, Salegio, et al. 2013).

Clinical trials of intraparenchymal injection of AAV serotypes 2 and rh.10 have demonstrated excellent tolerability despite the inherent invasiveness of this delivery method(Kaplitt et al. 2007, McPhee et al. 2006, Tardieu et al. 2013). Several studies of intrathecal AAV9 administration in nonhuman primates have indicated that it is similarly well tolerated. However, one study reported that macaques treated with intrathecal AAV9 expressing GFP developed neurologic deficits 2-3 weeks following vector administration (Samaranch et al. 2014). These animals also exhibited histological signs of inflammation in the brain, including MHC class II upregulation and microglial

activation. This was presumed to be due to an immune response against the foreign GFP transgene. We did not identify similar clinical or histological findings in any treated animals. It is possible that we did not observe the same phenomenon due to our shorter follow up period (two vs three weeks). However, the same group previously reported treating four macaques with intrathecal AAV9, as well as two with AAV7, both expressing GFP, without any complications during the same three week follow up period (Samaranch et al. 2012, Samaranch, Salegio, et al. 2013). Likewise, another group reported no adverse events or histological abnormalities after four weeks of follow up in 10 macaques treated with intrathecal AAV9 expressing GFP (Gray et al. 2013). It therefore appears that this isolated observation of an inflammatory response following intrathecal AAV9 delivery was unlikely due to the vector itself, though future studies should continue to monitor subjects for such a response. Although we did not observe any clinical or histological abnormalities, we did observe elevated CSF lymphocytes in two of the treated animals. This suggests that there may be some degree of immune activation by the vector or GFP transgene, although we have not observed any clinical or histological consequences of this response.

Our results demonstrate that delivery of an AAV9 vector into the cisterna magna is an effective approach to achieve transduction of cells throughout the nonhuman primate CNS. The excellent safety and feasibility of this route of administration should enable rapid deployment into the clinic for a wide range of diseases affecting the CNS.

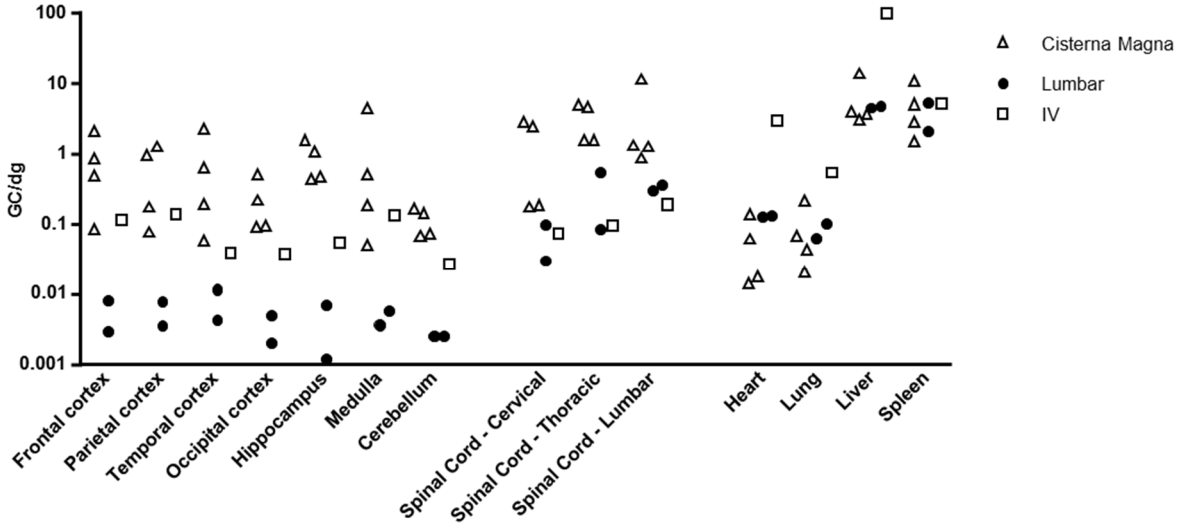

Figure 2-1. AAV9 biodistribution following intrathecal delivery in nonhuman primates

AAV9 was administered to six cynomolgus macaques at doses of 2.5 – 5 x 10^{12} GC/kg by injection into the cisterna magna (n = 4) or the lumbar subarachnoid space (n = 2). An additional animal was treated intravenously with a high dose (2 x 10^{13} GC/kg) of AAV9. All animals were sacrificed two weeks after injection and vector genomes were quantified in tissue samples by Taqman PCR.

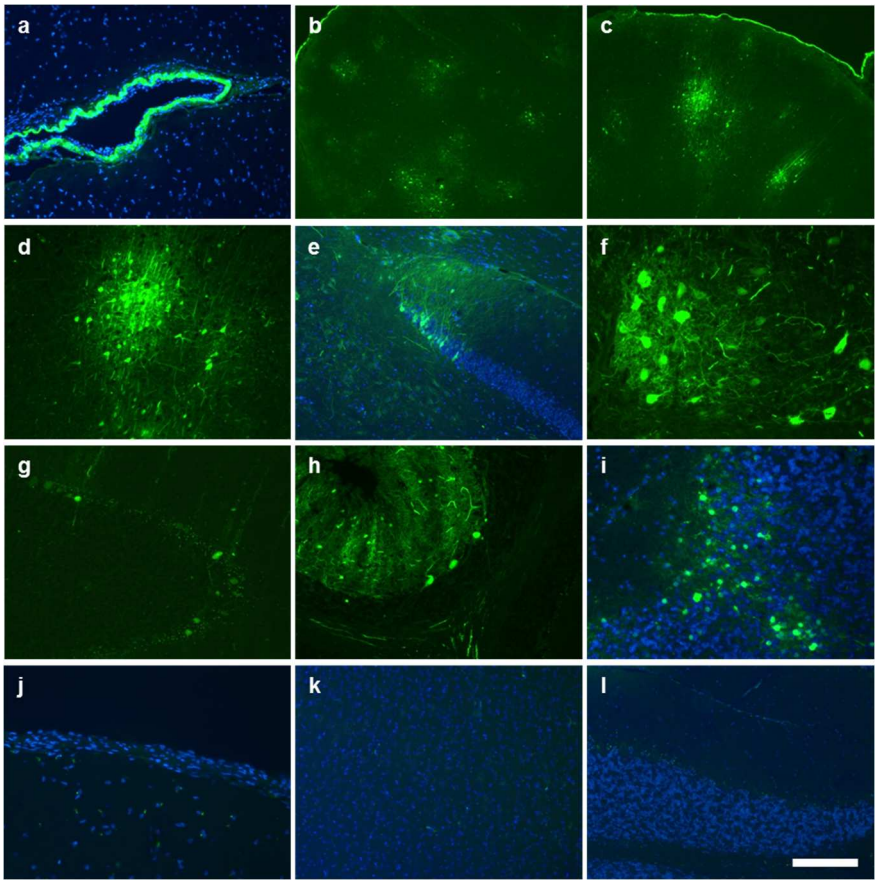

Figure 2-2. Transduction throughout the brain following intracisternal AAV9 delivery

AAV9 was administered to six cynomolgus macaques at doses of 2.5 – 5 x 10^{12} GC/kg by injection into the cisterna magna (n = 4) or the lumbar subarachnoid space (n = 2). Brain sections from animals treated by intracisternal injection (a-i) and those treated by lumbar puncture (j-l) were imaged for native GFP fluorescence. Counterstain is DAPI (a, e, i-l). All images shown were negative for fluorescence in the red channel. (a) Meninges (b-d) Cerebral cortex (e) Dentate gyrus (f) Thalamus (g, h) Cerebellum with large Purkinje cells. (i) Cerebellum with transduced neurons in granular layer. (j-l). Direct GFP fluorescence in meninges (j), cerebral cortex (k), and cerebellum (l) after treatment by lumbar puncture. Scale bar: 100 μm (f, i, j), 200 μm (a, d, e, g, h, k, l), 500 μm (b, c).

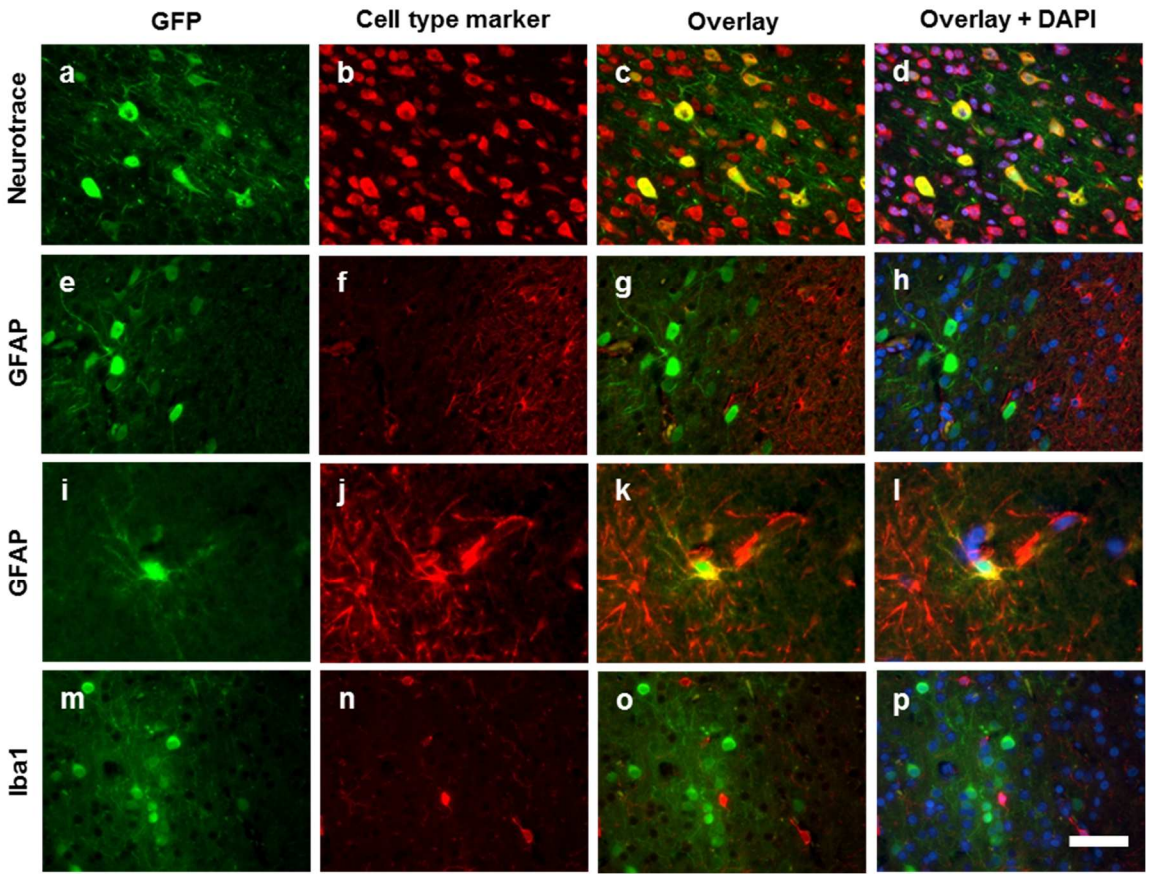

Figure 2-3. Predominantly neuronal transduction of intrathecal AAV9

Cortical brain sections from animals treated by intracisternal injection were imaged for native GFP fluorescence (a, e, i, m). Images are overlaid with a fluorescent Nissl stain (NeuroTrace) for detection of neurons (b, c, d), GFAP immunostaining for astrocytes (f, g, h, j, k, l), or Iba1 staining for microglia (n, o, p). Counterstain is DAPI (d, h, l, p). Scale bar = 50 μm.

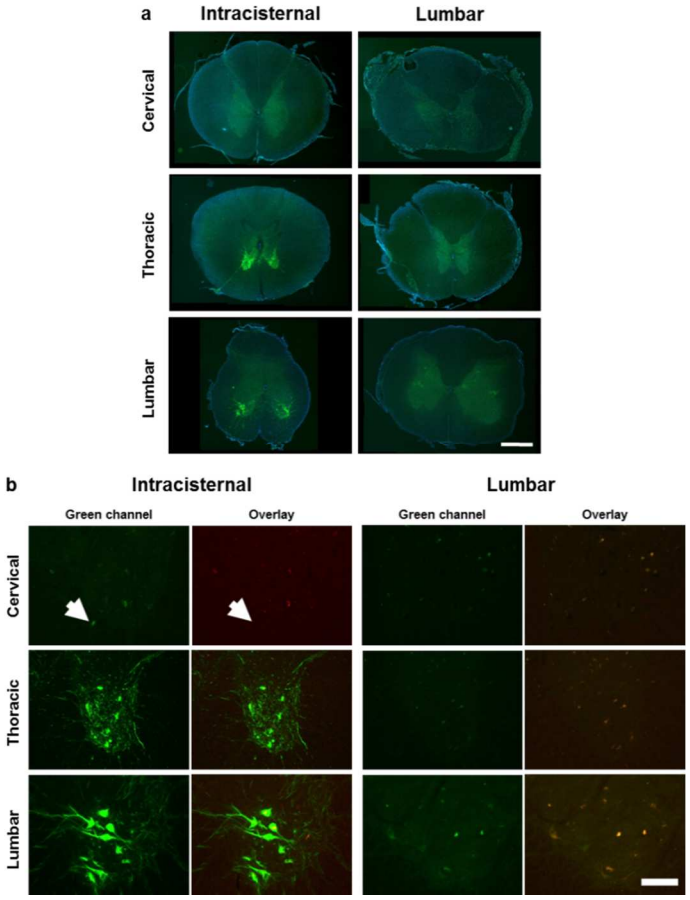

Figure 2-4. Spinal cord transduction following intrathecal AAV9 administration by intracisternal or lumbar injection

Direct fluorescence images were captured for three spinal cord segments from all treated animals. Low magnification images show transduction primarily in the ventral gray matter (a). High magnification images of the ventral horn demonstrate transduction primarily of large neurons in the thoracic and lumbar segments, with occasional transduced cells in the cervical segment (white arrow). Scale bar: 1 mm. (b). As autofluorescence was observed in some spinal cord sections, an overlay of the red and green channels is shown to identify false positive GFP signal (yellow). Scale bar: 200 μm.

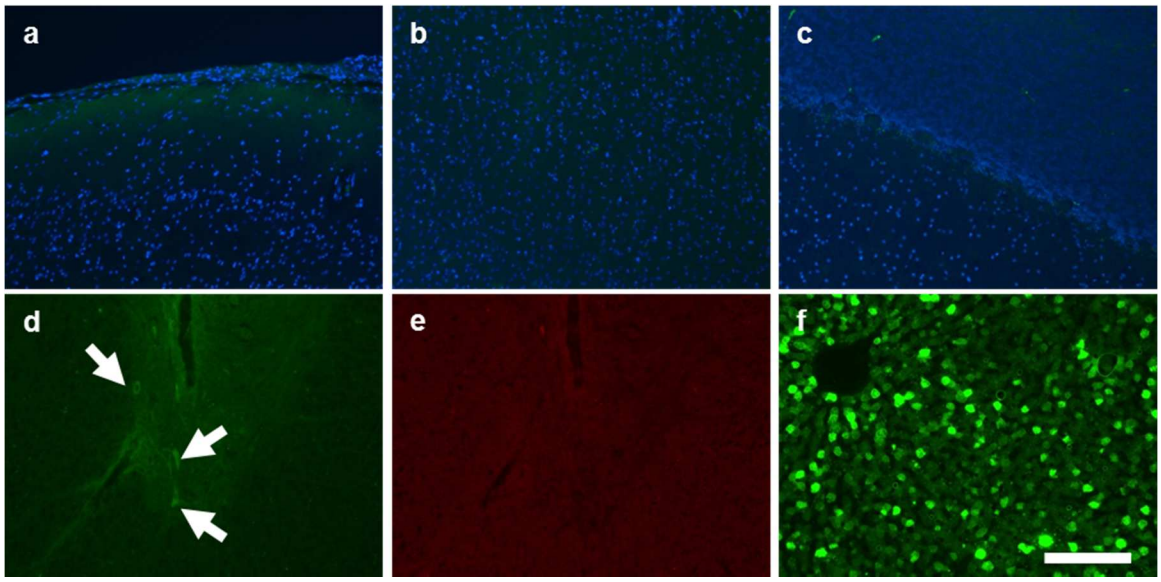

Figure 2-5. Limited CNS transduction following intravascular AAV9 delivery

A rhesus macaque was treated intravenously with an AAV9 vector (2 x 10^{13} GC/kg) expressing GFP. Sections were imaged for native GFP fluorescence from cerebral meninges (a), cortex (b) and cerebellum (c). Some GFP expressing cells (arrows) were noted in the thoracic spinal cord (d). GFP expression was confirmed by absence of fluorescence in the red channel (e). In contrast to the CNS, peripheral organs including liver were heavily transduced (f). Counterstain is DAPI (a-c). Scale bar: 200 μm.

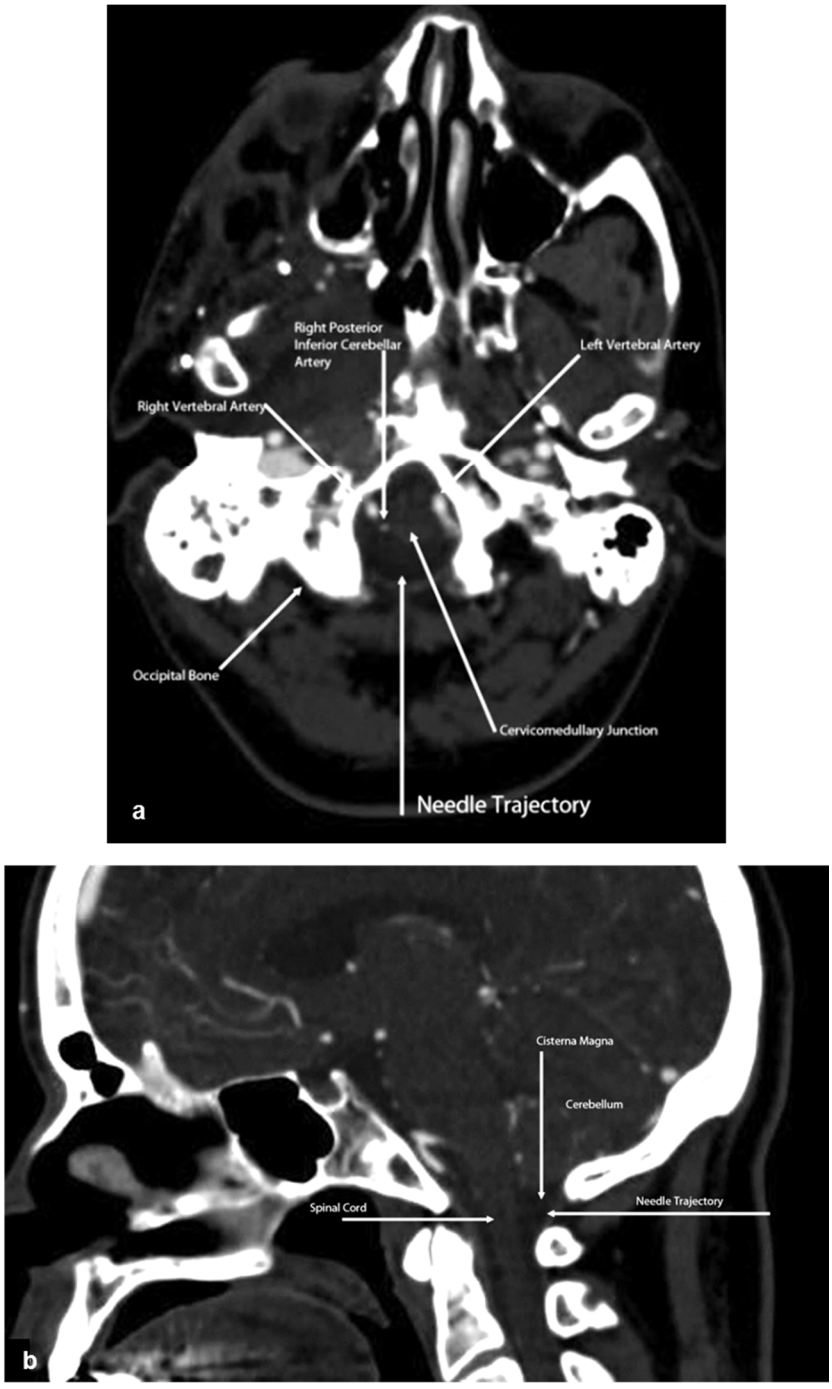

Figure 2-6. Evaluation of anatomic landmarks for suboccipital puncture

Axial (a) and sagittal (b) contrast enhanced CT images illustrating key structures to identify when performing a suboccipital puncture.

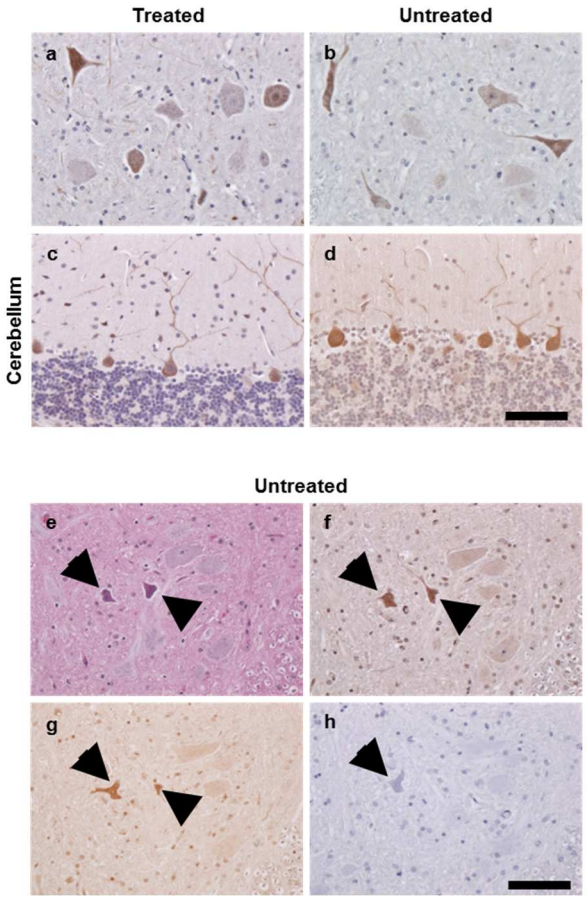

Figure 2-7. Detection of false positive GFP expressing cells by immunohistochemistry Sections from cerebrum and cerebellum from the AAV9 treated animals (a and c) and an untreated control (b and d) were stained with a chicken anti-GFP antibody followed by a horseradish peroxidase labeled anti-chicken secondary. In order to identify the cause of nonspecific staining, sequential brain sections from an untreated animal were stained with H&E (e), primary and secondary antibodies for GFP detection as well as hematoxylin counterstain (f), IHC antibodies without counterstain (g), or hematoxylin and peroxidase substrate only (h). Scale bar: 100 μm.

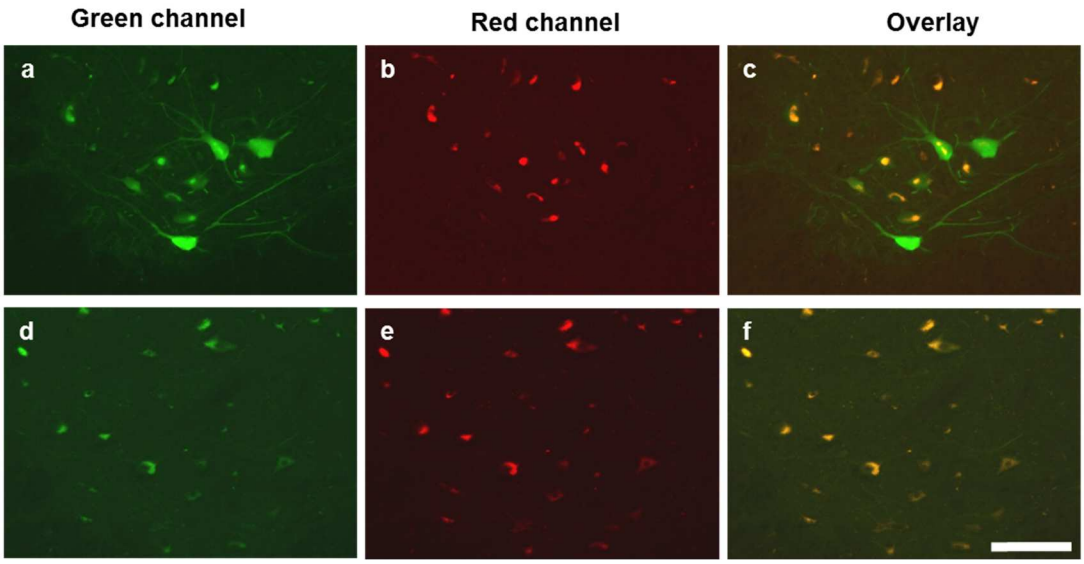

Figure 2-8. Differentiating GFP fluorescence from autofluorescence in spinal cord

Fixed frozen sections of a spinal cord expressing GFP (A-C) or not expressing GFP (D-F) were imaged by fluorescence microscopy in both red and green channels. The overlaid images (C and F) distinguish autofluorescent material by its broader emission spectrum, which results in equal red and green channel signal. Scale bar: 200 μm.

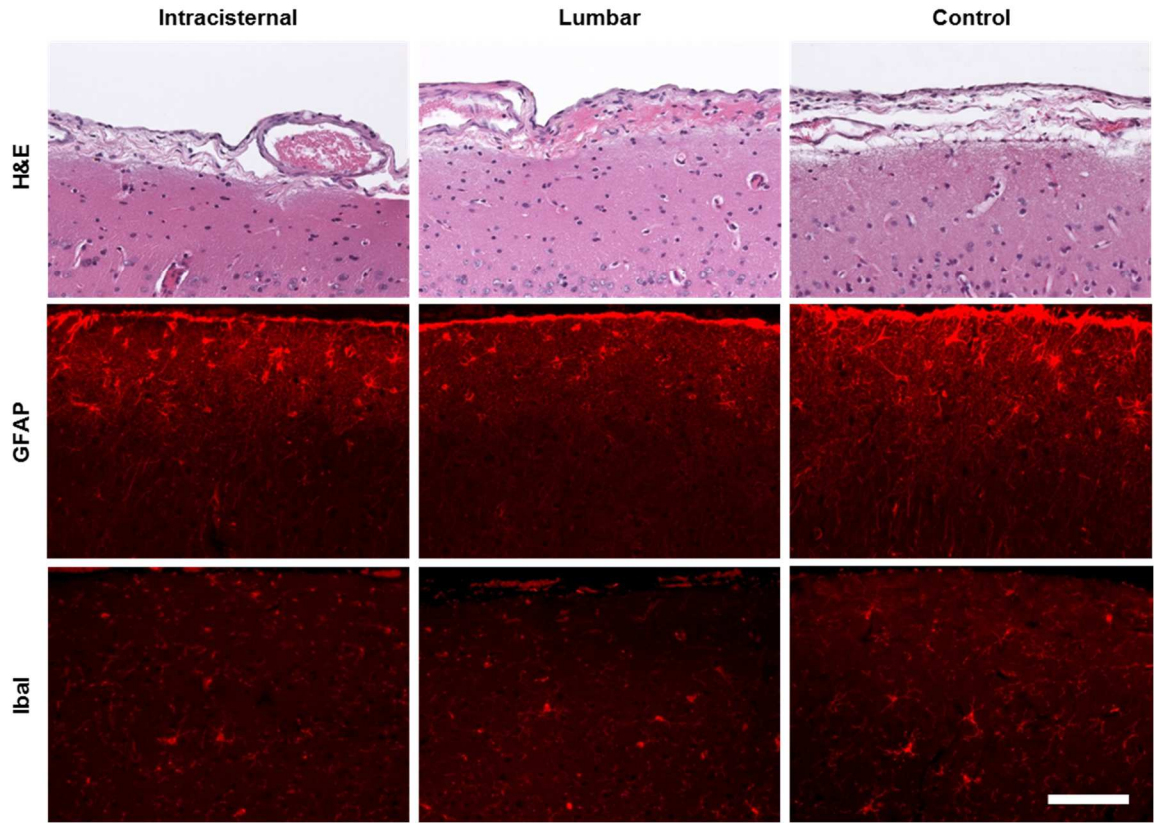

Figure 2-9. Absence of an inflammatory response following intrathecal delivery of AAV9 expressing GFP

Brain sections from intrathecal AAV9 treated animals and control animals were stained with H&E, and immunostained for the astrocyte marker GFAP and the microglial marker Iba1. Scale bar: 100 μm.

Table 2-1. Summary of study subjects

Animal #	ROA[A]	Vector	Dose	Weight (kg)	Sex	Age
17	**CM**	AAV9.CMV.eGFP	5 x 10^{12} GC/kg	3.60	F	8 years
18	**CM**	AAV9.CB7.eGFP	5 x 10^{12} GC/kg	3.85	F	8 years
20	**CM**	AAV9.CB7.eGFP	2.5 x 10^{12} GC/kg	5.40	F	8 years
21	**CM**	AAV9.CB7.eGFP	2.5 x 10^{12} GC/kg	8.75	F	8 years
04	**L**	AAV9.CB7.eGFP	2.5 x 10^{12} GC/kg	4.25	F	8 years
05	**L**	AAV9.CB7.eGFP	2.5 x 10^{12} GC/kg	4.85	F	8 years
49	**IV**	AAV9.CMV.eGFP	2.0 x 10^{13} GC/kg	3.30	F	8 years

A. L = lumbar injection, CM = cisterna magna, IV = intravenous

Table 2-2. Quantification of transduced motor neurons throughout the spinal cord

Animal #	ROA[A]	Promoter	Percent GFP+ motor neurons[B]		
			Cervical	Thoracic	Lumbar
17	**CM**	**CMV**	ND	10.7 ± 11.4	14.5 ± 17.6
18	**CM**	**CB**	0 ± 0	8.4 ± 2.3	20.3 ± 4.9
20	**CM**	**CB**	0.3 ± 0.6	25.1 ± 17.0	19.3 ± 11.0
21	**CM**	**CB**	1.5 ± 2.1	48.0 ± 15.6	38.2 ± 23.4
04	**L**	**CB**	0.3 ± 0.6	0 ± 0	0.6 ± 1.3
05	**L**	**CB**	0 ± 0	1.7 ± 2.9	2.6 ± 5.2
49	**IV**	**CMV**	0 ± 0	7.7 ± 10.5	0.2 ± 0.5

A. L = lumbar injection, CM = cisterna magna, IV = intravenous

B. Mean ± standard deviation in four fields

Table 2-3. Quantification of GFAP and Iba1 positive cells in brain sections

Animal #	ROA[A]	Vector	GFAP[B]	Iba1
17	**CM**	AAV9.CMV.eGFP	15.1 +/- 12	4.6 +/- 1.6
18	**CM**	AAV9.CB7.eGFP	14.1 +/- 8.4	4 +/- 1.6
20	**CM**	AAV9.CB7.eGFP	11.8 +/- 9.2	4.7 +/- 1.7
21	**CM**	AAV9.CB7.eGFP	19.6 +/- 16	4.8 +/- 0.3
04	**L**	AAV9.CB7.eGFP	9.6 +/- 11.2	4.7 +/- 1.4
05	**L**	AAV9.CB7.eGFP	16.5 +/- 19	4.2 +/- 1.8
80	**IV**	AAV2.TBG.EPO	14.6 +/- 7.5	9.2 +/- 2.9
86	**IV**	AAV2.TBG.EPO	12.7 +/- 3.8	8.4 +/- 1.9

A. L = lumbar injection, CM = cisterna magna, IV = intravenous

B. Mean number of positive cells ± standard deviation in 15 fields

Table 2-4. CSF analysis

			Nucleated Cells/µl		Total Protein (mg/dL)	
Animal #	**Treatment**	**ROA[A]**	**Day 0**	**Day 14**	**Day 0**	**Day 14**
04	AAV9.CB7.eGFP	L	1	ND	12	ND
05	AAV9.CB7.eGFP	L	0	2[B]	15	25[B]
20	AAV9.CB7.eGFP	CM	2	41[C]	11	25
21	AAV9.CB7.eGFP	CM	4	13[C]	20	14

A. L = lumbar injection, CM = cisterna magna

B. traumatic tap; RBC count = 2090/µL

C. >70% lymphocytes

CHAPTER 3: Intrathecal gene therapy corrects CNS pathology in a feline model of mucopolysaccharidosis I

Chapter 3 is adapted from: C. Hinderer, P. Bell, B. L. Gurda, Q. Wang, J.-P. Louboutin, Y. Zhu, J. Bagel, P. O'Donnell, T. Sikora, T. Ruane, P. Wang, M. E. Haskins, J. M. Wilson, *Molecular therapy* (2014).

Abstract

Enzyme replacement therapy has revolutionized the treatment of the somatic manifestations of lysosomal storage diseases (LSD), although it has been ineffective in treating central nervous system (CNS) manifestations of these disorders. The development of neurotrophic vectors based on novel serotypes of adeno-associated viruses (AAV) such as AAV9 provides a potential platform for stable and efficient delivery of enzymes to the CNS. We evaluated the safety and efficacy of intrathecal delivery of AAV9 expressing α-l-iduronidase (IDUA) in a previously described feline model of mucopolysaccharidosis I (MPS I). A neurological phenotype has not been defined in these animals, so our analysis focused on the biochemical and histological CNS abnormalities characteristic of MPS I. Five MPS I cats were dosed with AAV9 vector at 4-7 months of age and followed for 6 months. Treated animals demonstrated virtually complete correction of biochemical and histological manifestations of the disease throughout the CNS. There was a range of antibody responses against IDUA in this cohort which reduced detectable enzyme without substantially reducing efficacy; there was no evidence of toxicity. This first demonstration of the efficacy of intrathecal gene therapy in a large animal model of a LSD should pave the way for translation into the clinic.

Introduction

Mucopolysaccharidosis type I (MPS I, Hurler, Scheie, Hurler-Scheie syndromes) is a recessively inherited disease caused by deficiency of a ubiquitous lysosomal enzyme, α-l-iduronidase (IDUA), which is required for the degradation of the glycosaminoglycans (GAGs) heparan sulfate and dermatan sulfate. Accumulation of these undegraded lysosomal substrates results in widespread tissue pathology, often

characterized by skeletal deformities, cardiac and pulmonary disease, upper airway obstruction, and in some cases, progressive neurological disease (Xing et al. 2014). The central nervous system manifestations of MPS I vary, with profound developmental decline occurring in early childhood in severely affected patients, while those with a more mild phenotype often maintain normal intelligence(Kachur and Del Maestro 2000, Taccone et al. 1993, Vijay and Wraith 2005, Zafeiriou and Batzios 2013, Furukawa et al. 2011, Ahmed et al. 2014). However, even the patients with attenuated disease sometimes face serious neurological complications such as communicating hydrocephalus, as well as spinal cord compression secondary to GAG storage in the meninges.

The currently available treatments for MPS I include bone marrow transplantation (BMT) and intravenous enzyme replacement therapy (ERT). Both modalities exploit the observation that the mannose-6-phosphate receptor, which is responsible for sorting lysosomal proteins from the *trans*-Golgi, is also expressed at the cell surface, allowing for receptor-mediated uptake and lysosomal trafficking of IDUA infused intravenously or secreted from donor-derived leukocytes following BMT (Dahms, Lobel, and Kornfeld 1989)(Kakkis et al. 1994). While both ERT and BMT have demonstrated efficacy against many of the somatic features of MPS I, only BMT is believed to alter the course of CNS disease, presumably through IDUA secretion by donor derived cells that migrate into the CNS(Aldenboven, Boelens, and de Koning 2008). Despite the promise of this approach, BMT has been associated with engraftment rates as low as 50% and mortality rates in excess of 10% in MPS I patients(Aldenboven, Boelens, and de Koning 2008). Studies in the canine model of MPS I and small clinical trials have indicated that it may be possible to instead achieve IDUA delivery throughout the CNS using intrathecal

injection of the enzyme, which would allow for distribution via the cerebrospinal fluid(Chen et al. 2011, Dickson, Ellinwood, et al. 2010, Dickson, Naylor, Mlikotic, Victoroff, Chen, Passage, and Le 2008, Dickson et al. 2009, Dickson, Hanson, et al. 2010, Dickson, Naylor, Mlikotic, Victoroff, Chen, Passage, Le, et al. 2008, Kakkis, McEntee, et al. 2004, Munoz-Rojas et al. 2008). While intrathecal ERT provides important proof of principle for achieving enzyme distribution in CNS via the CSF, it does not represent a practical treatment approach due to the need to repeatedly access the CSF for enzyme delivery for the lifetime of the patient. This leaves a significant unmet need for a safe and effective long-term treatment for the CNS manifestations of MPS I.

Gene therapy offers an attractive alternative to BMT and intrathecal ERT for targeting the CNS in MPS I. Gene transfer to the brain using adeno-associated viral (AAV) vectors has been found safe in multiple human trials, and delivery of the therapeutic transgene to quiescent cells within the CNS could provide a permanent source of secreted enzyme, obviating the need to repeatedly access the CSF (Mandel and Burger 2004, McPhee et al. 2006, Mittermeyer et al. 2012, Kaplitt et al. 2007). In murine MPS models, CNS-directed AAV gene transfer has demonstrated complete correction of tissue lesions and improvements in disease-specific behavioral phenotypes (Wolf et al. 2011, Haurigot et al. 2013). The primary obstacle to this approach has been translation to large animal models. Direct intra-parenchymal brain injection of AAV vectors results in transgene expression constrained to the area surrounding the injection site, with histological correction limited to the adjacent tissue (Vite et al. 2005). Although studies in both canine and feline models of lysosomal enzyme deficiencies have shown that this limitation can be overcome using multiple vector injections, this strategy is not readily scalable to the human brain (Vite et al. 2005, Ciron et al. 2006). Further, intra-

parenchymal injections have been shown to induce a local inflammatory response that can be accompanied by elimination of transduced cells (Ciron et al. 2006). A potential alternative delivery approach has been highlighted by recent studies of intrathecal AAV delivery, which show that in dogs, cats and nonhuman primates, an AAV9 vector delivered into the CSF transduces glial and neuronal cells throughout the brain and spinal cord (Gray et al. 2013, Haurigot et al. 2013, Bucher et al. 2014a). This potential to transduce cells across the neuraxis in a large animal via a single minimally invasive injection could radically transform the therapeutic potential of AAV-mediated gene therapy for CNS disease. We hypothesized that this capacity of intrathecal AAV9 to effect such widespread CNS transduction, coupled with the ability of genetically corrected cells to secrete enzyme to cross-correct untransduced cells, would make this a highly effective approach for the long-term treatment of CNS manifestations of MPS I.

In the present study, we tested the capacity of intrathecal delivery of an AAV9 vector to correct storage lesions throughout the CNS in a large animal model of MPS I. We selected the feline MPS I model for these experiments because the CNS lesions in these animals closely resemble those of MPS I patients, with accumulation of gangliosides in neurons and GAGs in the meninges and around cerebral blood vessels(Vite et al. 2011). We found that intrathecal delivery of a vector bearing the normal feline IDUA sequence resulted in global CNS correction of the histological and biochemical features of MPS I. IDUA-specific antibody responses were elicited in the CNS of most treated animals, but were not associated with adverse clinical sequelae or loss of efficacy. Together these results strongly support the development of intrathecal AAV9-mediated gene delivery as a therapeutic approach for MPS I.

Materials and Methods

Vector production: The feline *IDUA* sequence was isolated as described (Wang et al., manuscript in preparation). A codon-optimized version of the cDNA was cloned into expression constructs flanked by AAV2 terminal repeats that contained the CMV or CB promoter, a chimeric intron, and an SV40 or rabbit globin polyadenylation sequence. The constructs were packaged in an AAV9 capsid by triple transfection of 293 cells and purified as previously described (Wang et al. 2011).

Animal procedures: The MPS I cat colony was maintained at the University of Pennsylvania School of Veterinary Medicine under NIH and USDA guidelines for the care and use of animals in research. All protocols were approved by the Institutional Animal Care and Use Committee of the University of Pennsylvania. Approximately 3 mL of blood was collected from the jugular vein for serum analysis. For intrathecal injections, propofol-anesthetized animals were intubated, and the suboccipital region was clipped of hair and scrubbed. Using sterile technique, a suboccipital puncture was performed with a 22 gauge spinal needle. Placement was confirmed by CSF return. After collecting 1 -2 mL of CSF, vector diluted in sterile PBS (1-2 mL) was slowly injected by hand. The animals were monitored to confirm complete recovery after the procedure. Euthanasia was by an intravenous overdose of sodium barbiturate, 80 mg/kg.

Enzyme assays: Tissue, serum, and CSF samples were immediately frozen on dry ice and stored at -80 degrees until analysis. Serum and CSF were used directly in IDUA and Hexosaminidase (Hex) assays. Tissue samples were homogenized in lysis buffer (0.2 % Triton-X100, 0.9% NaCl, pH 4.0), and briefly sonicated. Samples were then freeze-thawed and clarified by centrifugation. Protein concentrations were determined by Bradford assay. IDUA activity was measured by incubating sample diluted in 0.1 mL

water with 0.1 mL of 100 mM 4MU-iduronide (Toronto Research Chemicals; Glycosynth) in IDUA buffer (0.15 M NaCl, 0.05% Triton-X100, 0.1 M sodium acetate, pH 3.58) at 37 degrees for 1-3 hours. The reaction was stopped by addition of 2 mL 290 mM glycine, 180 mM sodium citrate, pH 10.9. The liberated 4MU was quantified by comparing fluorescence to standard dilutions of 4MU. Units are given as nmol 4MU liberated per hour per mg of protein (tissues) or per mL of serum or CSF. Hex assays were performed as described(Wendeler and Sandhoff 2009).

HCII-thrombin western blot: 0.5 µL of serum in 1x LDS buffer was separated on a 4-12% Bis-Tris polyacrylamide gel (Novex) in MOPS buffer at 120 V for 2 hours. Protein was transferred to a PVDF membrane at 30 V for 1.5 hours. The membrane was blocked for 1 hour in 5% NFDM, and then incubated overnight at 4 degrees in 5% NFDM containing a 1:25,000 dilution of HRP-conjugated goat anti-HCII antibody (Enzyme Research). The blot was washed and developed with a chemiluminescent substrate (Thermo Scientific).

GAG assay: Tissue samples were processed as for enzyme assays. Tissue GAGs were quantified using the Blyscan assay (Biocolor, Carrickfergus, UK) according to the manufacturer's instructions.

ELISA for detection of antibodies to feline IDUA: A C-terminal his-tag was added to the feline *IDUA* cDNA by PCR. The tagged cDNA was cloned into an expression cassette driven by a CB promoter. This plasmid was transfected into six 90% confluent 10 cm plates of HEK 293 cells using lipofectamine 2000 (Invitrogen, Carlsbad, CA). Supernatant was collected twice at 24-hour intervals; each time the supernatant pH was immediately titrated to pH 5.8, which vastly increased enzyme stability, and stored at 4 degrees. The enzyme was purified on a 1 mL HisTrap FF column (GE). The eluted fractions were immediately adjusted to pH 5.8. The fractions containing purified feline IDUA were identified by enzyme assay and SDS-PAGE. The purified protein was

incubated at 3 μg/mL in PBS, pH 5.8 on polystyrene ELISA plates overnight at 4 degrees. The plates were washed twice in PBS, pH 5.8, blocked in 3% BSA, pH 5.8, and then incubated with diluted samples for one hour at room temperature. The plates were washed 5 times, incubated 1 hour with a 1:10,000 dilution of HRP-conjugated goat anti-feline IgG (Peirce, Rockford, IL) in blocking solution, washed 5 times, and developed using TMB substrate.

Quantitative PCR: Quantification of vector genomes in tissue was performed as previously described (Wang et al. 2011).

Histology: Brains were divided into left and right hemisphere. The right half was sliced and, except for the distal occipital part, fixed in paraformaldehyde to be further processed for GM3 and cholesterol detection. Slices from the left half were used for all other stains as well as for PCR analysis and enzyme assays. For PCR and enzyme analysis samples were collected from the frontal, temporal and occipital cortices as well as medulla, hippocampus and cerebellum. Hippocampus samples included the entire dissected hippocampus, spanning from CA1 to the DG.

Hematoxylin and eosin staining (H&E): H&E staining was performed on 6 μm sections from formalin-fixed paraffin-embedded tissues according to standard protocols.

GM3 immunohistochemistry: Brain slices were fixed overnight in 4% paraformaldehyde/PBS, equilibrated sequentially in 15% and 30% sucrose, and frozen in OCT embedding medium.

Immunostaining was performed on 30 μm thick floating cryosections as described (McGlynn, Dobrenis, and Walkley 2004) using monoclonal antibody DH2 (Glycotech, Gaithersburg, MD) as primary antibody followed by a biotinylated secondary anti-mouse antibody (Jackson Immunoresearch, West Grove, PA) and detection with a Vectastain Elite ABC kit (Vector Labs, Burlingame, CA). Stained sections were transferred onto

glass slides and mounted with Fluoromount G (Electron Microscopy Sciences, Hatfield, PA).

GAG histochemistry: Brain samples were fixed overnight in methacarn (60% methanol, 30% chloroform, 10% glacial acetic acid) at 4ºC, dehydrated through an ethanol series and xylene, and paraffin embedded. Deparaffinized 6 µm sections were stained in 1% Alcian Blue (Sigma)/0.1 N HCl (pH1.0) for 15 min, rinsed in water for 2-3 min, and counterstained with Nuclear Fast Red (Vector Labs).

Filipin stain: Cholesterol was detected on 30 µm thick cryosections prepared as described for GM3 immunohistochemistry. Floating sections were stained with filipin (Sigma, St Louis, MO, 10 µg/ml prepared from 3 mg/ml stock solution) for 1.5 h. After washing in PBS (2 x 5 min), sections were mounted with Fluoromount G.

Immunofluorescence: Immunostaining was performed on 6 µm sections from formalin-fixed paraffin-embedded tissue samples. Sections were deparaffinized through an ethanol and xylene series, boiled in a microwave for 6 min in 10mM citrate buffer (pH 6.0) for antigen retrieval, and blocked with 1% donkey serum in PBS + 0.2% Triton for 15 min followed by sequential incubation with primary (1 h) and labeled secondary (45 min) antibodies diluted in blocking buffer. Primary antibodies used were rabbit antibodies against GFAP (Abcam, Cambridge, UK, 1:1000) and LIMP2 (Novus Biologicals, Littleton, CO, 1:200), and FITC- or TRITC-labeled donkey anti-rabbit (Jackson Immunoresearch) served as secondary antibody.

Morphometric analyses: Images taken for quantification purposes were acquired using either a 4x (GM3), 10x (filipin), or 20x objective (GFAP,LIMP2, H&E) depending on the lowest magnification that still allowed accurate visualization of neurons or astrocytes. Images for GFAP and LIMP2 were taken from the area directly below the cerebral cortex surface and include the cerebral molecular layer; all other images were centered on the

middle to upper neuron layers of the cortex. The images shown for LIMP2, filipin and H&E stained sections correspond to the region depicted in the second column of Figure 4. Five images from each brain were taken for analyzing storage in H&E sections as well as GM3 and filipin staining which showed low variation between different brain parts, while a total of 20 images (10 each from two different sections) were acquired for GFAP and LIMP2 analyses. For quantification of GM3 and filipin positive neurons, ImageJ software (Rasband W. S., National Institutes of Health, USA; http://rsb.info.nih.gov/ij/) was used to first threshold images, i.e. to mark positively stained cells, and then to count the number of these cells with the "Analyze Particles" tool of ImageJ. GFAP and LIMP2 positive cells as well as storage-positive H&E-stained neurons were counted manually.

Results

Intrathecal AAV9 delivery induced robust IDUA expression in CSF and serum

Eight MPS I cats between four and seven months of age were included in this study (Table 3-1). These animals carried a three base pair deletion in the *IDUA* gene, resulting in omission of a single aspartate residue (He et al. 1999). Three cats heterozygous for the *IDUA* mutation and two wild type animals from the same colony served as unaffected controls. Five of the affected animals at ages 4 to 7 months were treated with a single intrathecal injection via the cisterna magna of 10^{12} GC/kg of an AAV9 vector bearing a codon-optimized normal feline *IDUA* sequence. The vector administered to two of the cats carried a chicken beta actin (CB) promoter; the other three treated animals received a vector carrying a cytomegalovirus (CMV) promoter. One additional animal assigned to receive the CB vector died under anesthesia during

the pre-treatment CSF collection. There were no other adverse events throughout the study period.

Serum and CSF were serially collected from the treated and naïve animals and assayed for IDUA enzyme activity (Fig. 3-1). IDUA activity was not detected in samples from untreated MPS I cats. Treated animals exhibited a rapid elevation in both CSF and serum IDUA activity following vector injection, with peak activity exceeding that measured in normal cats. The CB promoter appeared to be more active, inducing higher enzyme levels in both CSF and serum. Following a peak at 21 days post injection, CSF enzyme levels rapidly declined to near baseline in two animals, although activity remained detectable at most time points. CSF IDUA activity stabilized at approximately normal levels in the other three cats. Serum activity varied between the normal range and baseline values, although high background in the serum assay precluded accurate assessment of low levels of circulating enzyme.

Heterogeneous antibody responses were elicited against the therapeutic enzyme

The sharp decline in IDUA activity in some of the treated animals did not appear to be consistent with a cellular immune response against the transduced cells, as residual expression was detectable and there were no clinical signs of meningitis or encephalitis. CSF analysis revealed normal nucleated cell counts and only mildly elevated protein, which was also observed in untreated MPS I cats (Table 3-2). We suspected that this decline in CSF enzyme could be due to the induction of antibodies against IDUA. Indirect ELISA using purified feline IDUA as a target for capture of antibodies showed clear antibody responses in the CSF of some of the treated animals (Fig. 3-2a). Within the CMV vector treated group, CSF IDUA activity decreased in

proportion to antibody titer, with animal 8982 having the highest titer corresponding to nearly undetectable CSF enzyme levels. The same was true for the animals treated with the CB vector; animal 9050 exhibited elevated antibody titers and very low CSF IDUA activity whereas 9058 maintained normal CSF IDUA and did not have a detectable antibody response. The correlation was not as clear between the groups treated with the different vectors, as the CB vector-treated animals appeared to have lower steady state CSF antibody titers overall. Considering that these animals also had higher initial enzyme expression, it is likely that the additional antigen either sequestered antibody or interfered with ELISA-based detection, resulting in lower overall titer measurements in this group. In summary there was a correlation between CSF IDUA antibody and steady state level of CSF IDUA for all animals except 8911, which developed moderate levels of CSF antibodies but retained high levels of steady state CSF enzyme.

Normalization of CSF hexosaminidase (Hex) activity despite antibody induction to the therapeutic enzyme

IDUA deficiency has been shown to induce secondary elevation of activity of other lysosomal glycohydrolases. We found that elevated activity of one such enzyme, beta hexosamindase, was detectable in the CSF of MPS I cats (Fig. 3-2b). This elevated Hex activity in CSF provided a potential non-invasive biomarker to detect aberrant cellular regulation in the CNS of MPS I cats. Following vector delivery, we observed an approximately 2-fold decrease in CSF Hex activity in all treated animals. Animals receiving the CB vector, which induced higher initial expression, exhibited the most rapid normalization of CSF Hex. Only one animal (8982), which had high anti-IDUA titers and very low CSF IDUA activity, exhibited incomplete normalization of CSF

Hex. This demonstrated that all treated animals, even those that lost nearly all CSF enzyme activity, exhibited a persistent biochemical response to gene transfer.

Intrathecal AAV9 delivery resulted in global CNS transduction and normalization of tissue Hex activity

All treated animals were euthanized between 160 and 170 days following vector delivery. We performed quantitative PCR analysis on DNA from tissue samples, which revealed substantial vector deposition throughout the brain and spinal cord (Fig. 3-3a). There were no differences in copy number in samples from animals with very low CSF IDUA levels, further confirming that elimination of transduced cells played no role in the decrease in circulating activity. Vector bio-distribution to peripheral organs was limited, except to the liver, which contained very high vector copy numbers. All subsequent analyses of transduction activity and biochemical and pathological correction are presented in subgroups of cats with high (8911, 8932 and 9058) or low (8982 and 9050) CSF IDUA.

IDUA activity was measured in tissue samples collected from various regions of the brain and spinal cord (Fig. 3-3b). Activity was undetectable in untreated MPS I cats. All treated animals exhibited elevated tissue IDUA activity, exceeding that of heterozygous control animals in several brain regions. Tissue IDUA was lower in many regions of the CNS in the animals with the lowest CSF enzyme activity, although in all cases it was greater than that found in untreated MPS I cats. To evaluate tissue correction of the MPS I phenotype in the CNS, Hex activity was measured in CNS tissue lysates (Fig. 3-3c). Similar to observations in the CSF, untreated animals had significantly elevated tissue Hex activity, which was normalized in all brain regions of

treated animals, including sites with very low IDUA activity. This indicates an extremely low threshold for the expressed enzyme to effect changes in the abnormal cellular processes associated with MPS I in the CNS. We also attempted to quantify total GAG concentrations in the brain, but we found that the dimethylmethylene blue assay used for these measurements exhibited high background in brain tissue and thus could not reliably distinguish between normal and MPS I cats.

IDUA reconstitution reverses lysosomal storage lesions throughout the CNS

The CNS manifestations of MPS I are characterized histologically by intracellular accumulation of cholesterol and the gangliosides GM2 and GM3 in the brain parenchyma, with storage of GAGs prominent in the meninges and surrounding the cerebral vasculature (Vite et al. 2011, McGlynn, Dobrenis, and Walkley 2004). Untreated MPS I cats exhibited marked GM3 staining throughout multiple brain sections, which was absent in normal controls (Fig. 3-4, Table 3-3). In treated animals, GM3 storage was cleared throughout all brain regions analyzed, although scattered cells showing residual GM3 staining were visible in the animals with the lowest CSF enzyme activity. The reduction in GM3 staining correlated with a reduced frequency of abnormal neurons exhibiting distended cytoplasm visible on histopathology; while these were frequently observed in the cortex of untreated cats, they were absent in treated animals with high CSF IDUA activity, and rare in treated animals with lower CSF enzyme (Fig. 3-5, Table 3-3). Filipin staining for cholesterol revealed a similar pattern of correction, with an average of 239 +/- 60 positive cells per field in untreated animals, which was reduced to an average of 2 positive cells per field in animals with high CSF IDUA activity and 38 and 52 cells per field in treated animals with low CSF IDUA activity (Fig. 3-5, Table 3-3). We also stained for LIMP2, a lysosomal integral membrane protein, which has been

shown to accumulate in neurons in murine models of MPS (Haurigot et al. 2013). This marker also showed considerable lysosomal storage in the brains of MPS I cats that was almost completely normalized following intrathecal vector administration in all treated animals (Fig. 3-5, Table 3-3).

To evaluate correction of storage pathology in the meninges and perivascular spaces, Alcian blue staining for GAGs was performed on cortical tissue sections (Fig. 3-6). The untreated animals exhibited significant GAG accumulation in the thickened meninges, as well as in perivascular cells. This GAG storage was almost completely reversed in all treated animals.

Intrathecal AAV9 delivery corrects somatic lesions

It has previously been reported that AAV9 delivery into the CSF in a murine MPS model results in both CNS and peripheral organ transduction, with corresponding correction of peripheral pathology (Haurigot et al. 2013, Gray et al. 2013). It has also been demonstrated that this distribution of vector to the periphery occurred after intrathecal administration in primates and dogs, an observation confirmed by our PCR analysis in the present study [29,](Gray et al. 2013). Given the distribution of vector to the periphery and significant serum IDUA activity, we evaluated somatic tissues for evidence of disease correction. Quantitative analysis of GAGs in liver and spleen showed normalization in the liver of all treated animals, whereas splenic GAG storage was corrected in animals which exhibited the lowest antibody titers in their treatment groups (8911, 8932, 9058) but not in those that had the highest antibody titers within their treatment group and had reduced CSF enzyme activity (Fig. 3-8). This is consistent with IDUA being expressed primarily from the heavily transduced liver, with cross correction

of distant organs such as the spleen occurring only in the absence of an interfering antibody response. Histological evaluation of GAG storage by Alcian blue stain confirmed correction in the liver and spleen, as well as improvement in the heart and lungs, which was more pronounced in the animals with lower antibody titers (Fig. 3-7). The kidney appeared to have significant GAG storage that did not respond as readily to treatment.

Serum levels of the covalent complex formed by thrombin and the protease inhibitor heparin cofactor II (HCII) have been proposed as a biomarker in MPS I, as formation of this complex is catalyzed by GAGs such as dermatan sulfate (Langford-Smith et al. 2011, Randall et al. 2008). We saw reductions in serum HCII-thrombin in all treated animals, consistent with reduction in peripheral GAGs (Fig. 3-9). The response appeared less robust in the two animals with high residual spleen GAGs.

Intrathecal AAV9 does not induce an inflammatory response in the CNS

One report has suggested that intrathecal AAV9 delivery can result in a robust inflammatory response and cellular infiltration (Samaranch, San Sebastian, et al. 2013). We evaluated hematoxylin and eosin stained tissue sections from cerebrum and cerebellum for evidence of cellular infiltrates (Fig. 3-10). We also immunostained tissue sections for GFAP, an astrocyte intermediate filament protein that is highly upregulated in the context of inflammation (Fig. 3-11, Table 3-3). We observed no evidence of cellular infiltration or astrocyte activation in any of the treated animals based on standard histopathology or GFAP staining.

Discussion

The goal of this study was to evaluate the feasibility of intrathecal gene therapy for treating CNS manifestations of MPS I in an authentic large animal model as a necessary step toward human trials. A previously described feline model of MPS I was further characterized for biochemical and histological abnormalities as a prelude to an evaluation of gene transfer. Our study demonstrated diffuse CNS pathology in this model, including neuronal storage lesions staining strongly for gangliosides and cholesterol as well as pronounced meningeal and perivascular GAG storage, consistent with previous reports (Vite et al. 2011). We also found accumulation of the lysomomal membrane protein LIMP2 and elevation of hexosaminidase activity in the brains of MPS I cats, as has been observed in other species (Haurigot et al. 2013). We found that a single intrathecal administration of AAV9 expressing normal feline IDUA resulted in virtually complete correction of the histological and biochemical features of MPS I in the CNS. We could not directly assess the clinical consequences of treatment because MPS I cats do not have a well-defined neurological phenotype, although mouse studies suggest that correction of CNS storage pathology correlates with normalization of cognitive deficits(Wolf et al. 2011).

Intrathecal AAV9 delivery could potentially be applied to many lysosomal storage diseases affecting the CNS. However, MPS I may represent a particularly tractable target due to the extremely low levels of enzyme required to correct lysosomal storage. *In vitro* studies have shown that IDUA concentrations below 1 pM can reduce GAG accumulation in MPS I patient fibroblasts, which would predict extremely efficient cross correction of untransduced cells by enzyme secreted from even a small number of genetically modified cells (Kakkis et al. 1994). MPS I is also an important target due to

the substantial CNS morbidity in this disease and the limited efficacy and availability of treatment options. BMT is currently the only therapeutic option with the potential to modify the course of cognitive decline in patients with a severe phenotype, but this comes with high morbidity and mortality. Other CNS manifestations such as communicating hydrocephalus and spinal cord compression also cause debilitating symptoms and necessitate surgical interventions such as ventriculoperitoneal shunting or spinal laminectomy (Kachur and Del Maestro 2000, Vijay and Wraith 2005, Taccone et al. 1993, Ahmed et al. 2014, Furukawa et al. 2011, Zafeiriou and Batzios 2013). Our results demonstrate that intrathecal AAV9 administration can reverse storage lesions in both the brain parenchyma and the surrounding meninges, indicating the potential to benefit patients with a variety of CNS sequelae of MPS I. In addition to the unmet clinical need in MPS I and strong preclinical data, this disease presents some practical benefits as a target for human trials. The ability to measure enzyme activity in the CSF would allow for direct confirmation of transgene expression, and a variety of potential biomarkers could be useful for assessing biological activity. In this study we found that CSF hexosaminidase activity was elevated in MPS I animals and was normalized in proportion to histological CNS correction, making this a strong candidate for a biomarker in human trials. Longitudinal evaluation of the MRI findings typical of MPS I— enhanced white matter signal intensity, enlarged perivascular spaces and meningeal thickening— could also provide useful correlates of therapeutic activity (Zafeiriou and Batzios 2013).

We found that a variable antibody response against normal feline IDUA was elicited by intrathecal AAV9-mediated expression. This might be expected, given that nearly all MPS I patients develop antibodies against the enzyme during the course of ERT. The heterogeneity of clinical responses and high prevalence of antibodies make it

difficult to discern a clear effect of antibodies on therapeutic outcomes in humans, but studies in MPS I dogs indicate that tissue correction from systemic ERT is significantly reduced by high antibody titers (Dickson, Peinovich, et al. 2008). A study examining the effect of antibody titer on the efficacy of intrathecal ERT in canine MPS I likewise showed that antibodies reduce treatment efficacy in the CNS (Dickson et al. 2012). Our results suggest that while anti-IDUA antibodies impact the efficiency of tissue correction, cross correction of untransduced cells remains reasonably effective in the setting of an antibody response. Some degree of residual efficacy after antibody induction against IDUA could also be explained by intracellular enzyme production alone; however, a previous study demonstrated that intracisternal AAV9 delivery at the dose tested transduces only a small fraction of cells in the feline brain, suggesting that widespread reversal of storage lesions is due to cross-correction. Most critically, development of an antibody response against IDUA in the CSF was not associated with adverse clinical events or histological evidence of inflammation. Together these data strongly support the safety and efficacy of this approach, even with the risk of developing antibodies against the therapeutic enzyme. Given the correlation we observed between antibody titer and histological evidence of efficacy, measuring CSF antibody titers may be informative for predicting clinical outcomes in human trials. Long-term follow up of patients treated with systemic ERT has shown that antibody titers fall to baseline levels in most patients within two years of treatment initiation, suggesting that a similar decline in titer may be seen in the context of gene therapy, which would further support the potential for robust long-term clinical benefit(Kakavanos et al. 2003). Long-term evaluation of AAV9 intrathecal gene therapy in feline MPS I is currently underway.

Here, we have demonstrated proof-of-principle that intrathecal AAV9 delivery can globally correct CNS manifestations of MPS I in a high-fidelity large animal model, even when antibodies are elicited against the therapeutic enzyme. The excellent tolerability and efficacy of this approach support progression into human trials for MPS I. These promising results also suggest that this approach may serve as a broad platform for the treatment of other lysosomal storage diseases affecting the CNS.

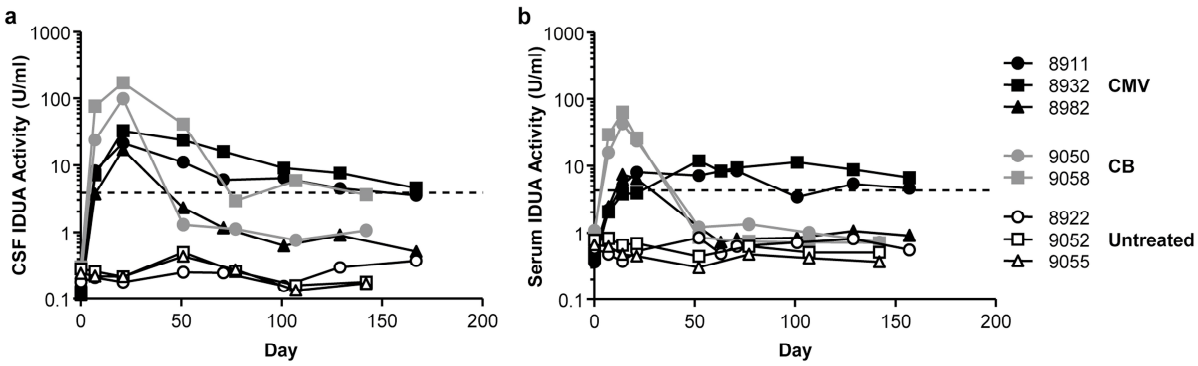

Figure 3-1. IDUA expression in CSF and serum following IT AAV9 delivery

Five MPS I cats were treated with an intracisternal injection of an AAV9 vector (10^{12} GC/kg) expressing feline *IDUA* from a CB (gray symbols) or CMV (black symbols) promoter. CSF and serum were serially collected from the treated animals as well as three untreated MPS I cats. IDUA activity was measured using the fluorogenic substrate 4MU-iduronide in CSF (a) and serum (b). All values are the mean of duplicate assays. Normal serum and CSF activity (dashed line) are the mean values from two wild type animals.

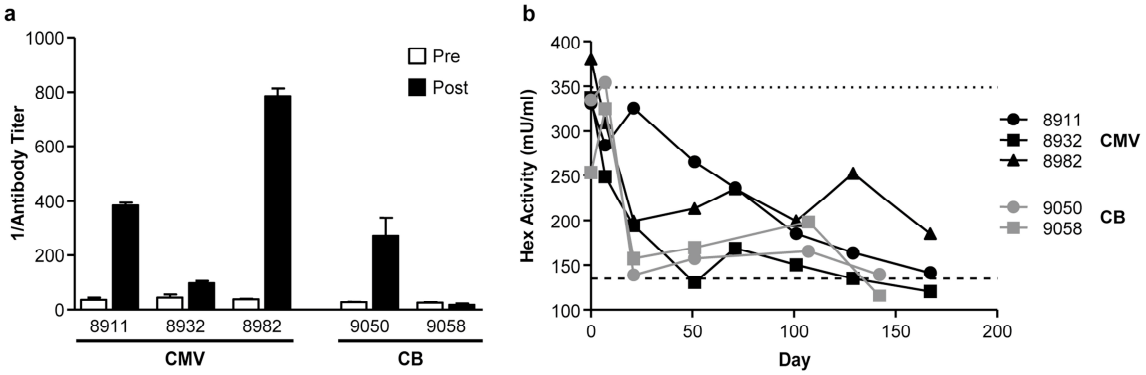

Figure 3-2. Normalization of CSF hexosaminidase activity despite a transgene-specific antibody response

CSF samples collected before vector administration and at the end of the study were tested for the presence of antibodies against IDUA by indirect ELISA (a). Titers are based on a standard curve of a serially diluted positive sample, which was arbitrarily assigned a titer of 1:1000. (b) Total Hex activity was measured in CSF using the fluorogenic substrate MUG. Normal activity (dashed line) is the mean of two heterozygous control samples. The untreated MPS I level (dotted line) is the mean of untreated controls.

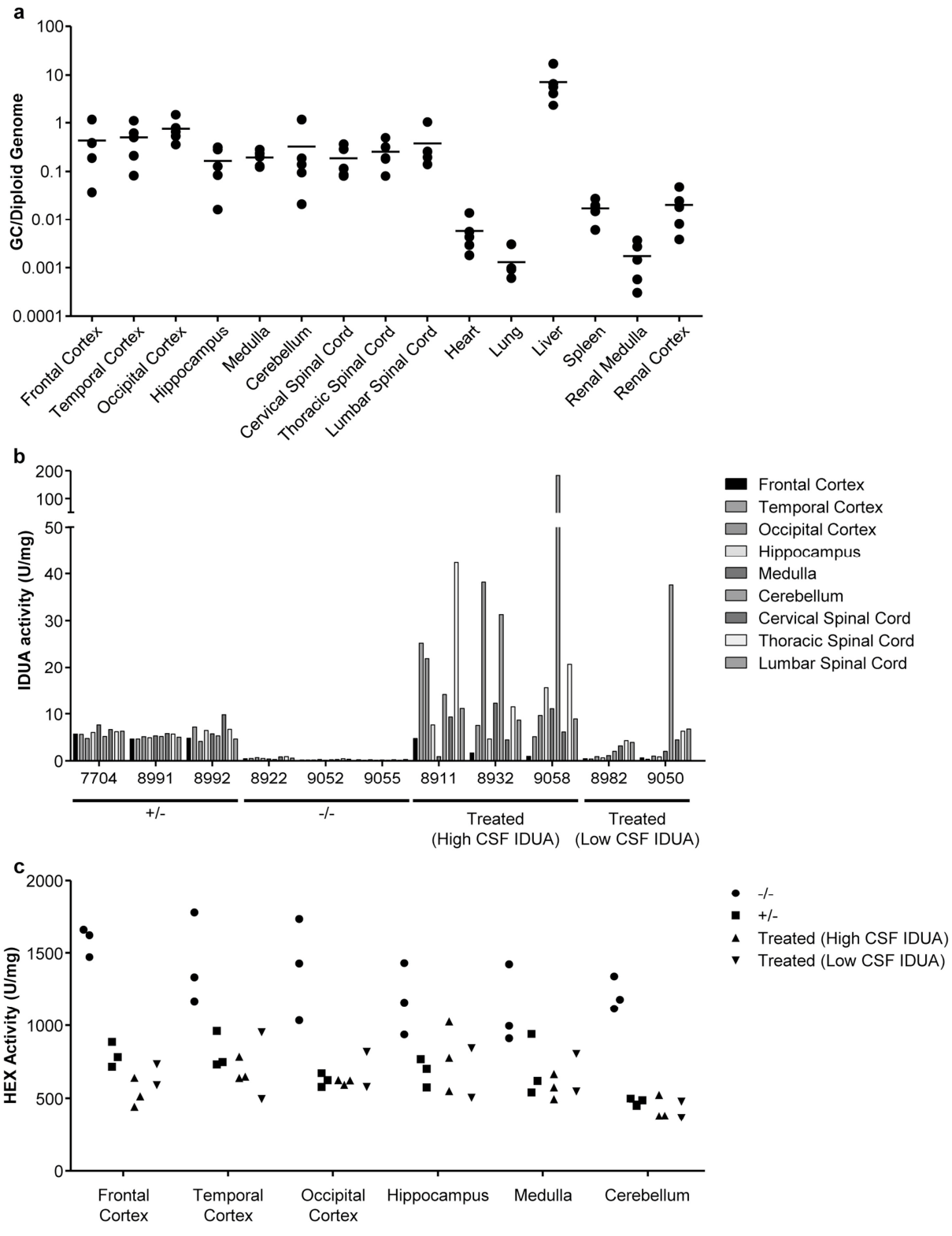
a
GC/Diploid Genome
100
10
1
0.1
0.01
0.001
0.0001
Frontal Cortex
Temporal Cortex
Occipital Cortex
Hippocampus
Medulla
Cerebellum
Cervical Spinal Cord
Thoracic Spinal Cord
Lumbar Spinal Cord
Heart
Lung
Liver
Spleen
Renal Medulla
Renal Cortex
b
IDUA activity (U/mg)
200
100
50
40
30
20
10
0
7704
8991
8992
8922
9052
9055
8911
8932
9058
8982
9050
+/-
-/-
Treated (High CSF IDUA)
Treated (Low CSF IDUA)
Frontal Cortex
Temporal Cortex
Occipital Cortex
Hippocampus
Medulla
Cerebellum
Cervical Spinal Cord
Thoracic Spinal Cord
Lumbar Spinal Cord
c
HEX Activity (U/mg)
2000
1500
1000
500
0
Frontal Cortex
Temporal Cortex
Occipital Cortex
Hippocampus
Medulla
Cerebellum
-/-
+/-
Treated (High CSF IDUA)
Treated (Low CSF IDUA)

Figure 3-3. Global CNS transduction and biochemical correction following IT gene transfer

Vector genomes were quantified in DNA extracted from CNS and peripheral tissues of treated cats by TaqMan PCR (a). Tissue samples from MPS I cats and heterozygous controls were collected from sites throughout the CNS for measurement of IDUA activity (b) and Hex activity (c). Treated animals are stratified into those with normal CSF IDUA activity (8911, 8932, 9058) and those with low CSF activity (8982, 9050). All enzyme activities are normalized to protein concentration.

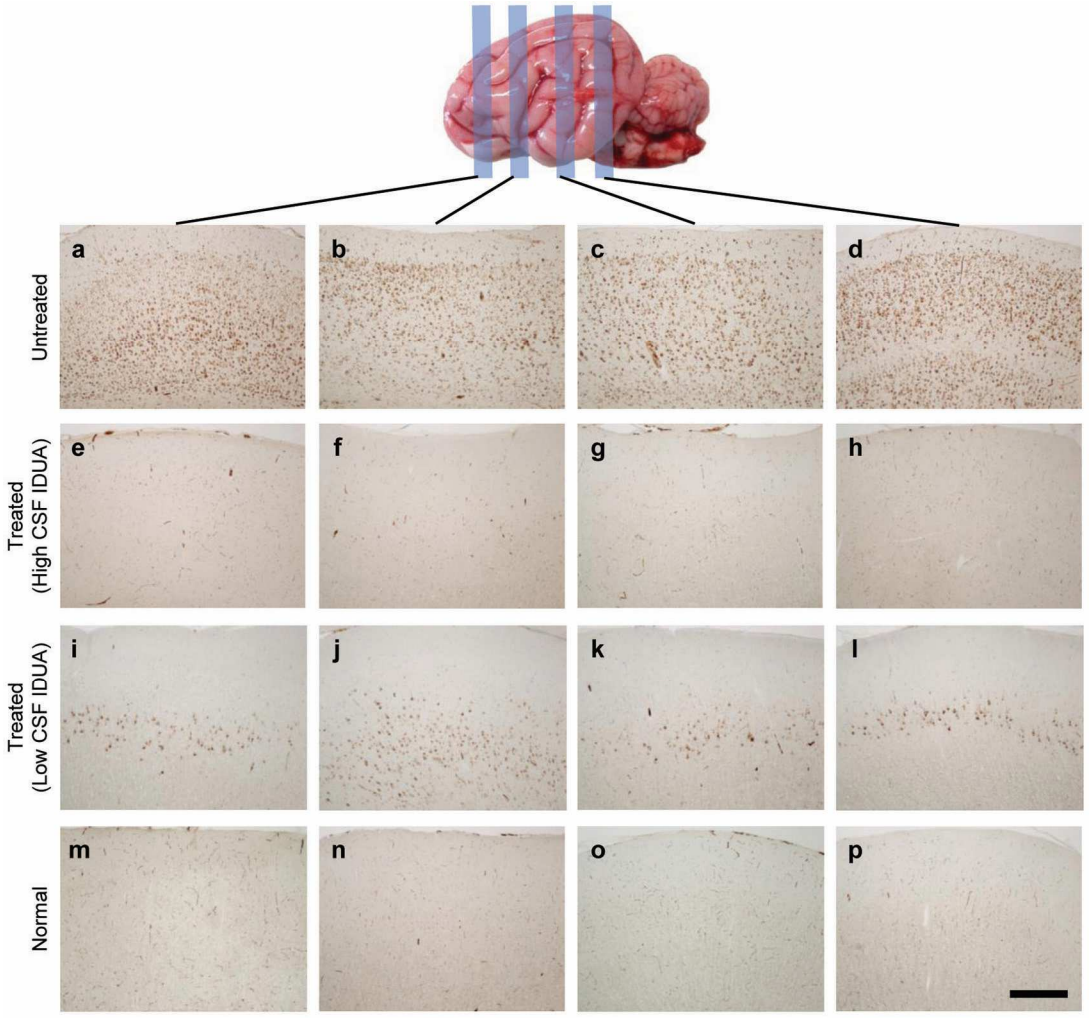

Figure 3-4. Reversal of brain ganglioside storage

Immunostaining for the ganglioside GM3 was performed on tissue sections from four brain regions in untreated MPS I cats (a-d), treated cats with high CSF IDUA activity (E-H) and low CSF activity (i-l), as well as normal controls (m-p). Scale bar = 500 μM.

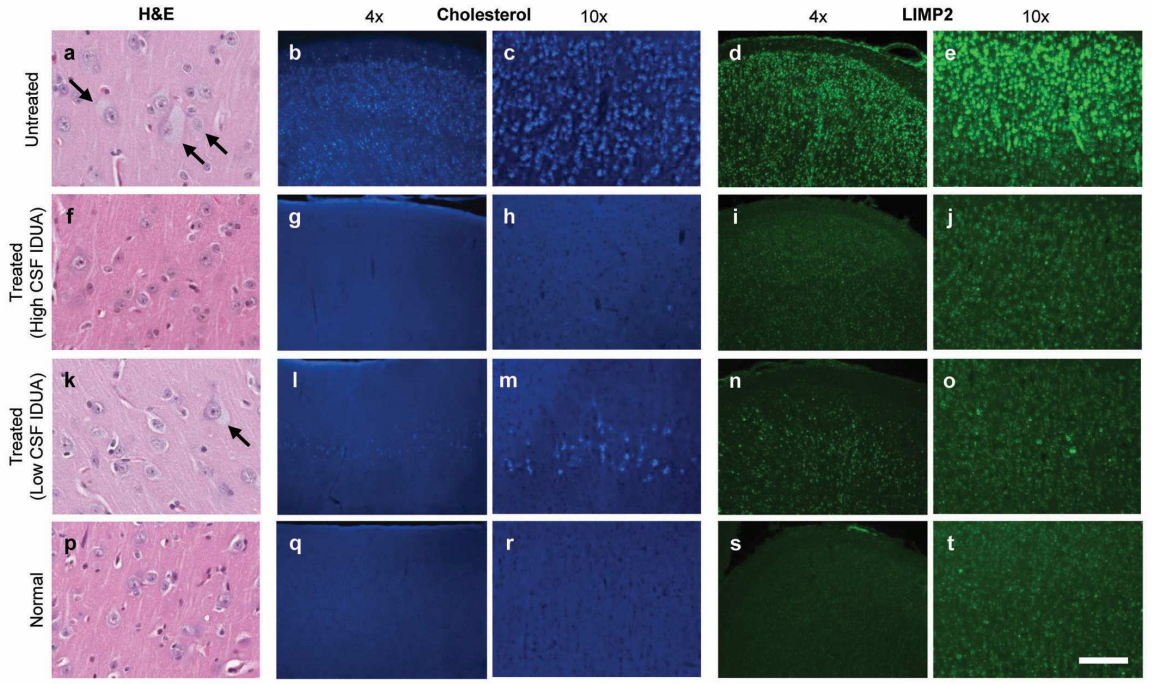

Figure 3-5. Correction of neuronal storage lesions

Sections from the cerebral cortex were stained with H&E (a, f, k, p). Arrows indicate the distended neuron cell bodies typical of MPS I. The treated cats were stratified into those with low CSF IDUA activity and those with high activity. Cholesterol accumulation was evaluated in matched brain sections by filipin staining in untreated (b,c), treated (g, h, l, m) and normal control (q, r) cats. Immunostaining for the lysosomal integral membrane protein LIMP2 was performed on corresponding sections from each animal (d, e, i, j, n, o, s, t). Scale bar = 500 μM (4x), 200 μM (10x) or 100 μM (H&E).

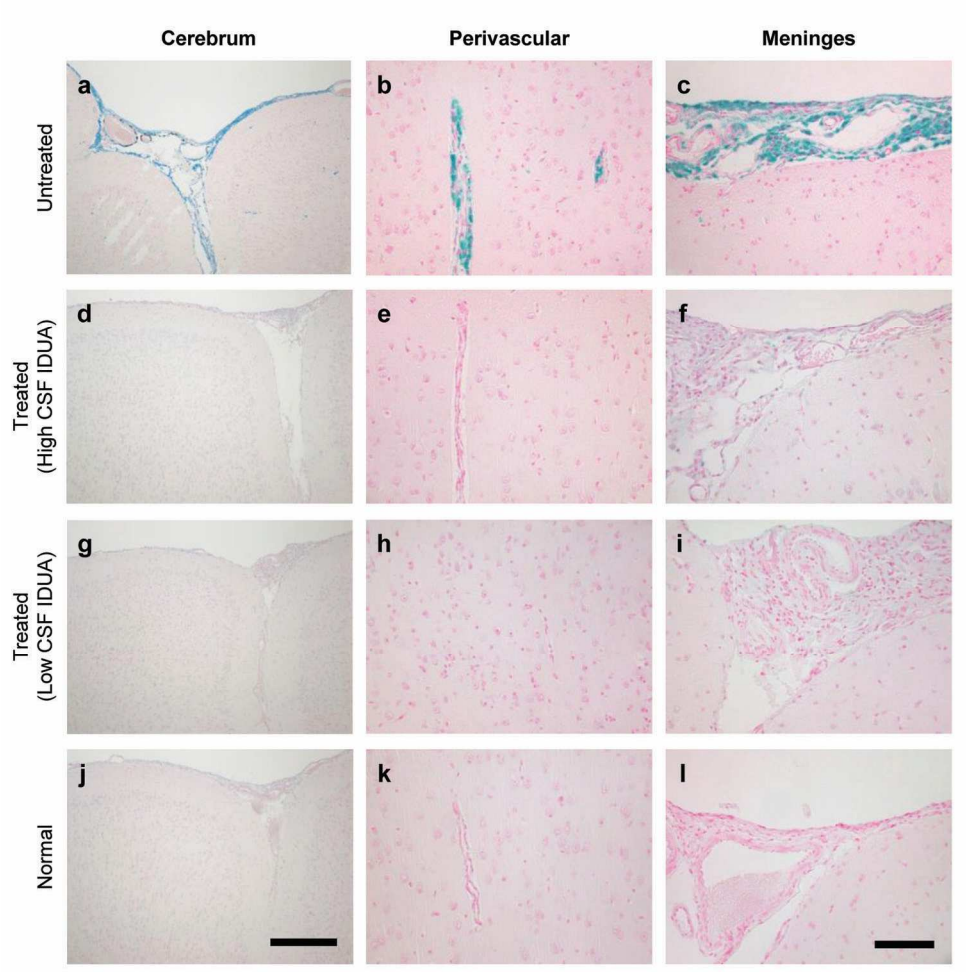

Figure 3-6. Reduced GAG storage in the cerebral vasculature and meninges

Cortical brain sections were stained for GAGs using alcian blue. Low magnification images (a,d, g, j) show the cerebral cortex with the associated meninges. High magnification images show representative cortical blood vessels (b, e, h, k) and segments of meninges (c, f, i, l). Scale bars = 500 μM (left column) and 100 μM (middle and right columns).

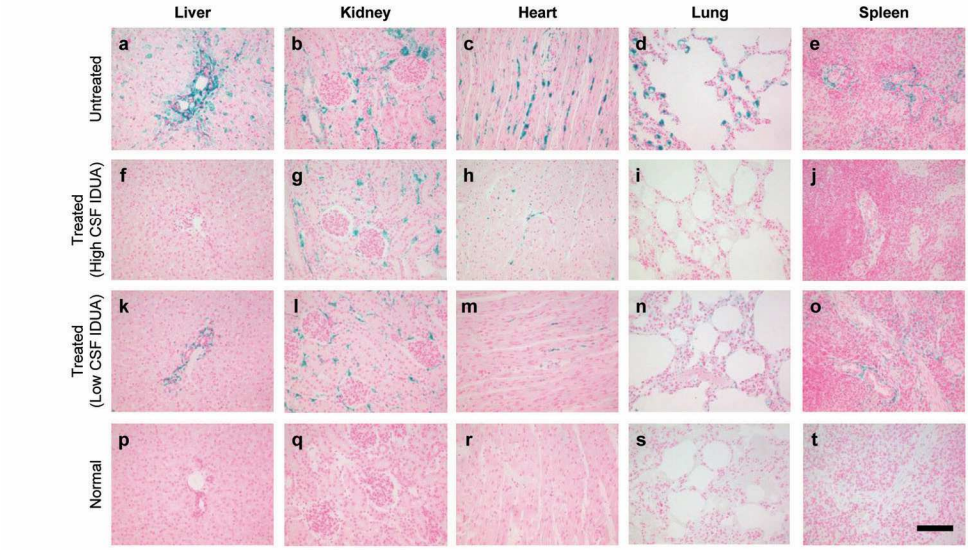

Figure 3-7. Correction of somatic lesions

Sections from heart, lung, liver, spleen and kidney were stained with Alcian blue. Animals are stratified according to antibody response and circulating enzyme activity as in Figure 6. Scale bar = 100 μM.

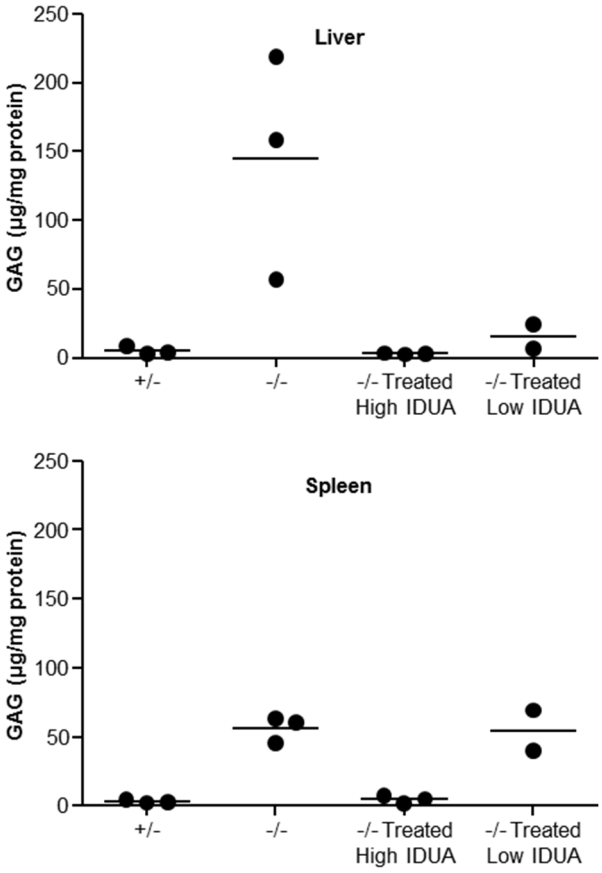

Figure 3-8. Peripheral GAG clearance following intrathecal AAV9 delivery

GAG content of liver and spleen lysates was measured by dimethylmethylene blue binding assay. Animals are stratified into those that had the highest antibody titers and the lowest circulating CSF enzyme in their treatment group (9050, 8982) and those that exhibited more stable expression (8911, 8932, 9058). Values are normalized to sample protein concentration.

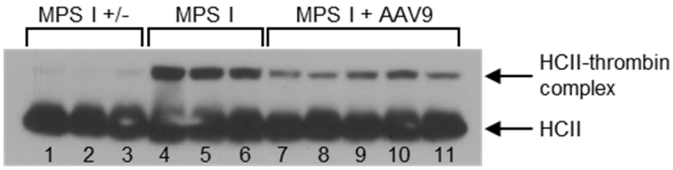

Figure 3-9. Reduced serum heparin cofactor II-thrombin complex concentration following intrathecal gene therapy

Serum concentrations of the heparin cofactor II-thrombin complex were assessed by western blot, using a polyclonal anti-human HCII antibody for detection. Lane 1-3: heterozygous controls, lane 4-6: untreated controls, lane 7: 8911, lane 8: 8932, lane 9: 8982, lane 10: 9050, lane 11: 9058.

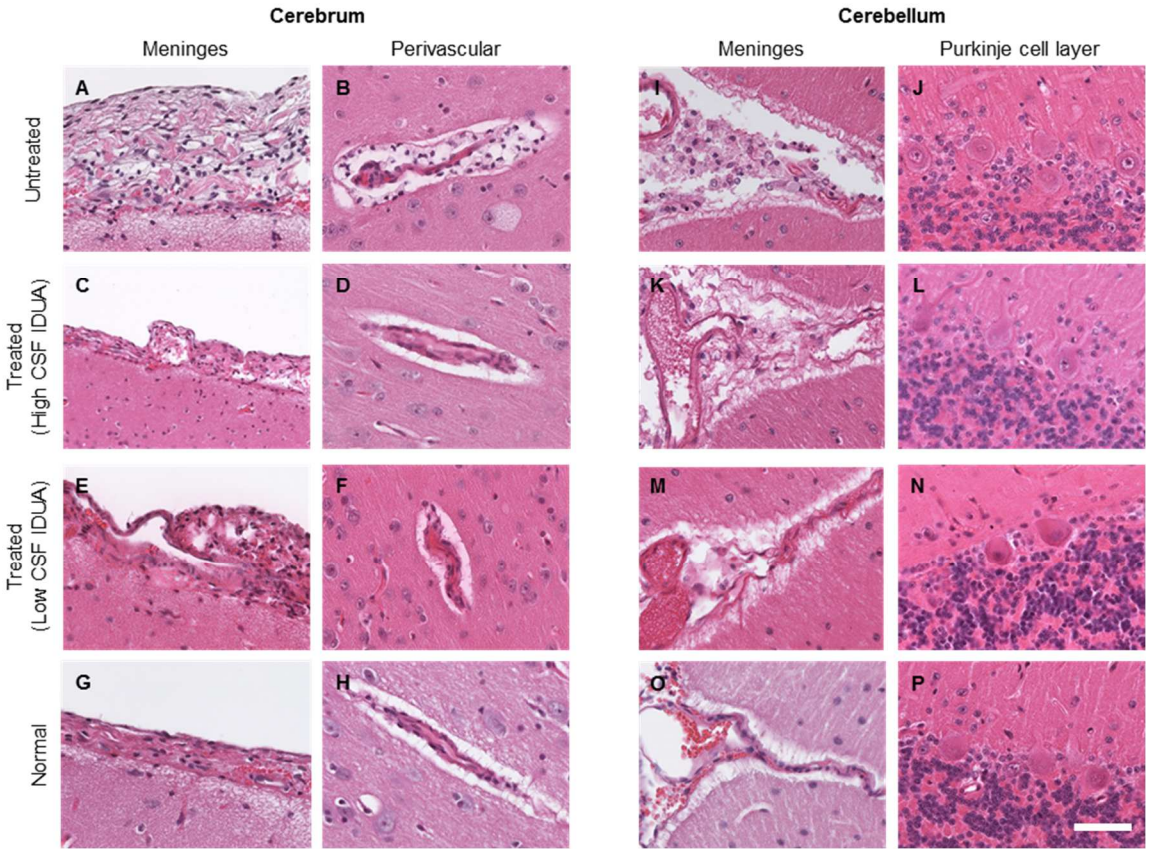

Figure 3-10. Absence of inflammation or cellular infiltration in treated animals

Tissue sections from cerebrum (A-H) and cerebellum (I-P) were stained with H&E. Images depict representative segments of meninges and blood vessels. Scale bar = 50 μM.

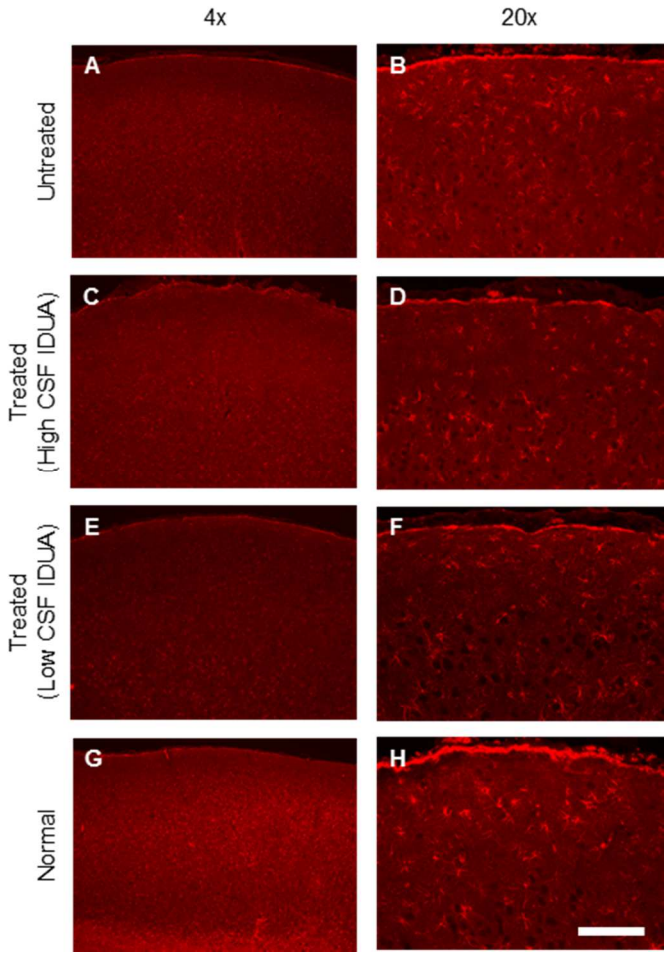

Figure 3-11. Absence of astrocyte activation in treated animals

Tissue sections from cerebral cortex were stained with an anti-GFAP antibody. Scale bars = 500 μM (low magnification) and 100 μM (high magnification).

Table 3-1. Summary of study subjects

Animal #	Genotype	Treatment	Dose	Weight at injection	Sex	Age at study end
9110	WT	Untreated	-	-	M	7 months
9115	WT	Untreated	-	-	F	7 months
7704	MPS I Het	Untreated	-	-	F	58 months
8991	MPS I Het	Untreated	-	-	F	6 months
8992	MPS I Het	Untreated	-	-	F	6 months
8922	MPS I	Untreated	-	-	F	13 months
9052	MPS I	Untreated	-	-	F	10 months
9055	MPS I	Untreated	-	-	M	10 months
8911	MPS I	AAV9-CMV-fIDUA	10^{12} GC/kg	2.43 kg	F	13 months
8932	MPS I	AAV9-CMV-fIDUA	10^{12} GC/kg	2.89 kg	M	12 months
8982	MPS I	AAV9-CMV-fIDUA	10^{12} GC/kg	1.83 kg	F	10 months
9050	MPS I	AAV9-CB-fIDUA	10^{12} GC/kg	1.14 kg	F	10 months
9058	MPS I	AAV9-CB-fIDUA	10^{12} GC/kg	1.35 kg	F	10 months

Table 3-2. CSF analysis in treated and control MPS I cats

		Nucleated Cells/µl[A]				Total Protein (mg/dL)[B]			
Animal ID	**Treatment**	**Day 21**	**51**	**77**	**101-7**	**21**	**51**	**77**	**101-7**
8911	AAV9.CMV.fIDUA	0	1	ND	2	<25	<25	ND	<25
8932	AAV9.CMV.fIDUA	1	0	ND	1	<25	26	ND	29
8982	AAV9.CMV.fIDUA	1	1	ND	1	<25	<25	ND	33
9050	AAV9.CB7.fIDUA	ND	1	1	1	ND	29	<25	26
9058	AAV9.CB7.fIDUA	ND	0	1	3	ND	30	29	25
8922	Untreated	0	1	ND	1	<25	<25	ND	27
9052	Untreated	ND	0	0	1	ND	<25	<25	<25
9055	Untreated	ND	0	1	1	ND	26	28	41

A. Normal range ≤ 2 cells / µl

B. Normal range ≤ 25 mg/dL

Table 3-3. Quantification of histopathology and GM3, LIMP2, filipin and GFAP positive cells per field in matched brain sections[A]

Animal ID	Treatment	Genotype	GM3	H&E[B]	LIMP2	Filipin	GFAP
9110	Untreated	WT	2.6 ± 1.9	0.4 ± 0.5	0.2 ± 0.4	3.5 ± 2	17.7 ± 8.1
9115	Untreated	WT	8.4 ± 7.3	0.8 ± 0.8	0.2 ± 0.4	3.8 ± 2.4	11.1 ± 8.2
7704	Untreated	MPS I Het	0.2 ± 0.45	0.2 ± 0.4	13.4 ± 3.2	0 ± 0	19.3 ± 7.4
8992	Untreated	MPS I Het	0.8 ± 0.84	0.2 ± 0.4	6.1 ± 3.8	0 ± 0	20.7 ± 6.6
8991	Untreated	MPS I Het	7.2 ± 6.0	0.6 ± 0.9	14.1 ± 4.5	0 ± 0	11.9 ± 2.9
8922	Untreated	MPS I	380.4 ± 88.8	9.4 ± 3.6	85.2 ± 6.2	274.6 ± 54.7	29.4 ±5.7
9052	Untreated	MPS I	239 ± 89.13	8.2 ± 2.4	75.8 ± 7.9	271.8 ± 82.9	28.8 ± 12.6
9055	Untreated	MPS I	272.2 ± 66.2	5.4 ± 4.7	80 ± 7.6	169.2 ± 23.4	25 ± 7.1
8911	AAV9.CMV.fIDUA	MPS I	7.2 ± 3.83	0.6 ± 0.9	16.3 ± 5.5	5.2 ± 4.3	18.6 ± 6.8
8932	AAV9.CMV.fIDUA	MPS I	8 ± 6.48	0.6 ± 0.5	11.4 ± 6.7	0.6 ± 1.3	23.3 ± 6.9
8982	AAV9.CMV.fIDUA	MPS I	46.8 ± 10.75	1 ± 1	34.7 ± 21.7	52 ± 12.4	25.1 ± 5.8
9050	AAV9.CB.fIDUA	MPS I	24 ± 15.95	1.8 ± 0.8	9.2 ± 6.7	38 ± 26.5	16.4 ± 5.9
9058	AAV9.CB.fIDUA	MPS I	14 ± 5.43	0.4 ± 0.5	2.6 ± 1.2	0 ± 0	17.1 ± 7.1

A. Cells staining positive for the indicated marker were quantified in 5 fields (GM3, Filipin, H&E) or 20 fields (LIMP2 and GFAP) from matched brain regions. Quantification is per 20x field for GFAP, LIMP2, and H&E, 10x field for filipin, and 4x field for GM3.

B. Indicates number of cells exhibiting distended, asymmetric pale cytoplasm characteristic of neuronal storage

CHAPTER 4: Neonatal systemic AAV induces tolerance to CNS gene therapy in MPS I dogs and nonhuman primates

---

Chapter 4 is adapted from: C. Hinderer, P. Bell, J. P. Louboutin, Y. Zhu, H. Yu, G. Lin, R. Choa, B. L. Gurda, J. Bagel, P. O'Donnell, T. Sikora, T. Ruane, P. Wang, A. F. Tarantal, M. L. Casal, M. E. Haskins, J. M. Wilson. *Molecular therapy* (2015).

Abstract

The potential host immune response to a non-self protein poses a fundamental challenge for gene therapies targeting recessive diseases. We demonstrate in both dogs and nonhuman primates that liver directed gene transfer using an adeno-associated virus (AAV) vector in neonates induces a persistent state of immunological tolerance to the transgene, substantially improving the efficacy of subsequent vector administration targeting the central nervous system (CNS). We applied this approach to a canine model of mucopolysaccharidosis type I (MPS I), a progressive neuropathic lysosomal storage disease caused by deficient activity of the enzyme α-l-iduronidase (IDUA). MPS I dogs treated systemically in the first week of life with a vector expressing canine IDUA did not develop antibodies against the enzyme and exhibited robust expression in the CNS upon intrathecal AAV delivery at one month of age, resulting in complete correction of brain storage lesions. Newborn rhesus monkeys treated systemically with AAV vector expressing human IDUA developed tolerance to the transgene, resulting in high CSF IDUA expression and no antibody induction after subsequent CNS gene therapy. These findings suggest that inducing tolerance to the transgene during a critical period in immunological development will improve the efficacy and safety of gene therapy.

Introduction

The lysosomal storage diseases (LSDs) are a broad class of inherited disorders caused by deficient activity of enzymes involved in the lysosomal catabolism of ubiquitous polysaccharides, glycoproteins, and lipids, leading to intracellular accumulation of these undegraded enzyme substrates and multi-organ pathology. LSDs are excellent targets for gene therapy because many of the associated lysosomal enzymes can be secreted by genetically corrected cells and endocytosed by neighboring

cells, allowing for widespread cross-correction even with modest gene transfer efficiency (Dahms, Lobel, and Kornfeld 1989, Sando and Neufeld 1977). Gene therapy may play a particularly important role in treating the central nervous system (CNS) manifestations associated with LSDs, because the CNS cannot be effectively targeted by intravenous (IV) delivery of the deficient enzymes, and chronic direct CNS administration is impractical as a long-term therapy. One LSD in which gene therapy has shown particular promise for treating CNS disease is mucopolysaccharidosis type I (MPS I), which is caused by deficient activity of the lysosomal enzyme α-l-iduronidase (IDUA). Currently, the only treatment capable of curbing the severe cognitive decline experienced by many MPS I patients is hematopoietic stem cell transplantation, which is associated with substantial morbidity and mortality (Aldenboven, Boelens, and de Koning 2008, Boelens et al. 2007, Clarke et al. 2009, Langford-Smith et al. 2011, Sifuentes et al. 2007, Souillet et al. 2003, Whitley et al. 1993). Using a naturally occurring cat model of MPS I, we found that a minimally invasive intrathecal injection of an AAV serotype 9 vector into the cerebrospinal fluid (CSF) achieved widespread gene transfer in the brain and sufficient secretion of the therapeutic enzyme into the CSF to correct storage pathology throughout the CNS (Hinderer, Bell, et al. 2014a). Intrathecal AAV delivery could, therefore, represent a vast improvement over the current standard of care for CNS disease in MPS I patients.

Despite the promise of intrathecal AAV delivery for MPS I, we found that the efficacy of gene transfer was diminished in some MPS I cats due to development of antibodies to IDUA, resulting in reduced circulating enzyme in the CSF and less efficient correction of storage lesions. Here we report that MPS I dogs, another naturally occurring disease model, also develop antibodies to the normal canine enzyme following

intrathecal gene therapy leading to less efficient correction of brain lesions. These findings reflect the clinical experience with enzyme replacement therapy in MPS I, as patients treated with recombinant IDUA almost universally develop antibodies to the enzyme, which correlate with a poor response to therapy (Wraith et al. 2007, Langereis et al. 2014).

With the goal of developing a safe and effective method for the prevention of anti-transgene immune responses, we explored the possibility of exploiting the normal processes by which the immune system learns to distinguish self from non-self. Decades of evidence from transplantation studies suggest that neonatal rodents and humans, unlike adults, are prone to develop tolerance rather than immunity to alloantigens (Fan et al. 2004, McCarthy and Bach 1983, Billingham, Brent, and Medawar 1953). While this phenomenon has often been ascribed to an immature and poorly functional immune system, it has since become clear that neonates are indeed capable of eliciting functional immune responses, albeit with higher activation thresholds (Adkins 1999). The development of tolerance to neoantigens in newborns is instead an active process involving peripheral anergy and deletion of reactive T and B cells, as well as induction of regulatory T cells (Fan et al. 2004, McCarthy and Bach 1983, Wang et al. 2010). One recent report demonstrated that this phenomenon could be exploited to induce durable tolerance to factor VIII in hemophilic mice by performing gene transfer in neonates (Hu et al. 2011). While this effect in mice could be attributed to the relative immaturity of the murine immune system at birth, evidence for neonatal tolerance to a foreign transgene has also emerged in studies using retroviral vectors in newborn dogs (Traas et al. 2007, Xu et al. 2007). These experiments demonstrated sustained expression of relatively immunogenic transgenes after neonatal retroviral vector administration, although the

ineffectiveness of these vectors in adults precluded direct comparison of immune responses to the transgene in animals of different ages.

In this study, we evaluated the potential for neonatal AAV-mediated systemic expression of a therapeutic protein to induce immunological tolerance that could subsequently allow for safe and effective CNS directed gene therapy. We found that MPS I dogs treated intravenously in the first week of life with an AAV vector expressing canine IDUA from a liver specific promoter did not develop antibodies to the transgene, and following subsequent intrathecal gene transfer at one month of age exhibited 3- to 100-fold higher IDUA levels in CSF than naïve dogs, with complete resolution of brain storage lesions. Likewise, rhesus monkeys administered liver-directed human *IDUA* gene transfer at birth exhibited tolerance to the protein, allowing for robust CSF IDUA expression without antibody induction after intrathecal AAV injection one month later. These findings suggest a potential approach to prevent immune responses to a non-self transgene through neonatal gene transfer, which could significantly improve the efficacy of gene therapy for many recessive diseases.

Materials and Methods

Vector production

The AAV8 vectors contained codon optimized canine or human IDUA cDNA downstream of the thyroid hormone binding globulin promoter. The AAV9 vector contained the chicken beta actin promoter with a cytomegalovirus immediate early enhancer. Both vectors included the rabbit beta-globin polyadenylation sequence. Vectors were produced by triple transfection of 293 cells and purified on iodixanol gradients as previously described (Wang et al. 2011).

MPS I dogs

The MPS I dog colony was maintained at the University Of Pennsylvania School Of Veterinary Medicine under NIH and USDA guidelines for the care and use of animals in research. All MPS I dog study protocols were approved by the University of Pennsylvania Institutional Animal Care and Use Committee. For vector injections in neonatal MPS I dogs, the AAV8 vector was diluted in 0.5-1 mL of sterile saline, and injected via the jugular vein. Intrathecal injections of AAV9 vectors and CSF collection were performed via the suboccipital approach as previously described (Hinderer, Bell, et al. 2014a). A total of 9 MPS I dogs were included in this study. Genotype was confirmed at birth by PCR and serum enzyme assay. Six dogs were administered an IV injection of the AAV serotype 8 vector (5×10^{12} genome copies per kilogram [GC/kg] body weight) on either the first (N=3) or seventh (N=3) day of life. One animal died on postnatal day 3. The remaining 5 treated animals as well as 3 naïve MPS I dogs were treated with intrathecal AAV9 (10^{12} GC/kg) at one month of age. Blood was collected from a peripheral vessel weekly for the first seven weeks of life then monthly thereafter. CSF (1 mL) was collected at the time of intrathecal vector injection (one month of age), on days 7 and 21 after injection, and monthly thereafter. Euthanasia was performed by administration of sodium pentobarbital (80 mg/kg IV). Five animals (I-549, I-550, I-552, I-553, I-554) were euthanized at 9 months of age; 3 (I-562, I-563, I-564) were euthanized at 11 months of age. Untreated MPS I and controls were euthanized between 6 and 26 months of age (Table 1). Tissues were collected and processed as previously described (Hinderer, Bell, et al. 2014a).

Rhesus Monkeys

All animal procedures conformed to the requirements of the Animal Welfare Act and protocols were approved prior to implementation by the Institutional Animal Care and Use Committee at the University of California, Davis. Activities related to animal care were performed as per California National Primate Research Center standard operating procedures. Normally cycling, adult female rhesus monkeys (*Macaca mulatta*; N=4) with a history of prior pregnancy were bred and identified as pregnant, using established methods (Tarantal 2005). All dams selected for the study were pre-screened to ensure they were seronegative for AAV antibodies. Fetuses were monitored sonographically during gestation to confirm normal growth and development (Tarantal 2005) and newborns were delivered by cesarean section at term (160±2 days gestation) according to established protocols (Tarantal et al. 2005). Newborns were placed in incubators post-delivery and nursery-reared for the study. Infant health, food intake, and body weights were recorded daily or weekly (dependent on age) in the nursery according to established protocols. At birth all animals were administered the selected AAV vector IV. At one month postnatal age and at subsequent monthly time points (up to 2 months post-transfer, to date) infants were sedated with ketamine (10 mg/kg intramuscularly, IM) and dexmedetomidine (0.015-0.075 mg/kg IM) in preparation for collection of CSF (~0.5 ml; pre-injection then weekly or monthly) and for intrathecal injection via the suboccipital approach (~ 0.5 ml volume; 1 month and immediately after collection of CSF), all under aseptic conditions. Blood samples were collected at birth then monthly from a peripheral vessel (~ 3-6 ml) to monitor CBCs and clinical chemistry panels, and for collection of serum and plasma. The reversal atipamezole was given IM at a comparable dose to dexmedetomidine when sample collection was completed.

Vector Biodistribution

DNA was isolated from tissues and vector genomes quantified by TaqMan PCR as described (Wang et al. 2011).

Enzyme activity assays

Assays for IDUA and Hex activity were performed as described (Hinderer, Bell, et al. 2014a).

CSF pGAG measurement

CSF pGAG measurement was performed by the Glycotechnology Core at the University of California, San Diego using previously described methods (Lawrence et al. 2012). Briefly, GAG was extracted from CSF samples and digested to disaccharides with heparinase I, II, and III. Disaccharides were tagged with aniline ^{12}C by reductive coupling and dried by speed vac. Dried samples were reconstituted in LC-MS grade water and spiked with a known concentration of ^{12}C-aniline tagged standard. Samples were analyzed on a LTQ Orbitrap Discovery electrospray ionization mass spectrometer (Thermo Scientific) equipped with Thermo Scientific Ultimate 3000 HPLC system.

ELISA

The ELISA for antibodies to canine IDUA was performed as described (Hinderer, Bell, et al. 2014a), except that the expression construct contained the canine cDNA under the control of the thyroid hormone binding globulin promoter, and the cIDUA protein was produced in Huh7 cells. The detection antibody used was HRP-conjugated sheep anti-canine (Pierce, Rockford, IL). The assay for antibodies to human IDUA in rhesus monkeys was identical, except that Aldurazyme (Genzyme, Cambridge, MA) 10 µg/mL,

was used for coating antigen and the detection antibody was polyclonal goat anti-human (Jackson ImmunoResearch Laboratories, West Grove, PA).

Histology

Histological analysis of MPS I dog brains was performed as previously described (Hinderer, Bell, et al. 2014a) with the following modifications for quantifying neurons positive for GM3, cholesterol, and LIMP2 storage: Images of LIMP2- and filipin-stained sections of cerebral cortex were taken with a 10x objective such that the border between layer I (molecular layer) and layer II formed the upper border of the image. A total of 10 images were acquired from each animal. Images of GM3-stained brain sections were taken with a 4x objective from the area directly below the cerebral cortex surface including the cerebral molecular layer. Seven images from each animal were analyzed. All images were processed with ImageJ software (Rasband W. S., National Institutes of Health, USA; http://rsb.info.nih.gov/ij/) using the “Threshold” and “Analyze particles” modules as described previously (3).

Results

Antibody Induction to Canine IDUA after Intrathecal AAV9-mediated Gene Transfer in MPS I Dogs

The canine model of MPS I faithfully recapitulates many of the manifestations of the human disease (Kakkis, McEntee, et al. 2004, Shull et al. 1984). These animals have no detectable IDUA activity due to a splice site mutation that results in retention of the first intron of *IDUA* (Menon, Tieu, and Neufeld 1992). Given the absence of detectable IDUA expression in these animals, we anticipate that they will model the immune response to intrathecal gene therapy that would occur in patients with the

severe form of MPS I, as these individuals generally carry alleles that produce no full length IDUA, leaving them immunologically naïve to the protein (Terlato and Cox 2003). The brains of MPS I dogs show the characteristic pathology associated with MPS I, including widespread storage of gangliosides such as GM3 in neurons, as well as abnormal accumulation of cholesterol and lysosomal membrane proteins including LIMP2 (Shull et al. 1984). MPS I dogs also exhibit prominent storage of glycosaminoglycans (GAGs) in the meninges, resulting in significant meningeal thickening, a process which contributes to spinal cord compression in some MPS I patients (Kachur and Del Maestro 2000, Taccone et al. 1993, Vijay and Wraith 2005).

We initially treated 3 dogs at one month of age with an intrathecal injection of an AAV9 vector carrying the canine IDUA sequence under the control of a ubiquitous promoter (Table 4-1). The injection was well tolerated in all animals; no clinical signs were observed throughout the study. CSF analyses were generally unremarkable, with only a mild transient elevation of CSF lymphocytes occurring in 2 animals (Table 4-2). A single CSF sample in one animal showed a marked pleocytosis consisting primarily of monocytoid cells. A subsequent tap showed no evidence of pleocytosis, and at the time of euthanasia, there was no histological evidence of inflammation in the brain or spinal cord of any treated animal.

The vector was distributed throughout the CNS, transducing cells in all analyzed regions of the brain and spinal cord (Table 4-3). All animals exhibited supraphysiologic expression of IDUA in CSF, which declined to the normal range in one animal (I-550) and to below normal levels in two animals (I-553 and I-554), after which CSF enzyme levels were essentially stable for 5 months until the animals were euthanized (Fig. 4-1a). The absence of clinical signs, vector genome loss, or histological evidence of

encephalitis indicated that the decline in CSF IDUA activity was not due to killing of transduced cells by cytotoxic T lymphocytes, which was also supported by persistent residual CSF IDUA activity. Instead, the decline in CSF IDUA activity was associated with the induction of high titer antibodies against canine IDUA in CSF (Fig. 4-1b).

Induction of Tolerance to IDUA by Neonatal Gene Transfer

To determine whether neonatal expression of canine IDUA could induce immune tolerance to the enzyme in MPS I dogs, we treated 6 animals with an IV injection of an AAV serotype 8 vector expressing canine IDUA from a liver selective promoter on either the first (N=3) or the seventh (N=3) day after birth (Table 4-1). One of the dogs treated on postnatal day one died two days after treatment. Overall survival of neonates was similar to historical data for untreated MPS I dogs, which have approximately 20% mortality in the first two weeks of life (Traas et al. 2007). The cause of this early mortality in MPS I dogs has not been determined; in this treated animal postmortem examination showed systemic lesions typical of MPS I as well as possible evidence of a systemic bacterial infection. Treated animals demonstrated an elevation in serum IDUA followed by a rapid decline (Fig. 4-5). This is consistent with observations of transient expression due to vector genome loss during hepatocyte division in previous studies utilizing non-integrating vectors for hepatic gene transfer in newborns (Wang et al. 2012).

At one month of age, the five surviving dogs that received IV AAV8 in the first week of life were given an injection of an AAV9 vector using an intrathecal approach. All 5 animals exhibited greater than 30-fold normal peak levels of IDUA in CSF following intrathecal vector injection, with long term CSF enzyme levels 3- to 100-fold higher than those achieved in naïve animals (Fig. 4-1a). Antibodies to canine IDUA in the CSF were reduced nearly 100-fold compared to the animals treated with IT AAV9 alone, with

undetectable CSF antibodies in the dogs treated on postnatal day 1, and low but detectable responses in the animals treated on postnatal day 7 (Fig. 4-1b). All animals treated as neonates exhibited no detectable serum antibodies against canine IDUA, whereas the animals treated with IT AAV9 alone at one month of age had elevated serum anti-cIDUA titers (Fig. 4-1c).

Induction of tolerance to canine IDUA in neonates is not due to hepatic expression

Previous studies in both mice and dogs have demonstrated tolerance induction to foreign proteins through AAV-mediated hepatic expression(LoDuca, Hoffman, and Herzog 2009, Crudele et al. 2015, Finn et al. 2010, Sun et al. 2010). To determine whether immune tolerance in the animals treated with intravenous AAV8 as neonates was due to liver targeted expression rather than the age of the animal at the time of treatment, we treated 4 MPS I dogs at 3 months of age with an intravenous injection of the AAV8 vector expressing canine IDUA from a liver specific promoter. All 4 animals developed serum antibodies against the transgene product (Fig. 4-1c). This indicates that the lack of antibody response to IDUA in the neonatal gene transfer cohort is related to the age of the animal at the time of exposure to the transgene product, rather than the presence of hepatic expression.

Correction of Biochemical and Histological Abnormalities in the CNS of MPS I Dogs

The lysosomal enzyme hexosaminidase (Hex) is upregulated in tissues of MPS I animals, and the elevated Hex activity in both brain tissue and CSF serves as a useful marker for the aberrant cellular processes occurring downstream of IDUA deficiency (Hinderer, Bell, et al. 2014c). Measurement of CSF Hex activity at the time of intrathecal vector delivery (~1 month postnatal) revealed abnormally elevated Hex activity in all

MPS I dogs (Fig. 4-2a). The animals treated with intrathecal AAV9 alone exhibited modest reductions in CSF Hex activity, with only the animal with the highest residual IDUA expression (I-550) reaching the normal range. All 5 animals treated with neonatal systemic gene transfer followed by intrathecal vector administration demonstrated complete normalization of CSF Hex. Hex activity in brain tissue samples showed a greater response to therapy than CSF Hex, with substantial reductions in brain Hex activity in all treated animals, although the effect was slightly diminished in the two intrathecal-only treated animals with the lowest CSF IDUA levels (Fig. 4-2b).

GAG concentrations in CSF were measured using an assay specific for the non-reducing end of the pathologic GAGs (pGAG) that accumulate due to IDUA deficiency (Fig. 4-2c) (Lawrence et al. 2012). All animals exhibited a marked reduction in CSF pGAG concentration 3 weeks after intrathecal AAV injection. This reduction was sustained at day 112, although the dogs that were not immune tolerant to IDUA maintained higher residual CSF pGAG than immune tolerant dogs.

Histological analysis revealed severe storage lesions throughout the brains of untreated MPS I dogs, with widespread neuronal accumulation of GM3, cholesterol, and LIMP2 (Fig. 4-3). The animals treated with intrathecal AAV9 alone demonstrated substantial improvements in storage lesions, although only the animal with the highest CSF IDUA (I-550) experienced complete resolution of neuronal storage. The other two intrathecal-treated dogs had residual storage lesions. CNS storage lesions were completely reversed in all 5 dogs treated with neonatal AAV8 systemic gene transfer followed by intrathecal AAV9 administration.

In addition to the storage lesions in the brain parenchyma, untreated MPS I dogs showed accumulation of GAGs in meninges visible by Alcian blue stain (Fig. 4-3). This meningeal GAG accumulation and the resulting thickening of the meninges is implicated in many cases of spinal cord compression requiring surgical intervention, and also likely contributes to the development of communicating hydrocephalus in some MPS I patients by interfering with normal routes of CSF resorption. All treated animals showed evidence of improvement in meningeal GAG storage. While the meninges appeared almost completely normal in all tolerant dogs and one nontolerant dog, the two nontolerant animals with the lowest CSF IDUA activity retained some meningeal GAG storage.

Induction of Tolerance to Human IDUA in Newborn Rhesus Macaques

To assess whether the neonatal window for immune tolerance induction that was observed in MPS I dogs could also be found in primates, a similar study was performed in newborn rhesus monkeys (N=4). Because these animals are not IDUA deficient, the human IDUA transgene was used to model the immune response that might be expected against a species-specific transgene in a patient lacking the endogenous protein. Two newborn rhesus monkeys were administered AAV8 vector expressing human IDUA from a liver specific promoter IV at birth. Both demonstrated a brief increase in serum IDUA activity (Fig. 4-6). Two additional newborns were administered an AAV8 vector expressing an irrelevant transgene (human factor IX) IV at birth. All four animals were administered AAV9 vector expressing human IDUA at one-month postnatal age by intrathecal injection. Similar to the MPS I dogs, the IDUA naïve animals exhibited declining CSF IDUA activity 3 weeks after injection, with a return to near baseline levels by 2 months post-administration (Fig. 4-4a). These animals also developed transgene specific antibodies in the CSF (Fig. 4-4b). The two animals

administered IDUA gene transfer IV at birth did not develop antibodies to human IDUA in CSF (Fig. 4-4b), and maintained CSF enzyme activity greater than 10-fold normal (Fig. 4-4a) two months after intrathecal AAV9 administration. Unlike the kinetics of CSF IDUA expression observed in dogs, CSF IDUA activity continued to increase 60 days after IT vector administration, although overall expression was lower in NHP as previously described(Nietupski et al. 2011). The animals developed neutralizing antibodies to the vector capsids following both the IV administration at birth and the subsequent IT injection (Table 4-2). All animals remained robust and healthy during the study period with no evidence of adverse effects, normal growth trajectories, and complete blood counts (CBCs) and chemistry panels within normal limits based on age and when compared to historical controls.

Discussion

Immune activation to a wild type therapeutic protein is a potential obstacle to the successful treatment of any recessive disease. Antibody responses to protein replacement therapy have been particularly challenging for some LSDs, as antibodies can interfere with the distribution and uptake of the intravenously delivered enzyme (Langereis et al. 2014). Antibodies may be equally problematic for gene therapies targeting these disorders, as they can interfere with cross-correction mediated by enzyme secreted from transduced cells.

In this study we demonstrated that intrathecal AAV9 delivery can effectively target cells throughout the CNS in dogs and achieve sufficient expression to correct the biochemical and histological abnormalities associated with MPS I in the brain of a large animal. Previous work has demonstrated that even doses of intrathecal AAV9 much

greater than those employed in this study result in transduction of a small fraction of cells in the canine brain, suggesting that the widespread reduction in storage pathology observed was due to cross-correction by secreted enzyme (Haurigot et al. 2013). However, of the three animals treated with intrathecal vector alone, two developed sufficiently robust anti-transgene antibody responses to prevent complete resolution of CNS storage lesions. Only the animal that maintained near-normal CSF IDUA activity after antibody induction to the transgene demonstrated a complete response to CNS gene therapy. From this outcome, we conclude that IDUA activity in CSF is a reasonable predictor of efficacy following intrathecal gene transfer, with approximately normal levels required for full therapeutic benefit. This is consistent with our findings with intrathecal gene therapy in MPS I cats(Hinderer, Bell, et al. 2014c). MPS I cats generally exhibited weaker antibody responses to intrathecal gene transfer and more stable CSF IDUA activity than MPS I dogs. This may relate to the underlying mutation in the two models, as MPS I cats express an inactive mutant IDUA, potentially rendering them partially immunologically tolerant to the enzyme. Importantly, the present data in MPS I dogs indicate that even for MPS I patients with severe disease who, like the dogs, have no residual IDUA expression, the anti-transgene antibody response that may occur after intrathecal gene transfer does not result in adverse clinical events, and substantial efficacy is retained despite the antibody response. However, these data also suggest that preventing antibody responses against IDUA in the CNS could improve the efficacy of intrathecal gene therapy for MPS I.

Using liver-directed gene transfer, we tested the effect of early exposure to IDUA on subsequent immune responses following intrathecal gene therapy. Neonatal IDUA expression induced tolerance to the enzyme in MPS I dogs, which markedly increased

CSF enzyme levels achieved with intrathecal gene therapy at one month of age. The high CSF IDUA levels in the immune tolerant group consistently resulted in complete reversal of neuropathology, providing a strong example of the efficacy that is possible with intrathecal gene therapy for LSDs when interfering antibody responses are overcome. The finding that this neonatal window for induction of immune tolerance to a transgene also exists in nonhuman primates appears promising for translation to the clinic. Interestingly, neutralizing antibodies were elicited against the vector capsid in newborn NHPs, demonstrating that while neonates may be relatively tolerant to foreign proteins, they are fully capable of eliciting functional immune responses to pathogens. This finding has important clinical implications; while neonatal gene transfer may provide a method to circumvent immunity to the transgene, it does not provide a means of avoiding the antibody response to the AAV capsid. Thus vector readministration—a likely necessity in the setting of a life-saving gene therapy administered to a newborn—will depend on the development of alternative serotypes or other methods to evade capsid antibodies. In the case of intrathecal AAV delivery, readministration may be possible due to the remarkable insensitivity of this approach to pre-existing capsid antibodies (Haurigot et al. 2013).

Previous studies in mice, cats, and nonhuman primates have demonstrated vector escape to the peripheral circulation following intrathecal AAV delivery, often resulting in significant hepatic gene transfer and therapeutic levels of systemic transgene expression (Hinderer, Bell, et al. 2014c, Hinderer, Bell, Vite, et al. 2014, Haurigot et al. 2013). We did not directly evaluate somatic disease correction in treated MPS I dogs due to the confounding effects of anti-IDUA antibodies in the naïve cohort or previous systemic gene transfer in the immune-tolerant cohort. Notably we observed minimal

hepatic gene transfer following intrathecal AAV9 injection, consistent with the relatively low permissivity of canine liver to AAV-mediated transduction(Bell et al. 2011). Given the low level of hepatic gene transfer and serum IDUA activity in treated dogs, improvement in somatic disease is unlikely. However it should be emphasized that this inefficient peripheral transduction is inconsistent with that observed following intrathecal AAV delivery in other species, and may be specific to the canine model.

There are several limitations of the present study. Due to the increased risks associated with performing intrathecal vector injections in newborn MPS I pups, we chose to use systemic gene transfer as a means of inducing tolerance rather than performing CNS directed gene therapy in neonates. We therefore cannot conclude whether route of administration plays a role in the induction of tolerance. Hepatic gene transfer has often been associated with transgene specific tolerance, although we observed antibody responses against IDUA in 3-month-old MPS I dogs treated with AAV8-mediated hepatic gene therapy, indicating that liver directed gene transfer alone is insufficient to induce tolerance in this model (Crudele et al. 2015, Finn et al. 2010, LoDuca, Hoffman, and Herzog 2009, Sun et al. 2010). In this study we also did not rule out the possibility that prior liver directed gene therapy contributed to the improved correction of brain pathology in immune tolerant animals, although this appears unlikely given that IDUA was undetectable in CSF in these animals at the time of intrathecal vector injection, and CSF Hex activity and pGAG concentration showed no evidence of correction before intrathecal gene transfer. This is consistent with our studies in MPS I cats, in which even extremely high serum IDUA activity had no impact on brain lesions (Hinderer, Bell, et al. 2014b). Additionally, while we focused this study entirely on the observation of neonatal tolerance and its potential utility for therapeutic applications, we

did not evaluate the mechanisms responsible for this phenomenon. This model could serve as a powerful tool for better understanding the development of immunological recognition of self and non-self, and future studies should explore possible mechanisms. Finally, the present study did not define the temporal window in which tolerance induction is possible. Based on the observation that detectable antibody responses began to appear in the MPS I dogs treated on postnatal day 7, we estimate that this period lasts no more than one to two weeks, which could serve as a useful starting point for human studies.

If human neonates are found to exhibit the same potential for transgene-specific immunological tolerance that we have demonstrated in dogs and nonhuman primates, neonatal gene transfer could have enormous potential to treat many genetic disorders for which immune responses limit the safety or efficacy of therapy. In order for clinical trials to be feasible, newborn screening will be essential for identifying patients sufficiently early for this approach to be effective. For MPS I, newborn screening is now being implemented in several states, providing a potential opportunity to conduct first-in-human trials (Hopkins et al. 2014).

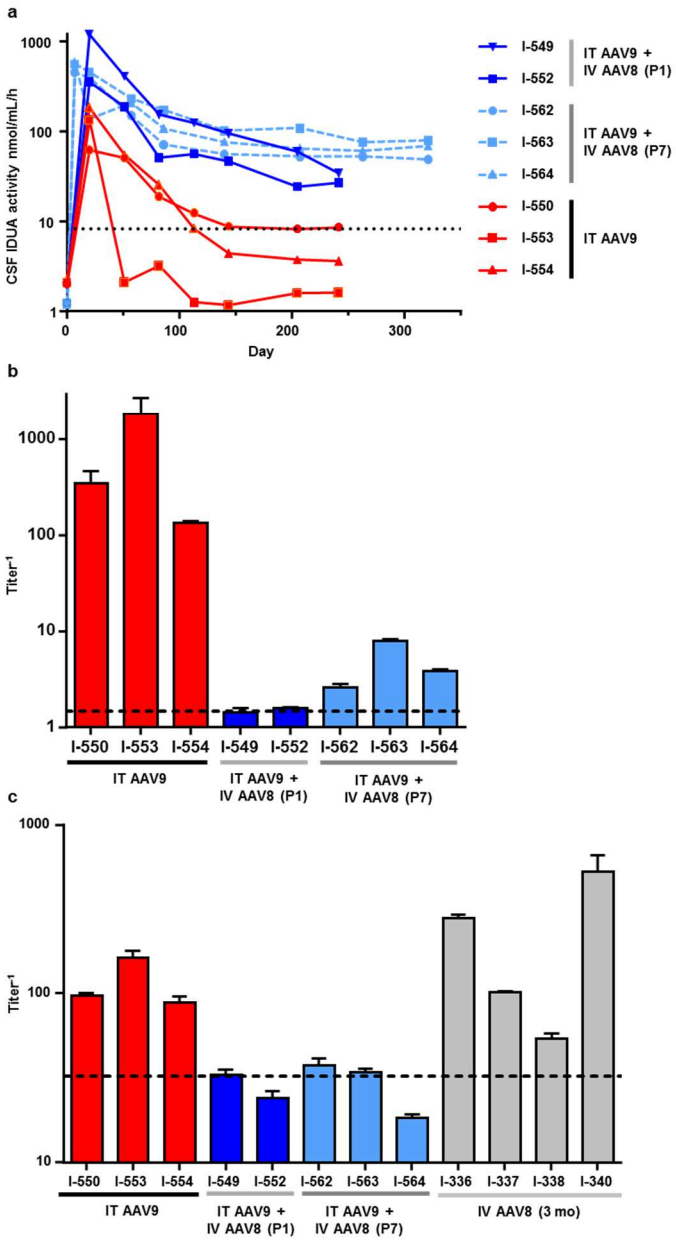

Figure 4-1. Neonatal systemic IDUA gene transfer induces tolerance to subsequent CNS gene therapy in MPS I dogs. MPS I dogs were treated with an intrathecal injection of an AAV9 vector encoding canine IDUA at one month of age (I-550, I-553, I-554) or were first treated with an intravenous injection of an AAV8 vector encoding IDUA under control of a liver specific promoter on postnatal day 1 (I-549, I-552) or postnatal day 7 (I-562, I-563, I-564) followed by intrathecal vector injection at one month of age. (a) CSF was serially collected from treated animals and assayed for IDUA enzyme activity. The dotted line represents the mean CSF IDUA activity in normal control animals. (b) Antibodies against canine IDUA were detected in CSF samples at baseline and on day 80 after intrathecal vector injection by indirect ELISA. Error bars represent standard error of replicate wells. The dashed line is the upper limit of pretreatment samples.

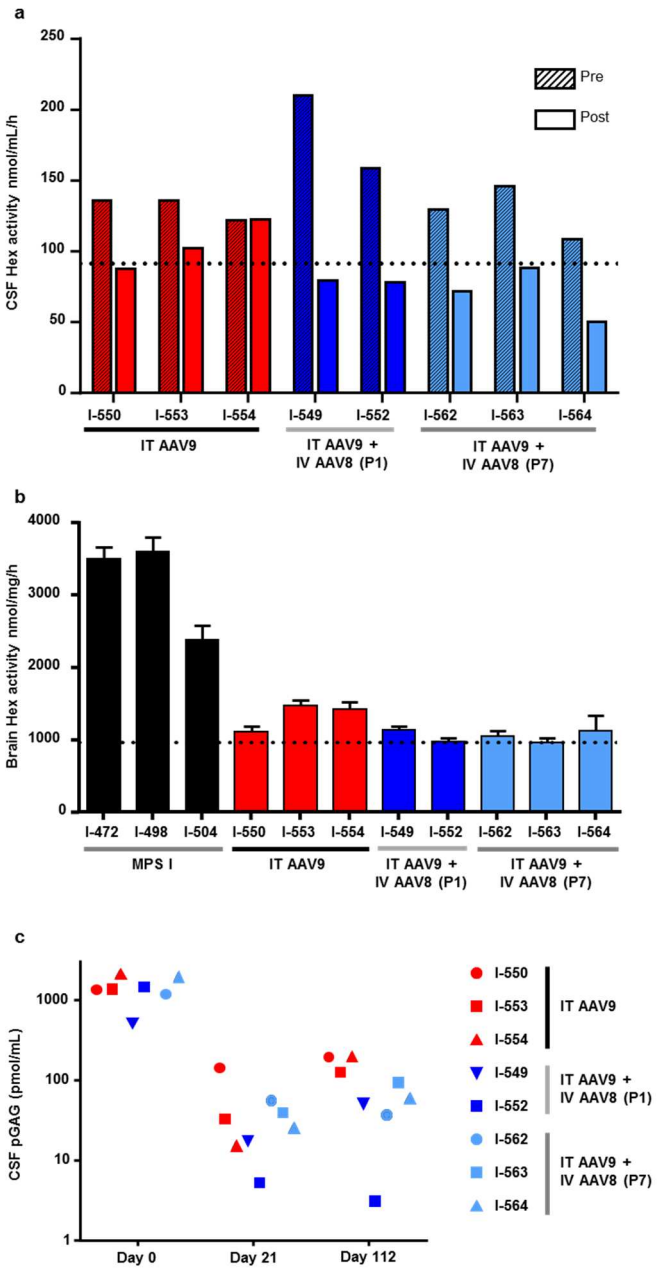

Figure 4-2. Biochemical markers are normalized following intrathecal gene therapy in MPS I dogs. (a) CSF samples from treated dogs and untreated controls were analyzed for Hexosaminidase (Hex) activity at the time of intrathecal vector injection (pre) and at the time of tissue harvest (post). The dotted line indicates the upper limit of CSF Hex activity in normal control samples. (b) Hex activity was also measured in brain lysates. Values are the mean +/- SEM of samples collected from six brain regions (frontal cortex, temporal cortex, occipital cortex, hippocampus, medulla, cerebellum). (c) Pathogenic GAGs were measured in CSF at the time of intrathecal vector injection and on day 21 and 112 post injection.

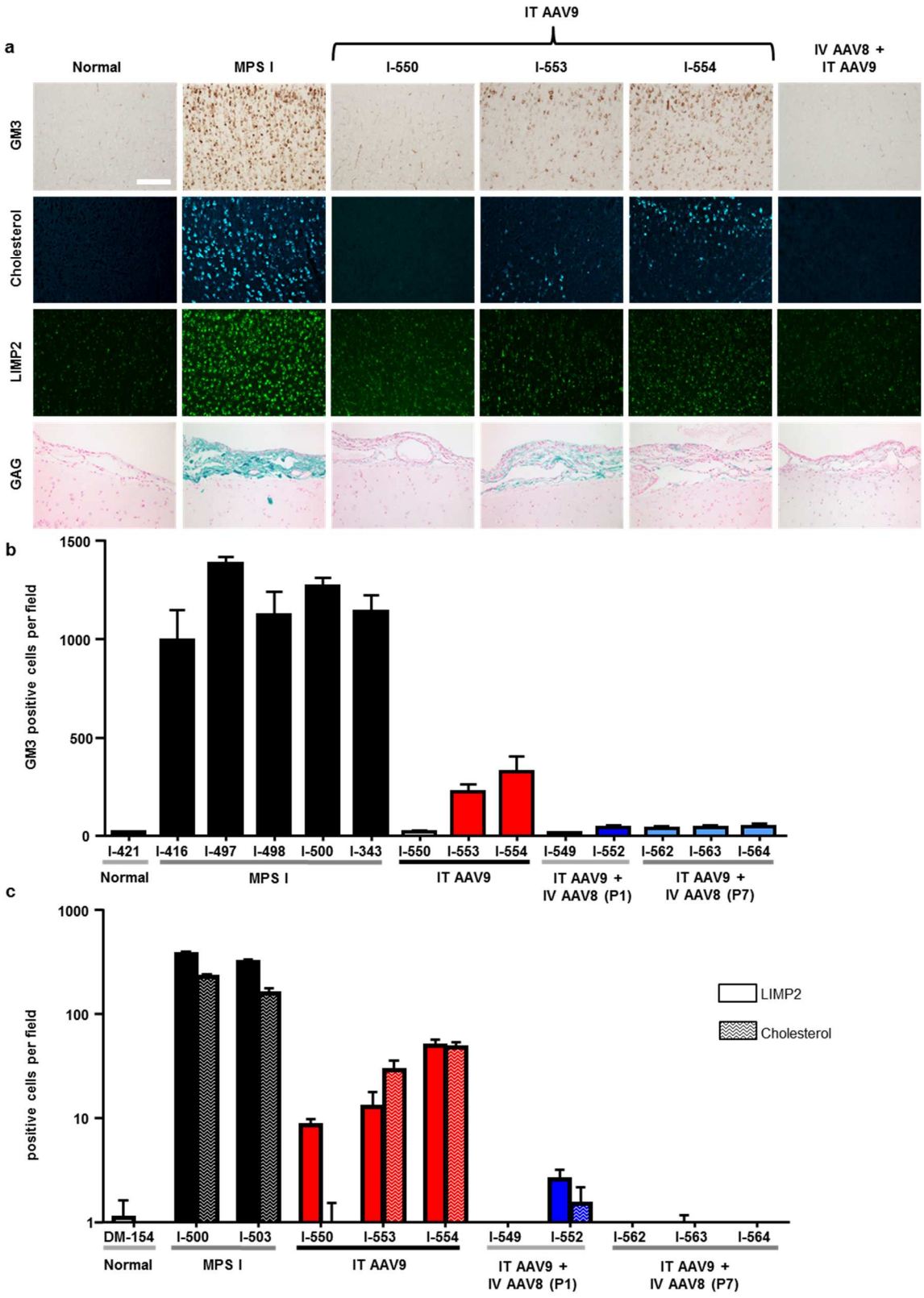
a
IT AAV9
Normal
MPS I
I-550
I-553
I-554
IV AAV8 +
IT AAV9
GM3
Cholesterol
LIMP2
GAG
b
GM3 positive cells per field
1500
1000
500
0
I-421
I-416
I-497
I-498
I-500
I-343
I-550
I-553
I-554
I-549
I-552
I-562
I-563
I-564
Normal
MPS I
IT AAV9
IT AAV9 +
IV AAV8 (P1)
IT AAV9 +
IV AAV8 (P7)
c
positive cells per field
1000
100
10
1
LIMP2
Cholesterol
DM-154
I-500
I-503
I-550
I-553
I-554
I-549
I-552
I-562
I-563
I-564
Normal
MPS I
IT AAV9
IT AAV9 +
IV AAV8 (P1)
IT AAV9 +
IV AAV8 (P7)

Figure 4-3. CNS storage lesions are more effectively cleared by intrathecal gene therapy in MPS I dogs tolerized to IDUA as neonates. (a) Representative brain sections are shown for normal, untreated MPS I, and tolerized intrathecal treated MPS I dogs. For the three animals treated with AAV9 alone, images are shown for each animal. Immunostaining was performed on cortical brain sections for the ganglioside GM3 and the lysosomal membrane protein LIMP2. Unesterified cholesterol was detected by filipin stain. GAG storage in meninges is stained with Alcian blue. Scale bar = 200 μM. (b) Automated quantification was performed on GM3, and (c) LIMP2, and filipin stained sections. Values are the mean +/- SEM of 10 sections.

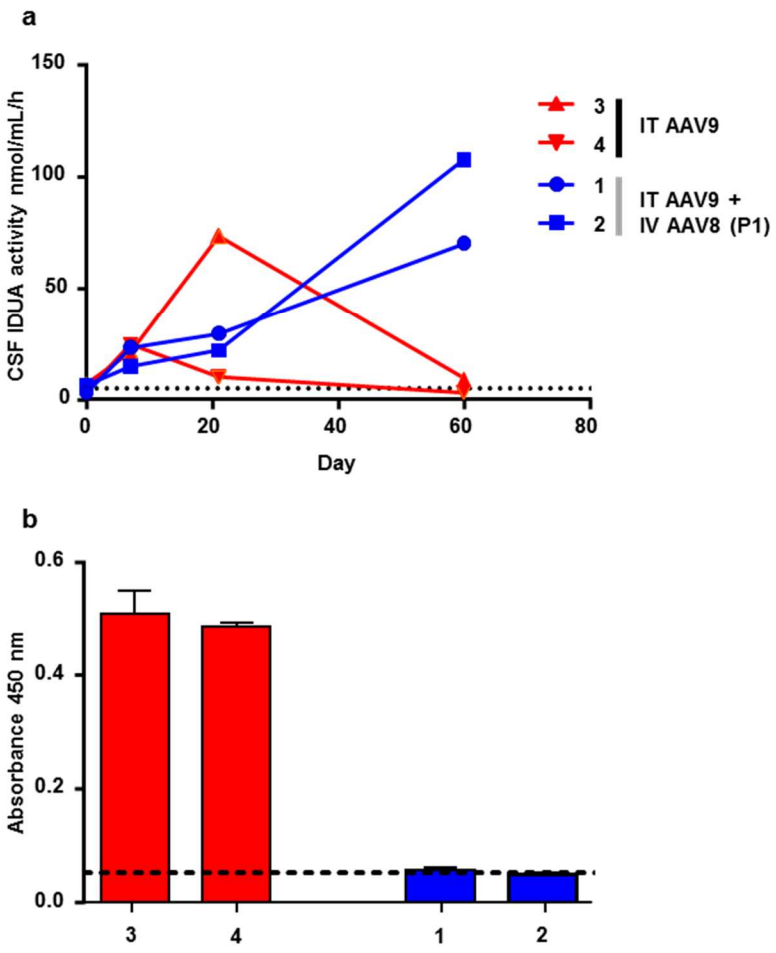

Figure 4-4. Neonatal gene transfer induces tolerance in nonhuman primates. Four newborn rhesus monkeys were administered an AAV8 vector expressing either human IDUA (Animal #s 1 and 2) or human factor IX (3 and 4) intravenously. All animals were administered AAV9 expressing human IDUA using the intrathecal approach at 1 month postnatal age. (a) IDUA activity was measured in CSF after intrathecal vector injection weekly then monthly. The dotted line represents the mean IDUA activity in pretreatment CSF samples. (b) Antibodies were detected in CSF by indirect ELISA 2 months after intrathecal vector administration. The dashed line indicates the upper limit of baseline samples. Error bars represent SEM.

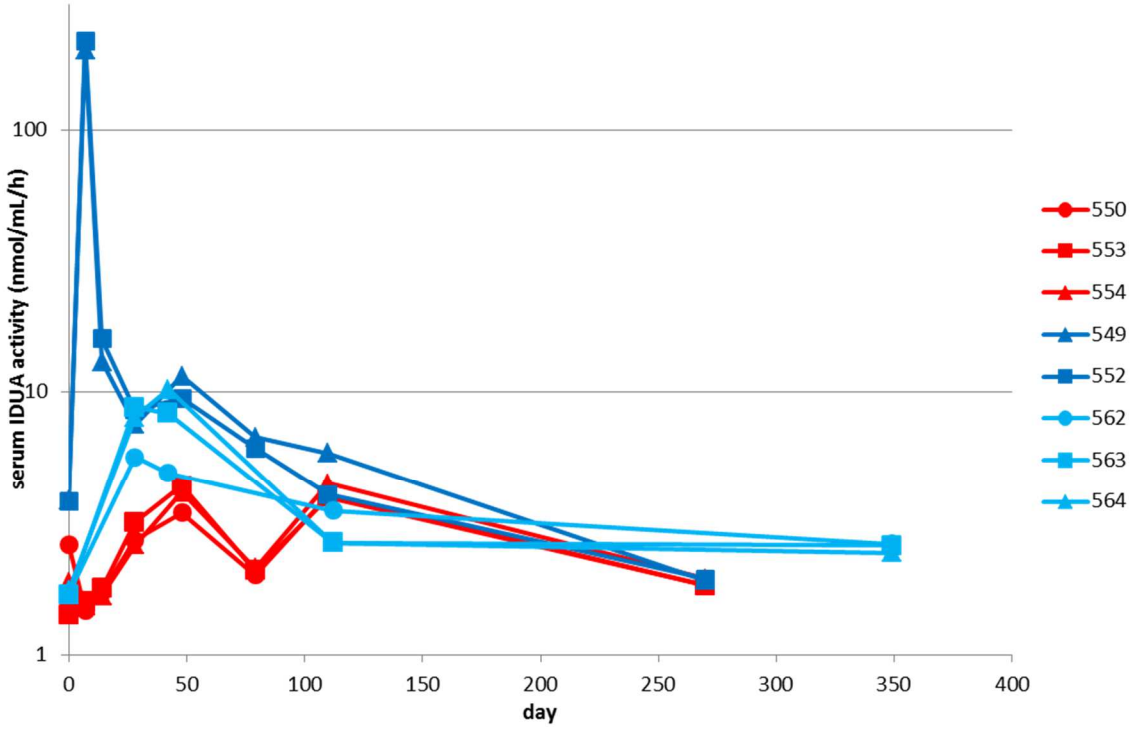

Fig 4-5: Serum IDUA activity in MPS I dogs. MPS I dogs were treated with an intravenous injection of an AAV8 vector encoding canine IDUA under control of a liver specific promoter on postnatal day 1 (I-549, I-552) or postnatal day 7 (I-562, I-563, I-564) followed by intrathecal injection of an AAV9 vector at one month of age. Serum was serially collected from treated animals and assayed for IDUA enzyme activity.

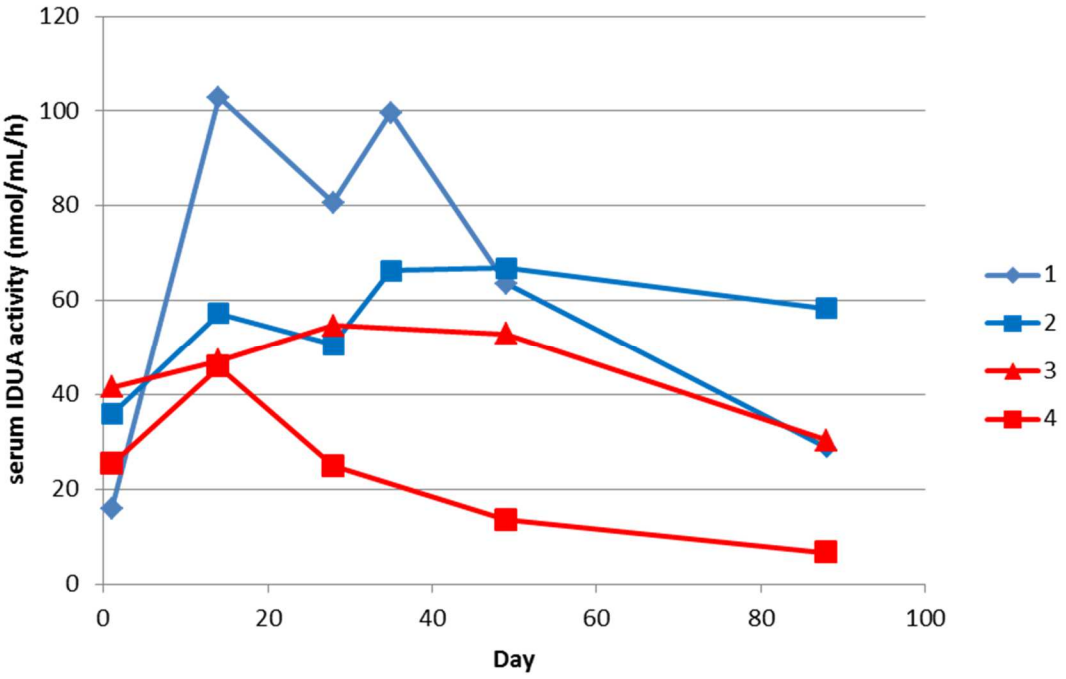

Fig 4-6. Serum IDUA activity in rhesus monkeys.

Newborn rhesus macaques were administered an AAV8 vector intravenously expressing human IDUA (animal 1 and 2) or human factor IX (3 and 4). All four were administered an intrathecal injection of an AAV9 vector expressing human IDUA at one month of age. Serum was serially collected from treated animals and assayed for IDUA enzyme activity.

Table 4-1. Summary of Study Subjects

	Animal ID	Genotype	IV vector	Age at IV treatment (days)	IT vector	Age at IT treatment (days)	Age at necropsy (months)
MPS I dogs							
	I-550	MPS I	-	-	AAV9.CB.cIDUA[C]	28	9
	I-553	MPS I	-	-	AAV9.CB.cIDUA	28	9
	I-554	MPS I	-	-	AAV9.CB.cIDUA	28	9
	I-549	MPS I	AAV8.TBG.cIDUA[A]	1	AAV9.CB.cIDUA	28	9
	I-552	MPS I	AAV8.TBG.cIDUA	1	AAV9.CB.cIDUA	28	9
	I-562	MPS I	AAV8.TBG.cIDUA	7	AAV9.CB.cIDUA	28	11
	I-563	MPS I	AAV8.TBG.cIDUA	7	AAV9.CB.cIDUA	28	11
	I-564	MPS I	AAV8.TBG.cIDUA	7	AAV9.CB.cIDUA	28	11
	I-497	MPS I	-	-	-	-	12
	I-498	MPS I	-	-	-	-	12
	I-500	MPS I	-	-	-	-	12
	I-503	MPS I	-	-	-	-	12
	I-504	MPS I	-	-	-	-	12
	I-343	MPS I	-	-	-	-	18
	I-416	MPS I	-	-	-	-	6
	I-472	MPS I	-	-	-	-	18
	I-421	Normal	-	-	-	-	26
	DM-154	Normal	-	-	-	-	12
Rhesus macaques							
	1	Normal	AAV8.TBG.hIDUA[B]	1	AAV9.CB.hIDUA[D]	30	ongoing
	2	Normal	AAV8.TBG.hIDUA	1	AAV9.CB.hIDUA	30	ongoing
	3	Normal	AAV8.TBG.hFIX	1	AAV9.CB.hIDUA	30	ongoing
	4	Normal	AAV8.TBG.hFIX	1	AAV9.CB.hIDUA	30	ongoing

A. 5 x 10^{12} genome copies per kilogram (GC/kg); IV=intravenous; IT=intrathecal

B. 10^{12} GC/kg

C. 10^{12} GC/kg D. 3 x 10^{12} GC/kg

Table 4-2: CSF nucleated cell counts in MPS I dogs following vector injection (Cells/μL)

	Day post IT vector				
Animal No.	**0**	**7**	**21**	**51**	**81**
549	1	ND	2	0	0
550	2	ND	11[A]	BC	2
552	0	ND	ND	2	2
553	2	ND	1485[C]	2	2
554	0	ND	14[B]	1	2
562	2	BC	1	0	0
563	BC	1	29[B]	1	0
564	1	1	4	0	0

ND = not done, BC = Blood contamination of CSF sample (>500 erythrocytes/μL), IT=intrathecal. Normative range ≤ 5 cells/μL.

A. 317 erythrocytes/μL
B. >70% lymphocytes
C. >70% monocytes

Table 4-3: Vector biodistribution[A]

	I-550	I-553	I-554	I-549	I-552	I-562	I-563	I-564
Frontal cortex	0.207224	0.032837	0.037931	0.195879	0.311028	0.053383	0.014606	0.41984
Temporal cortex	0.324461	0.015715	0.042556	0.682856	0.024615	0.075457	0.539041	0.541367
Occipital cortex	0.240198	0.03092	0.068607	0.585868	0.158689	0.006249	0.021576	0.724321
Hippocampus	0.007486	0.032587	0.058214	0.008692	0.336849	0.01288	0.056152	0.065506
Medulla	0.156078	0.012703	0.004936	0.063498	0.194763	0.294345	0.032355	0.020695
Cerebellum	0.022631	0.014178	0.010712	0.061944	0.046369	0.025023	0.026128	0.02586
Spinal cord cervical	0.257116	0.034117	0.014234	0.165666	0.509951	0.510722	0.046194	0.093024
Spinal cord thoracic	0.43775	0.063695	0.02829	0.359055	0.140467	0.120746	0.079992	0.100718
Spinal cord lumbar	0.190243	0.03037	0.116436	0.460682	0.313737	0.225627	0.241252	0.263238
Heart	0.001076	<0.0005[B]	0.001983	0.00145	0.001454	0.02967	0.005545	0.005753
Lung	0.000879	0.002424	0.001887	0.000491	0.000538	0.000667	0.001105	0.001883
Liver	0.001304	0.004242	0.001918	0.010545	0.206071	0.030681	0.006334	0.028654
Spleen	0.002579	0.001543	0.001228	0.002596	0.002229	0.044439	0.003144	0.008972

A. Values are genome copies (GC) per diploid genome. The assay does not distinguish between the AAV8 and AAV9 vectors.

B. Limit of detection

CHAPTER 5: Induction of transgene-specific immune tolerance enables evaluation of a human gene therapy for mucopolysaccharidosis type I in an authentic dog model

---

Chapter 5 is adapted from the manuscript: C. Hinderer, P. Bell, J. P. Louboutin, Y. Zhu, H. Yu, G. Lin, R. Choa, B. L. Gurda, J. Bagel, P. O'Donnell, T. Sikora, T. Ruane, P. Wang, M. L. Casal, M. E. Haskins, J. M. Wilson. In preparation.

Abstract:

High fidelity animal models of human disease are essential for preclinical evaluation of novel gene and protein therapeutics. However, these studies can be complicated by exaggerated immune responses against the human protein that preclude meaningful assessment of safety and efficacy. Here we demonstrate that dogs with a genetic deficiency of the enzyme α-l-iduronidase (IDUA), a model of the neuropathic lysosomal storage disease mucopolysaccharidosis type I (MPS I), can be rendered immunologically tolerant to human IDUA through neonatal exposure to the enzyme. Using MPS I dogs tolerized to human IDUA as neonates, we evaluated intrathecal delivery of an adeno-associated virus serotype 9 vector expressing human IDUA as a therapy for the central nervous system manifestations of MPS I. These studies established the efficacy of the human clinical candidate vector in the canine model, and allowed for estimation of the minimum effective dose, providing key information for the design of first in human trials. This approach has considerable potential to facilitate evaluation of human therapeutics in relevant animal models. If the neonatal tolerance induction strategy employed can be translated to humans, it may also have clinical applications for the prevention of immune responses to gene and protein replacement therapies.

Introduction

Mucopolysaccharidosis type I (MPS I) is a rare inherited lysosomal storage disease caused by deficiency of IDUA, an enzyme required for the catabolism of ubiquitous glycosaminoglycans (GAGs). GAG accumulation leads to a variety of clinical manifestations including bone and joint deformities, corneal clouding, and cardiac valve insufficiency. MPS I patients frequently experience neurological complications including

communicating hydrocephalus and spinal cord compression. The impact of the disease on cognitive function varies; in the attenuated form of MPS I (Scheie syndrome or Hurler-Scheie syndrome) in which there is residual IDUA activity, cognition is affected in only about one third of patients. In the more common severe form of MPS I (Hurler syndrome), patients universally exhibit rapid cognitive decline in early childhood(Wraith et al. 2007). MPS I is currently treated with intravenous infusion of the recombinant enzyme, which can be internalized by cells from the circulation via mannose 6-phosphate receptor binding (Sando and Neufeld 1977, Dahms, Lobel, and Kornfeld 1989). Enzyme replacement improves many disease symptoms, but does not reach the CNS, and therefore has no impact on cognitive function (Wraith et al. 2007). MPS I can also be treated with hematopoietic stem cell transplantation (HSCT) which provides a constant source of circulating IDUA through enzyme secretion by engrafted donor cells. Unlike enzyme replacement, HSCT can improve cognitive outcomes, apparently due to migration of donor derived cells across the blood-brain barrier, where they serve as a source of secreted enzyme within the CNS. However, HSCT suffers from numerous complications including graft failure, infection, graft versus host disease, and transplant-associated mortality as high as 20%(Aldenboven, Boelens, and de Koning 2008, Boelens et al. 2007, Braunlin et al. 2003, de Ru et al. 2011, Souillet et al. 2003, Staba et al. 2004, Whitley et al. 1993). After transplant many patients also exhibit residual cognitive deficits, which may be a consequence of disease progression during the slow engraftment of donor cells in the CNS (Kennedy and Abkowitz 1997). These shortcomings leave a significant unmet need for a safe and effective therapy for the CNS manifestations of MPS I.

Gene therapy is a promising alternative to HSCT for the treatment of cognitive decline in MPS I patients. Gene transfer has the potential to induce rapid reconstitution of IDUA in the CNS without the adverse effects of HSCT, and targeting even a small number of cells in the CNS could provide a depot of secreted IDUA in the brain, leading to widespread improvement of storage pathology. We previously demonstrated that injection of an adeno-associated virus serotype 9 vector into the cerebrospinal fluid (CSF) can efficiently deliver the IDUA gene to cells throughout the CNS, and that the enzyme secreted by transduced cells mediates global resolution of brain storage lesions. These proof-of concept studies for intrathecal AAV9 gene therapy relied on two naturally occurring large animal disease models, the MPS I dog and MPS I cat. The use of these models was critical for evaluating the efficacy of the approach, not only because they accurately reproduce the CNS pathology of MPS I, but also because these large animals better reflect the human CNS anatomy and CSF circulation than rodent models, allowing for realistic representation of the clinical route of administration and the resulting vector distribution. While these initial experiments in the MPS I dog and cat were carried out using vectors expressing species-specific transgenes, advancing this approach toward human trials necessitated the evaluation of a clinical candidate vector bearing the human IDUA transgene. However, studies of the clinical candidate vector in the MPS I dog model were complicated by an exaggerated immune response to the human enzyme. Building on our previous finding that neonatal gene transfer could induce persistent tolerance to the transgene product, we applied this approach to induce tolerance to human IDUA in MPS I dogs, which subsequently allowed for the evaluation of the efficacy of the human vector in this model.

Materials and Methods

Vector production: A codon optimized human IDUA cDNA was cloned into an expression construct bearing the cytomegalovirus immediate early enhancer, chicken beta-actin promoter and rabbit globin polyadenylation sequence flanked by AAV2 inverted terminal repeats. The construct was packaged in an AAV9 capsid, purified and titered as previously described.

Animal procedures:

The MPS I dog colony was maintained at the University Of Pennsylvania School Of Veterinary Medicine under NIH and USDA guidelines for the care and use of animals in research. All study protocols were approved by the University of Pennsylvania Institutional Animal Care and Use Committee. For infusions of recombinant human IDUA, laronidase (Genzyme) was diluted 5 –fold in saline immediately before use. Infusions were performed through a peripheral venous catheter over two hours. Vector injections, serum and CSF collection, and euthanasia were performed as previously described(Hinderer et al. 2015).

Enzyme assays:

IDUA and Hex activity were measured in tissue lysates and CSF as previously described(Hinderer, Bell, et al. 2014c).

Anti-hIDUA ELISA:

Polystyrene ELISA plates were coated overnight at 4 degrees with recombinant human IDUA (Genzyme) diluted to 5micrograms/mL in phosphate buffer pH 5.8. The plate was washed and blocked in 2% BSA in phosphate buffer. The plate was incubated 1 hour at

room temperature with CSF samples diluted 1:50 in PBS. The plate was washed and bound antibody detected with HRP conjugated anti-canine IgG (Pierce, Rockford, IL) diluted 1:10,000 in 2% BSA. The ELISA was developed with tetramethylbenzidine substrate for 15 minutes, then stopped with 2 N sulfuric acid and absorbance was measured at 450 nm. Titers were calculated from a standard curve of a serially diluted positive sample.

Histology:

Tissue processing, immunostaining and quantification were performed as previously described (Hinderer et al. 2015).

Biodistribution:

Vector biodistribution was evaluated as described (Hinderer et al. 2015).

Results

Intrathecal AAV9 expressing human IDUA elicits robust transgene-specific immunity in MPS I dogs

Five MPS I dogs were treated at one month of age with a single intrathecal injection into the cisterna magna of an AAV9 vector expressing human IDUA. Vector doses ranged from 10^{11} genome copies per kg (GC/kg) to 10^{12} GC/kg. The procedure was well tolerated in all subjects. IDUA activity in CSF rapidly increased following vector administration, exceeding that of normal controls by day 7 (Figure 5-1). However, by day 21 post vector administration CSF IDUA levels fell to baseline, accompanied by an elevation in CSF anti-hIDUA titers (Figure 5-2). Day 21 CSF samples also revealed a lymphocytic pleocytosis in all animals (Figure 5-3A). In these cohorts the elevated CSF

antibodies and cell counts were not associated with clinical signs or other laboratory abnormalities, and the pleocytosis spontaneously resolved. At the time of necropsy six months after injection, histological evaluation revealed no evidence of pathology in the brain or spinal cord. Vector biodistribution demonstrated widespread CNS transduction and persistence of the vector genome (Table 5-1). Histology also showed some improvement in brain storage lesions (Figure 5-7).

Based on the favorable safety profile observed in these dogs we dosed an additional two MPS I dogs with a 10-fold higher dose of vector (i.e., 10^{13} GC/kg). These dogs developed CSF pleocytosis with similar kinetics to the animals treated at the lower two doses; however in these two subjects the response was more pronounced, and the pleocytosis was temporally associated with the onset of neurological signs. Beginning 21 days after vector administration, the animals exhibited hyporeflexia and weakness of the hind limbs, and pain upon flexion of the neck. The animals were treated with corticosteroids and analgesics, after which the pain and CSF pleocytosis began to resolve. However, the hind limb weakness persisted, and the animals were euthanized two weeks after symptom onset. Histopathology demonstrated robust transduction of spinal motor neurons, particularly in the lumbar spinal cord, and lymphocytic infiltrates surrounding transduced neurons (Figure 5-4). Immunostaining revealed that the infiltrating mononuclear cells consisted primarily of B cells, with occasional CD4 and CD8 T cells infiltrating the associated spinal nerves. The correlation between the clinical signs of hind limb weakness and the histological evidence for high levels of transgene expression in the lumbar spinal motor neurons and selective lymphocytic infiltration at this level suggests that neurological toxicity was driven by a transgene specific immune response targeting heavily transduced motor neurons. An interferon gamma ELISPOT

assay performed on PBMCs collected at necropsy was negative for T cell responses to the transgene or the vector capsid (data not shown) although these results may be confounded by the preceding course of corticosteroids.

Neonatal exposure to human IDUA through hepatic gene transfer induces tolerance to subsequent intrathecal gene transfer

In order to evaluate the AAV9 vector expressing human IDUA in the absence of an exaggerated immune response to the human protein, 6 MPS I dogs were tolerized to human IDUA with a single intravenous injection of an AAV serotype 8 vector expressing human IDUA from a liver specific promoter on postnatal day 5. At one month of age the animals were treated with different doses of an intrathecal injection of the AAV9 vector expressing human IDUA in three cohorts (N=2 animals per cohort) as follows: 10^{10}, 10^{11} and 10^{12} GC/kg. All animals exhibited dose-dependent elevation in CSF IDUA activity similar to the non-tolerized dogs; however, in this cohort CSF enzyme expression persisted beyond day 21 and remained relatively stable for the duration of the experiment (Figure 5-1). CSF antibody responses were blunted compared to what was observed when naïve (i.e., non-tolerized animals) were dosed with intrathecal vector, with only two animals of the tolerized cohorts (I-602 and I-606) exhibiting detectable titers, which were approximately 20 fold lower than naïve animals treated with an equivalent vector dose (Figure 5-2). Only the dog with the highest antibody titer in this cohort exhibited elevated CSF lymphocytes at day 21, albeit at lower levels than in the naïve animals (Figure 5-3). There were no clinical adverse events in these cohorts.

Intrathecal AAV9-mediated hIDUA expression effects dose-dependent correction of brain biochemical abnormalities and storage lesions

The MPS I dog carries an IDUA mutation resulting in inclusion of the first intron in the mature mRNA, creating an immediate stop codon. The mutation in MPS I dogs yields no detectable IDUA activity (Menon, Tieu, and Neufeld 1992, Terlato and Cox 2003, He et al. 1999). In the absence of lysosomal IDUA activity, undegraded GAGs accumulate in the cell (Sando and Neufeld 1977). This primary GAG storage material in affected tissues can be directly detected histologically by Alcian blue staining (Shull et al. 1984, Shull et al. 1994, Clarke et al. 2009, Ellinwood et al. 2007, Haskins et al. 1983, Terlato and Cox 2003, Chen et al. 2011, Hinderer, Bell, et al. 2014c). In addition to the primary GAG storage pathology, lysosomal GAG accumulation leads to a characteristic cascade of cellular abnormalities. The un-degraded GAGs cause lysosomal distention, visible on histology by increased staining for lysosomal membrane proteins such as LIMP2. Neurons also exhibit secondary accumulation of substances such as gangliosides (e.g. GM3) and un-esterified cholesterol. These secondary storage materials can be detected by microscopy using immunostaining (GM3) or filipin staining (cholesterol). Lysosomal storage also induces aberrant overexpression of lysosomal enzymes such as hexosaminidase.

The six MPS I dogs tolerized to human IDUA through neonatal gene transfer were sacrificed 6 months post intrathecal AAV9 injection. Brain lysates demonstrated normalization of hexosaminidase activity, which correlated with vector dose (Figure 5-5). Hexosaminidase activity was normalized in CSF at all vector doses (Figure 5-8). There were also dose-dependent decreases in LIMP2 and ganglioside storage (Figure 5-6). CNS pathology was almost completely reversed at the highest vector dose. At the lowest dose, there were measurable improvements in some markers (LIMP2 and Hex) whereas ganglioside accumulation was not clearly reduced. The low dose of 10^{10} GC/kg

therefore appeared to be the minimum effective dose. Scaled to the 45g brain mass of a one-month old dog, and with an average body weight of 2 kg, this dose would correspond to an MED of 4.4 x 10^8 GC/g brain mass, or approximately 6.2 x 10^{11} GC in an adult human.

Infusion of recombinant hIDUA in newborn MPS I dogs is sufficient to induce tolerance to intrathecal AAV9-mediated hIDUA expression

In order to determine whether hepatic expression of human IDUA was necessary for tolerance induction, we treated two MPS I dogs (I-663 and I-664) with infusions of recombinant human IDUA (0.58 mg/kg) on postnatal day 7 and 14 before intrathecal AAV9 injection at one month of age. Similar to dogs treated as newborns with a vector expressing human IDUA, the enzyme treated dogs exhibited persistently high levels of CSF IDUA activity (Figure 5-1) and no antibody response against human IDUA (Figure 5-2) or CSF pleocytosis (Figure 5-3). Brain storage lesions were effectively cleared in both animals (Figure 5-6).

Discussion

Evaluating the efficacy of intrathecal AAV9 delivery for the treatment of MPS I required assessment of both the vector distribution that could be achieved via injection into the CSF, and the impact of that degree of transduction on measures of disease activity. These studies necessitated the use of an animal model that could accurately reflect the disease pathophysiology while also displaying sufficiently similar size and anatomy to allow for meaningful evaluation of the clinical delivery method and the resulting vector distribution. The canine model of MPS I faithfully replicates the human phenotype, exhibiting not only the same biochemical and histological lesions, but also

many of the same clinical manifestations (Ciron et al. 2006, Dickson, Ellinwood, et al. 2010, Dickson et al. 2009, Menon, Tieu, and Neufeld 1992, Shull et al. 1984, Shull et al. 1994, Traas et al. 2007). Due to the phenotypic similarity to MPS I in humans, MPS I dogs were used extensively in the development of enzyme replacement therapy for the treatment of systemic disease (Dickson, Peinovich, et al. 2008, Shull et al. 1994). MPS I dogs also mimic CNS manifestations of the disease, sporadically developing spinal cord compression and hydrocephalus (Dickson, Ellinwood, et al. 2010, Dickson et al. 2009, Vite et al. 2013). Though cognitive studies have not been reported for MPS I dogs, the histological and biochemical manifestations in the brain have been well characterized, and faithfully recapitulate the findings in humans with the severe from of the disease (Ciron et al. 2006, Shull et al. 1984, Walkley, Haskins, and Shull 1988). MPS I dogs demonstrate accumulation in the brain of lysosomal membrane proteins (LIMP2) and gangliosides (GM3), and upregulation of lysosomal enzymes such as hexosaminidase (Hex). Ganglioside accumulation correlates with cognitive function in MPS I and other lysosomal storage diseases, and thus is a critical marker for evaluating disease severity and therapeutic outcomes (Walkley and Vanier 2009, Constantopoulos, Iqbal, and Dekaban 1980). MPS I dogs also exhibit changes in neuronal morphology like those identified in patients (Walkley, Haskins, and Shull 1988). These striking similarities between this model and MPS I patients made this a compelling model for the evaluation of intrathecal AAV delivery as novel therapy for the CNS manifestations of the disease. The capacity of large animal models to replicate the route of administration that would be used clinically for IT AAV9 delivery, as well as the resulting vector distribution in the CNS, further supported the relevance of the MPS I dog for these studies.

Although the MPS I dog appeared to be an excellent model for evaluation of the clinical vector, the immune response to human IDUA presented a critical obstacle. From previous studies it is clear that the immune response to human IDUA in MPS I dogs is much more extreme than that observed in patients. Intravenous delivery of the protein in both dogs and MPS I patients often results in the development of serum antibodies; however in dogs these responses are more robust, less likely to decline upon continued administration, and more often associated with anaphylactic responses to subsequent infusions (Kakkis, Lester, et al. 2004, Shull et al. 1994). The difference in immune response to human IDUA in the CNS is even more striking; in MPS I dogs treated with intrathecal infusions of laronidase there was evidence of meningitis in addition to antibody responses detectable in CSF; in both pediatric and adult MPS I patients treated with repeated IT infusions of the protein there have been no similar adverse effects, and in the 5 patients that have been tested for CSF antibodies against IDUA only one has been positive(Chen et al. 2011, Dickson, Ellinwood, et al. 2010, Dickson et al. 2009, Dickson, Hanson, et al. 2010, Dickson, Naylor, Mlikotic, Victoroff, Chen, Passage, Le, et al. 2008, Kakkis, McEntee, et al. 2004, Lund et al. 2014, Vera et al. 2013). Interestingly MPS I dogs also develop antibodies to canine IDUA, albeit at lower levels than to the human enzyme, suggesting that this model has a greater overall tendency toward immunity to IDUA which is exacerbated by the use of the non-species specific protein (Hinderer et al. 2015). These marked differences in the outcome of both intravenous and intrathecal delivery of human IDUA in MPS I dogs and patients indicate a consistently exaggerated immune response to human IDUA in MPS I dogs, and suggest that preventing this response will be necessary to replicate the anticipated vector activity in humans. Inducing tolerance to the protein through neonatal exposure allowed for the evaluation of the efficacy of the human vector in this model without the interference of

the exaggerated immune response. This provided critical information, allowing for the determination of the minimum effective dose—an essential factor in the design of first-in human gene therapy trials—in the most relevant animal model. Without this approach, the only options would be to extrapolate efficacy data from vectors with species specific transgenes, which could have important differences in potency, or move studies to a less representative animal model that is more immune tolerant to the human protein. Pharmacologic immune suppression can also be employed in this setting, although the neonatal tolerance induction protocol has the clear advantage of avoiding secondary consequences of the immune suppressing drugs.

Though efficacy assessment was confounded by the immune response and loss of circulating IDUA in the non-tolerized dogs treated with the human vector, some useful data can be derived from these animals. While the strong immune response is not likely to represent the immune response in humans, it could inform monitoring plans for first in human studies by demonstrating key characteristics of immune-mediated toxicity. In this case we saw that immune-mediated toxicity was dose-dependent, the peak of the immune response occurred 3 weeks after vector administration, presented with focal motor symptoms likely due to high transduction of spinal motor neurons, and was accompanied by CSF pleocytosis. These findings could be directly integrated into the phase 1 trial protocol, with intensive monitoring for immune-mediated toxicity and neurological symptoms extending for several weeks after vector administration, and CSF analysis for pleocytosis occurring 3-4 weeks after injection. If neurological symptoms accompanied by pleocytosis appeared with similar kinetics in a human study subject, the findings in naïve dogs would suggest that the toxicity is due to an immune response (as opposed to overexpression toxicity, for example) and could guide therapeutic decisions.

The present findings indicate that neonatal exposure to human IDUA can induce tolerance regardless of the source of the enzyme. While we had previously found that AAV-mediated expression could induce tolerance in neonates, here we found that infusion of the recombinant enzyme could also induce tolerance. If this approach is generalizable to other proteins, it could be useful for preclinical evaluation of many human therapeutics in animal models. Further, if a similar approach could induce tolerance to foreign proteins in human neonates, it could have enormous potential to improve the efficacy of protein replacement therapies for diseases in which antibody responses to the normal protein limit efficacy. In the case of MPS I, while most patients appear to tolerate intrathecal IDUA infusions, the vast majority develop serum antibodies against intravenous enzyme replacement, and these antibodies can diminish the response to therapy. Combining neonatal tolerance induction with a gene or protein replacement therapy may substantially improve patient outcomes. The availability of an approved recombinant enzyme would make MPS I an excellent candidate for an initial human trial of this approach. If human neonates exhibit the same window of 1-2 weeks for tolerance induction, newborn screening would be essential for identifying patients early enough for successful intervention. The ongoing implementation of newborn screening for MPS I and other lysosomal storage diseases will therefore be critically important for clinical evaluation of a neonatal tolerance induction protocol.

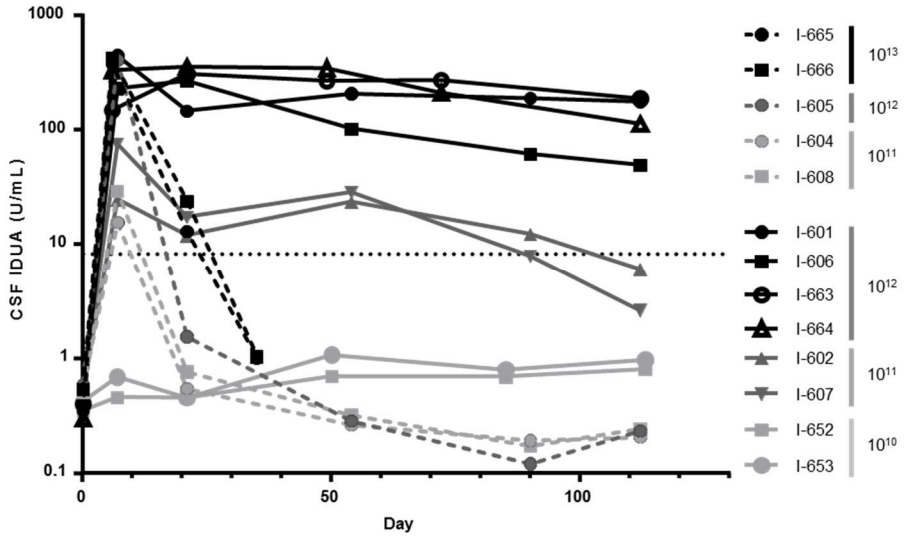

Figure 5-1. CSF IDUA activity in MPS I dogs treated with intrathecal AAV9 expressing human IDUA. Dogs were treated at one month of age with an intrathecal injection of the vector into the cisterna magna. IDUA activity was measured in subsequent CSF samples. Vector doses (GC/kg) are indicated for each animal. The dashed lines represent animals treated with intrathecal vector only. The solid lines with filled symbols represent animals pretreated on postnatal day five with intravenous AAV8 expressing human IDUA from a liver-specific promoter. Solid lines with open symbols represent animals pretreated on postnatal day 7 and 14 with intravenous infusion of recombinant human IDUA. Animals I-665 and I-666 were euthanized on day 36 due to neurological signs. The dotted line represents mean CSF IDUA activity in normal dogs.

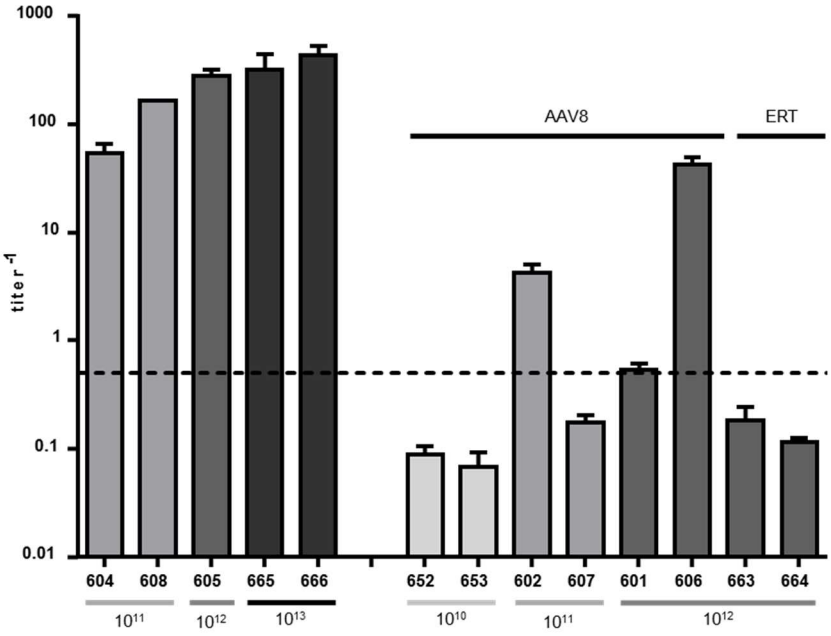

Figure 5-2. CSF antibody titer against human IDUA. Antibody titers against human IDUA were measured by ELISA in CSF samples collected 50 days post vector administration. CSF samples tested from I-665 and I-666 were collected at the time of necropsy (day 36 post injection). The dashed line represents the upper limit of CSF antibody titers measured in naïve control dogs. Error bars = SEM. Antibody titers were significantly lower in the animals pre-treated as neonates with AAV8 vector or recombinant human IDUA compared to controls (Mann-Whitney test).

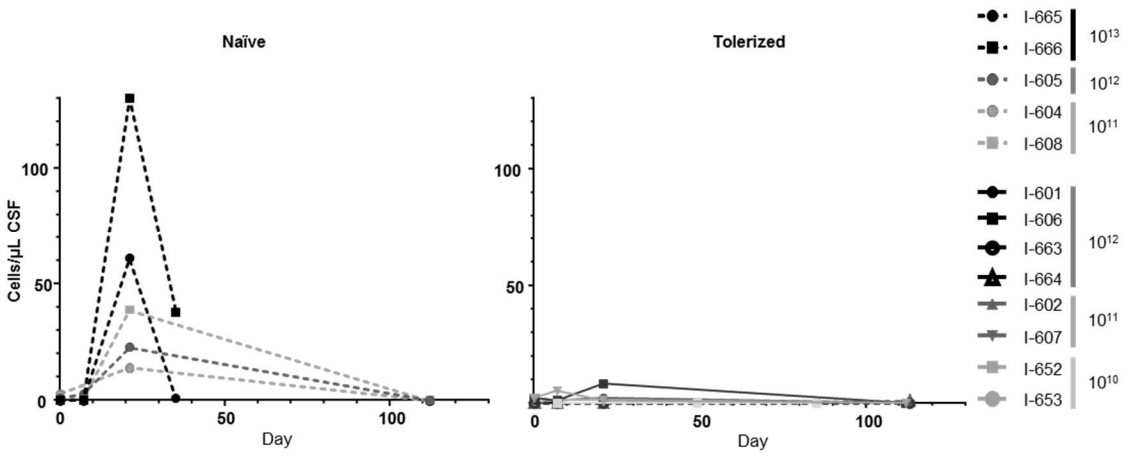

Figure 5-3. CSF nucleated cell counts following intrathecal AAV9 injection. Total nucleated cell counts were measured in CSF samples from naïve dogs treated with intrathecal AAV9 (left panel) as well as animals treated as neonates with systemic IDUA protein (I-663 and I-664) or IDUA expressing vector before receiving intrathecal AAV9 (right panel).

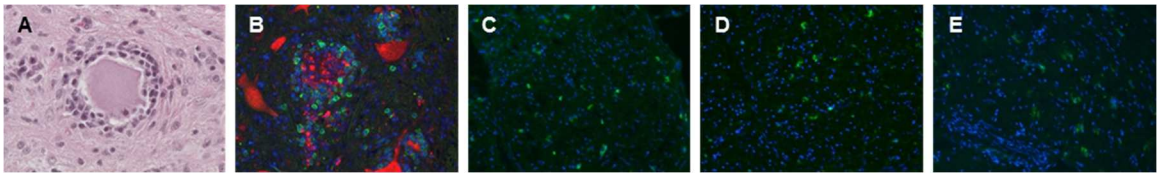

Figure 5-4. Lymphocyte infiltration of the lumbar spinal cord in MPS I dogs exhibiting hind limb weakness following human IDUA gene transfer. Representative sections of the lumbar spinal cord (A,B) and lumbar spinal nerve (C-E) are shown for the two naïve dogs (I-665 and I-666) treated with the highest dose of AAV9 expressing human IDUA. Sections were stained with H&E (A) or immunostained for human IDUA (red) and CD20 (green) (B,C), CD4 (D), or CD8 (E).

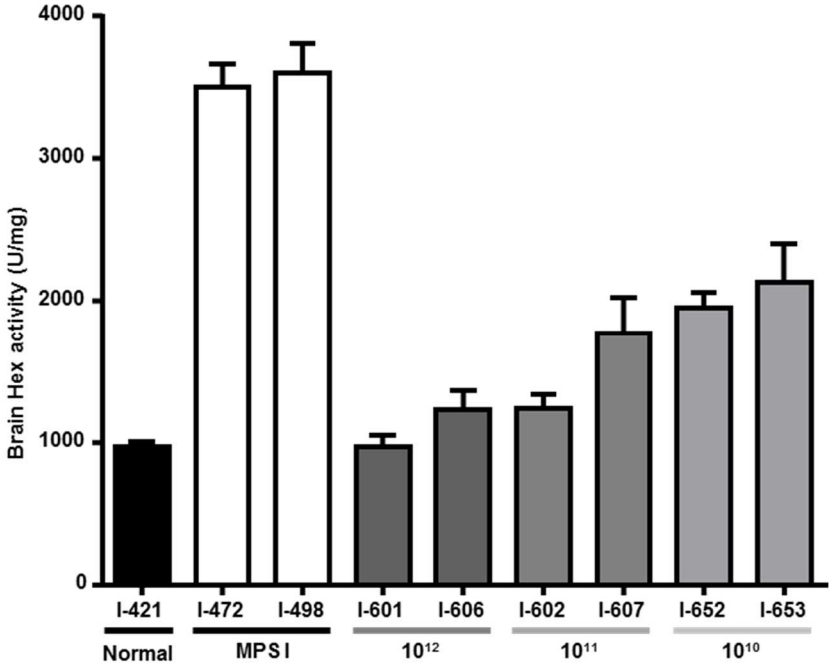

Figure 5-5. Normalization of brain hexosaminidase activity in human IDUA tolerant MPS I dogs treated with intrathecal AAV9. Hexosaminidase activity was measured in samples collected from six brain regions (frontal cortex, temporal cortex, occipital cortex, hippocampus, medulla and cerebellum). The mean activity is shown for a normal control dog, untreated MPS I dogs, and the six hIDUA tolerant dogs treated with intrathecal AAV9 expressing human IDUA. Error bars = SEM. Hex activity was significantly reduced in the high dose cohort compared to untreated controls (Kruskal-Wallis test followed by Dunn's multiple comparisons test).

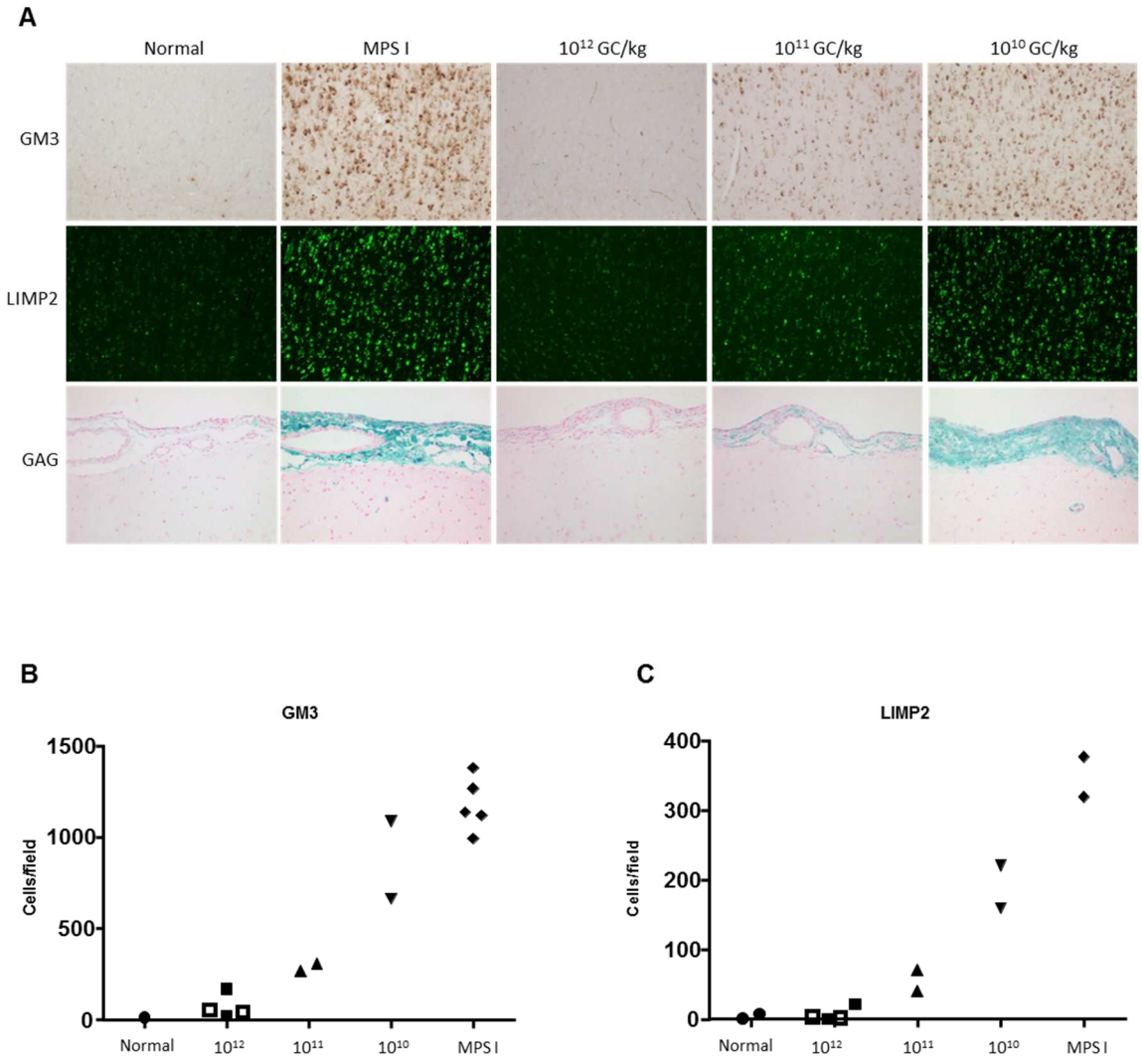

Figure 5-6. Dose-dependent correction of brain storage lesions in human IDUA tolerant dogs treated with intrathecal AAV9. Brains were sectioned and stained for LIMP2 and GM3 (A). Meningeal GAG accumulation was imaged using Alcian blue staining. Automated quantification of GM3 (B) and LIMP2 (C) positive cells was performed on cortical brain images (n = 10 per animal). Open symbols indicate animals tolerized with infusion of recombinant human IDUA. GM3 and LIMP2 were significantly reduced in the high dose cohort compared to untreated controls (Kruskal-Wallis test followed by Dunn's multiple comparisons test).

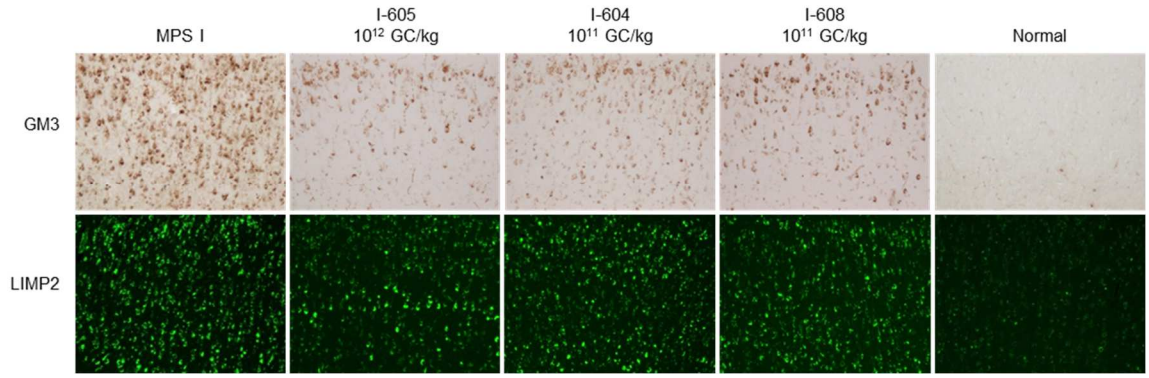

Figure 5-7. Partial correction of brain storage lesions in dogs treated with intrathecal AAV9 expressing human IDUA. Brains were sectioned and stained for LIMP2 and GM3.

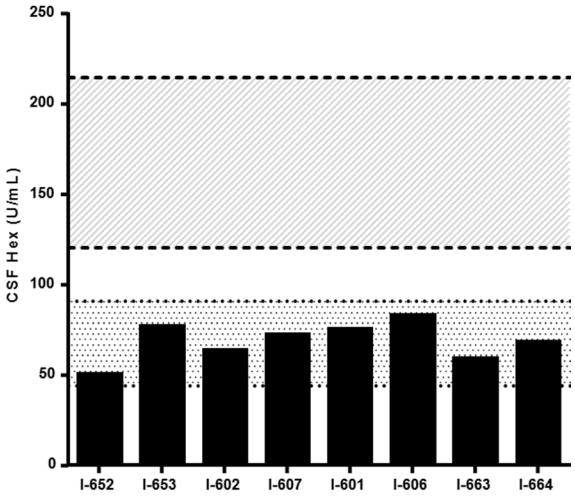

Figure 5-8. Normalization of CSF hexosaminidase activity after IT AAV9 treatment. Hex activity was measured in CSF of MPS I dogs tolerized to human IDUA at the end of the study. The shaded region represents CSF hex acitivity in untreated MPS I dogs. The dotted region indicates the normal range.

Table 5-1. Vector biodistribution

Dose	Animal Number	Frontal Cortex	Temporal Cortex	Occipital Cortex	Hippocampus	Medulla	Cerebellum	Cervical Spinal Cord	Thoracic Spinal Cord	Lumbar Spinal Cord	Heart	Lung	Liver	Spleen
1e10 GC / kg	652†	0.0021	0.0043	0.0620	0.0441	0.0980	0.0214	0.0123	0.0096	0.0170	0.0077	0.0022	0.0050	0.0015
	653†	0.0087	0.0046	0.0008	0.0054	0.0044	0.0011	0.0020	0.0016	NA	‹0.0005	0.0025	0.0010	0.0014
1e11 GC / kg	604	0.0078	0.0122	0.0033	0.0112	0.0071	0.0008	0.0150	0.0129	0.0063	‹0.0005	‹0.0005	0.0016	0.0031
	608	0.0480	0.0043	0.0031	0.0624	0.0087	0.0108	0.0025	0.0079	0.0063	‹0.0005	0.0005	0.0009	0.0014
	602†	0.0151	0.0033	0.0029	0.0178	0.0144	0.0011	0.1120	0.0006	0.0077	0.0012	‹0.0005	0.0054	0.0008
	607†	0.0069	0.0079	0.0025	0.0041	0.0030	0.0012	0.0028	0.0039	‹0.0005	0.0008	‹0.0005	0.0013	0.0025
1e12 GC / kg	605†	0.0153	0.0040	0.0166	0.0078	0.0325	0.0033	0.0447	0.2899	0.0592	0.0226	‹0.0005	0.0011	‹0.0005
	601†	0.1587	0.4328	0.1720	NA	0.1339	0.0113	0.1128	0.0701	0.0466	0.0013	‹0.0005	0.0010	0.0005
	606	0.0831	0.1264	0.0725	0.0209	0.0682	0.0188	0.0531	0.0242	0.0663	0.0008	‹0.0005	0.0025	0.0027
1e13 GC / kg	665	0.3790	0.7676	0.2262	0.0324	0.0484	0.0518	0.7661	0.5163	0.6688	0.0110	0.0055	0.3554	0.1286
	666	2.3428	0.4896	0.4006	NA	0.1169	0.0938	0.3797	1.5287	0.8769	0.0056	0.0008	0.2507	0.1418

† = Tolerized with 5e12 GC / kg hIDUA on postnatal day 5

NA = (sample) not analyzed

Limit of detection = 0.0005 GC/dg

CHAPTER 6: General discussion

Three decades ago it was demonstrated that the coding sequences of the adeno-associated virus genome could be provided in *trans*, allowing for the generation of infectious particles in which the endogenous genome was replaced with a transgene (Samulski, Chang, and Shenk 1989, 1987). This discovery would revolutionize gene therapy—for the first time it became possible to achieve *in vivo* gene transfer with a vector that did not cause insertional mutagenesis, nor elicit destructive immune responses against the transgene product. The emergence of AAV for *in vivo* gene therapy left only two major challenges: a relatively limited packaging capacity of around 5 kb, and because of the non-integrating nature of the vector, only quiescent tissues such as heart, skeletal muscle, liver, retina and brain could be stably transduced. The past two decades have seen rapid development of AAV based therapies targeting these tissues, with repeated demonstrations of efficacy in animal models. Targeting the retina yielded one of the first clinical successes; subretinal delivery of an AAV vector expressing *RPE65* rescued vision loss in a canine model of Leber's congenital amaurosis, and soon after demonstrated efficacy in children with the disease (Acland et al. 2001, Bainbridge et al. 2008, Maguire et al. 2009). Though many other early successes in animal models of liver and muscle directed gene therapy couldn't be replicated in the clinic, the development of a second generation of more efficient vectors made targeting these tissues a reality, leading to successful trials for hemophilia B and lipoprotein lipase deficiency (Nathwani et al. 2011, Bryant et al. 2013, Gao et al. 2002, Gao et al. 2004, Xiao et al. 1999).

Among the tissues initially targeted with AAV gene therapy, the brain has lagged behind in terms of clinical success. Trials of AAV mediated gene transfer to the brain

have demonstrated possible small benefits in Canavan disease and aromatic amino acid decarboxylase (AADC) deficiency, and expression of AADC in the brain has been demonstrated for several years after gene transfer by PET imaging (Mittermeyer et al. 2012, Janson et al. 2002, Leone et al. 2012, Hwu et al. 2012). While these studies and others have established a strong safety profile for AAV in the brain, there has yet to be a major clinical success for CNS-directed gene transfer. The primary obstacle to the field has been delivery—injection into the brain requires an invasive neurosurgical procedure, and can only transduce a small region surrounding the injection site (Vite et al. 2005). Some diseases affecting a single brain nucleus may be responsive to localized injection of the vector, but many genetic diseases affect cells throughout the CNS, making localized delivery ineffective. Studies in dog and cat models of genetic diseases demonstrated that reasonably widespread correction could sometimes be achieved with as few as 4-6 injections, however scaled from a 30-70 g cat or dog brain to a 1.4 kg human brain, more than 100 injections would be required for equivalent breadth of transduction (Vite et al. 2005, Ciron et al. 2006). Vector injection into the brain parenchyma can also induce inflammation that may elicit adaptive immune response to the transgene product; in studies in both dogs and NHP, transduced cells surrounding the injection site have been the target of T cell mediated killing (Ciron et al. 2006, Samaranch, San Sebastian, et al. 2013).

A critical advance for CNS gene therapy was the discovery that some novel AAV serotypes, particularly AAV9, could transduce neurons in the brain and spinal cord after intravascular delivery (Foust et al. 2009). This made it possible for the first time to achieve transduction of a large number of cells throughout the CNS without an invasive procedure. Intravenous AAV9 delivery demonstrated remarkable success in a mouse

model of spinal muscular atrophy (SMA), a disease affecting lower motor neurons throughout the spinal cord (Foust et al. 2010). Treating newborn animals allowed for transduction of a large fraction of spinal cord motor neurons, leading to increased survival and improved motor function. This approach is now progressing into clinical trials for SMA, as well as the lysosomal storage disease MPS IIIa. However, while intravenous AAV9 delivery has been an important step for the field, CNS transduction is much less efficient in large animals than in newborn mice, with very limited transduction in the brain even at extremely large vector doses (Hinderer, Bell, Vite, et al. 2014, Bevan et al. 2011, Gray et al. 2011). The resulting high levels of peripheral transduction limit this approach to diseases in which the vector has no peripheral toxicity even at very high doses. Intravenous AAV9 delivery is also very sensitive to the presence of pre-existing capsid antibodies, limiting the number of patients eligible for therapy. This approach may be clinically useful for select applications, but will not be sufficient for many diseases affecting the CNS.

The shortcomings of both intraparenchymal and systemic AAV delivery for CNS gene transfer have left a need for an efficient, non-invasive method to target a vector to large regions of the CNS. Delivery into CSF seems a reasonable option, given that this approach can theoretically achieve high vector concentrations in the CNS, and allow for broad distribution throughout the brain and spinal cord. However, intrathecal delivery has not often been pursued as a method for delivery of biologics to the CNS. This is rooted in a widely held perception that there is minimal interaction between CSF and the brain parenchyma, as the CSF is confined to the space between the arachnoid and the pia mater covering the brain (Papisov, Belov, and Gannon 2013). However, many studies have now demonstrated the exchange of CSF with brain interstitial fluid and the ability of

macromolecules to distribute to the brain following intrathecal delivery (Iliff et al. 2013, Iliff et al. 2012, Calias et al. 2012). This observation has extended to AAV vectors; there have been multiple demonstrations of transduction in the brain and spinal cord after intrathecal AAV delivery in mice, dogs, cats, and nonhuman primates (Haurigot et al. 2013, Gray et al. 2013, Samaranch, Salegio, et al. 2013, Hinderer, Bell, Vite, et al. 2014, Bucher et al. 2014b). These studies demonstrated widespread transduction of both neurons and glial cells throughout the brain following AAV9 delivery into the CSF. Transduction in the brain was not associated with inflammation or immune responses directed against transduced cells, as had been seen in some studies of intraparenchymal injection. In addition to brain transduction, a very large proportion of spinal cord motor neurons can be transduced by a single intrathecal vector injection. This approach thus offers the potential for widespread CNS transduction with a minimally invasive injection. An added advantage is that very little serum IgG crosses into the CSF, making intrathecal vector delivery insensitive to the presence of pre-existing antibodies against the AAV capsid, potentially extending this approach to individuals who would not be candidates for systemic vector delivery (Haurigot et al. 2013).

The transduction pattern achieved with IT AAV suggests some clear clinical applications. The efficient transduction of spinal cord motor neurons shows strong potential for the treatment of lower motor neuron disease. The transduction of a fraction of cells throughout the cerebrum may not be sufficient for many diseases in which a defective gene is essential for function of every cell. However, for many of the lysosomal storage diseases, in which some of the enzyme produced can be secreted and taken up by neighboring cells, even a relatively small number of cells spread throughout the brain

could lead to widespread correction (Sando and Neufeld 1977). Efficacy has already been demonstrated in animal models of diseases such as MPS IIIa, and MPS I, and other diseases that exhibit cross correction may also be good targets for intrathecal AAV delivery (Haurigot et al. 2013, Hinderer, Bell, et al. 2014a). For lower motor neurons, an extremely promising target is SMA. Intrathecal AAV9 delivery has been shown to efficiently rescue the neuromuscular phenotype in mice, and parallel studies in nonhuman primates demonstrate that levels of transduction required for efficacy can readily be achieved in large animals at moderate vector doses (Meyer et al. 2014, Passini et al. 2014). Intrathecal AAV9 expressing an shRNA against superoxide dismutase 1 (SOD1) has also shown promise in animal models of dominantly inherited amyotrophic lateral sclerosis, effectively reducing levels of the toxic protein in lower motor neurons (Foust et al. 2013). However, ALS also affects upper motor neurons residing in the cerebral cortex, and the impact of the vector on SOD1 expression in these cells has not been demonstrated.

Expanding on the success of intrathecal AAV delivery and bringing this approach to new disease targets will require that several issues are addressed. One is a problem of animal models. Preclinical studies should ideally be carried out in a model that not only reflects that pathophysiology of the disease, but also is amenable to the clinical route of administration and consequently exhibits the vector biodistribution expected patients. Knockout mouse models may be problematic for these studies, since some routes of intrathecal administration are technically challenging to replicate in these animals. Intraventricular delivery is readily carried out in mice, although the vector distribution resulting from intraventricular delivery in the small mouse CNS clearly differs from that in larger animals (Haurigot et al. 2013). For some diseases the availability of

large animal models will facilitate this process. We used canine and feline models to develop IT gene therapy for MPS I. Large animal models have been identified for many other lysososmal storage diseases, such as MPS VII, mannosidosis, GM1 and GM2 gangliosidoses, and an induced model was developed in pigs to evaluate IT gene transfer for SMA (Duque et al. 2015, Haskins 2009). For many other diseases, however, no large animal model will be available. Extrapolating biodistribution data from large animals may help to inform efficacy assessments in mouse models. For example, studies using SMA mice evaluated the extent of motor neuron transduction necessary to rescue the disease phenotype, then used reporter gene studies in nonhuman primates to identify a dose capable of similar transduction levels (Meyer et al. 2014, Passini et al. 2014). More creative approaches like this may be essential to developing IT gene therapy for diseases for which only mouse models are available.

A second important issue that will need to be considered is the potential for systemic distribution of a vector after IT delivery. Studies in dogs, mice, nonhuman primates, and cats have shown peripheral transduction after IT delivery (Hinderer, Bell, et al. 2014a, Hinderer, Bell, Vite, et al. 2014, Haurigot et al. 2013). This finding has revealed further limitations of the prevailing view of CSF circulation—in the past it was thought that CSF was resorbed entirely through arachnoid granulations of the meninges, which is inconsistent with the observation of efficient and rapid escape of viral particles from CSF to blood. This finding is, however, consistent with the more recent identification of perivascular channels and CNS lymphatics that allow for drainage of particles from CSF to the periphery (Iliff et al. 2012, Iliff et al. 2013). The implications of peripheral distribution will vary depending on disease—in the lysosomal storage diseases, systemic distribution and liver transduction may actually be beneficial, as

these enzymes are ubiquitously expressed and can treat somatic as well as CNS disease. However, for many other diseases hepatic targeting may be detrimental and additional measures such as tissue specific promoters may be needed to achieve adequate safety.

Another important issue for IT AAV delivery is that of dose scaling between animal models and patients. For systemic applications dosing has typically been based on body weight. For intrathecal delivery, the vector dose should presumably be based on the targeted compartment, since the primary activity and toxicity of the vector would be expected to be based on the concentration of vector in CSF. CSF volume does not exhibit a static relationship with body weight across species or animals of different ages, so it will be important to scale doses according to the actual size of CNS. Rather than basing doses on CSF volume, our approach has been to scale doses based on brain mass, since much more detailed data are available for humans and animals of different ages, and because brain size appears to have a linear relationship with CSF volume across species. Since there is systemic distribution of vector after IT delivery, it will be important to also consider the dose relative to body weight when comparing doses found to be safe in preclinical studies with those used in first in human trials to avoid potential systemic toxicity. This could be especially important in infants, whose brain to body mass ratio is greater than that of animal species commonly used for toxicology studies.

To expand IT AAV delivery to new targets it will be important to better elucidate the transduction patterns in the CNS. Motor neurons are clearly efficiently targeted in all species, but the other cell types transduced have varied between studies. In nonhuman primates we have observed predominately neuron-restricted expression, particularly the pyramidal cortical neurons and purkinje cells in cerebellum (Hinderer, Bell, Vite, et al.

2014). Others have reported more extensive glial transduction, including astrocytes and oligodendrocytes (Samaranch, Salegio, et al. 2013, Bucher et al. 2014b). For some disorders in which the transgene product can be secreted, targeting any cells in the CNS could potentially be beneficial. For other disorders, particular cell types and even very specific functional subsets of neurons may need to be transduced for efficacy, and transduction of other cell types may be toxic. This may necessitate careful capsid and promoter selection to achieve the required degree of selectivity.

Progressing IT gene transfer will also require a broader understanding of the factors leading to immune responses in CNS and the consequences of immunity. IT delivery appears to circumvent the T cell-mediated immune response to transgene products that has been observed with intraparenchymal delivery; however there has been one report of potential immunological toxicity after intrathecal AAV9 delivery expressing GFP in a nonhuman primate, indicating the need for careful monitoring and more detailed studies (Samaranch, San Sebastian, et al. 2013). The potential for antibody responses to secreted transgenes in the CNS will also be important. In MPS I dogs there was a high rate of antibody induction to the transgene product, which while not associated with toxicity, did reduce the efficacy of cross-correction. The clinical experience with intrathecal delivery of the enzyme indicates that antibody induction against the protein in CSF is not likely to occur in humans, but this provides an important example of a potential challenge for IT gene therapy with secreted transgene products (Vera et al. 2013). We have demonstrated that such responses can be prevented in MPS I dogs and nonhuman primates through exposure to the enzyme in the first week of life, which could be a viable approach for diseases in which newborn screening is commonly employed. This method can also be useful for preclinical studies of vectors

expressing human proteins as a means of preventing antibody responses to the non-species-specific transgene which would otherwise preclude evaluation of efficacy in animal models.

Another critical issue for IT AAV delivery will be the route of administration. There are many potential routes for CSF access; lumbar puncture is the most common, but cannulation of the lateral ventricle is also possible, and CSF can be accessed at the cervical level by lateral C1-2 puncture or suboccipital puncture. Our group and others have found that lumbar puncture results in very inefficient delivery of vector to the brain, whereas delivery into the cisterna magna by suboccipital puncture results in efficient transduction in both brain and spinal cord (Hinderer, Bell, Vite, et al. 2014). Suboccipital puncture is not commonly used clinically due to the greater risks that were associated with targeting near the brainstem and surrounding vessels in the pre-imaging era, although today the procedure can be readily performed with image guidance (Saunders and Riordan 1929, Pomerantz, Buchbinder, and Hirsh 2005). CSF access is also routinely achieved at approximately the same location by lateral puncture of the dorsal subarachnoid space between the first and second vertebrae. We have found that this approach is not feasible in MPS I patients due to abnormal thickening of the cervical meninges, although C1-2 puncture may be a reasonable option for many other applications. Future preclinical studies would be needed to verify similar distribution after C1-2 puncture relative to suboccipital puncture. Finally intraventricular delivery is a possibility, and has been shown to result in biodistribution similar to intracisternal delivery in dogs (Haurigot et al. 2013). However, ventricular delivery has the disadvantage of the requirement for a neurosurgical procedure. Also, the penetration of the brain parenchyma raises the possibility for the same type of localized inflammatory

response and induction of immunity against the transgene product that has been observed following intraparenchymal vector delivery.

IT AAV delivery represents a critical advance in our approach to the treatment of inherited neurologic disease. Gene therapy targeting the brain has slowly become possible through the advent of AAV vectors, followed by the discovery of more efficient serotypes for CNS gene transfer. The development of IT delivery represents a critical next step in this process, providing for the first time a minimally invasive method to deliver the vector to large portions of the brain and spinal cord. This will not be the final solution for CNS gene therapy—there are still many diseases for which more extensive transduction, precise regulation of transgene expression, or specific cell targeting will be necessary for successful treatment. However, IT AAV delivery has unlocked the possibility of gene therapy for many previously elusive targets, and could pave way for the first clinical successes for neurological disorders.

BIBLIOGRAPHY

Acland, G. M., G. D. Aguirre, J. Ray, Q. Zhang, T. S. Aleman, A. V. Cideciyan, S. E. Pearce-Kelling, V. Anand, Y. Zeng, A. M. Maguire, S. G. Jacobson, W. W. Hauswirth, and J. Bennett. 2001. "Gene therapy restores vision in a canine model of childhood blindness." *Nat Genet* 28 (1):92-5. doi: 10.1038/88327.

Adkins, B. 1999. "T-cell function in newborn mice and humans." *Immunol Today* 20 (7):330-5.

Ahmed, Alia, Chester B. Whitley, Renee Cooksley, Kyle Rudser, Stephanie Cagle, Nadia Ali, Kathleen Delaney, Brianna Yund, and Elsa Shapiro. 2014. "Neurocognitive and neuropsychiatric phenotypes associated with the mutation L238Q of the alpha-L-iduronidase gene in Hurler-Scheie syndrome." *Molecular Genetics and Metabolism* 111 (2):123-127. doi: 10.1016/j.ymgme.2013.11.014.

Aldenboven, M., F. Boelens, and T. F. de Koning. 2008. "The clinical outcome of Hurler syndrome after stem cell transplantation." *Biology of Blood and Marrow Transplantation* 14 (5):485-498. doi: 10.1016/j.bbmt.2008.01.009.

Ayer, J. B. 1920. "Puncture of the cisterna magna." *Archives of Neurology & Psychiatry* 4 (5):529-541. doi: 10.1001/archneurpsyc.1920.02180230052005.

Bainbridge, James W.B., Alexander J. Smith, Susie S. Barker, Scott Robbie, Robert Henderson, Kamaljit Balaggan, Ananth Viswanathan, Graham E. Holder, Andrew Stockman, Nick Tyler, Simon Petersen-Jones, Shomi S. Bhattacharya, Adrian J. Thrasher, Fred W. Fitzke, Barrie J. Carter, Gary S. Rubin, Anthony T. Moore, and Robin R. Ali. 2008. "Effect of Gene Therapy on Visual Function in Leber's Congenital Amaurosis." *New England Journal of Medicine* 358 (21):2231-2239. doi: doi:10.1056/NEJMoa0802268.

Bankiewicz, K. S., J. L. Eberling, M. Kohutnicka, W. Jagust, P. Pivirotto, J. Bringas, J. Cunningham, T. F. Budinger, and J. Harvey-White. 2000. "Convection-enhanced delivery of AAV vector in parkinsonian monkeys; in vivo detection of gene expression and restoration of dopaminergic function using pro-drug approach." *Exp Neurol* 164 (1):2-14. doi: 10.1006/exnr.2000.7408.

Bankiewicz, Krystof S., John Forsayeth, Jamie L. Eberling, Rosario Sanchez-Pernaute, Philip Pivirotto, John Bringas, Peter Herscovitch, Richard E. Carson, William Eckelman, Bryan Reutter, and Janet Cunningham. 2006. "Long-Term Clinical Improvement in MPTP-Lesioned Primates after Gene Therapy with AAV-hAADC." *Mol Ther* 14 (4):564-570.

Bartus, R. T., M. S. Weinberg, and R. J. Samulski. 2014. "Parkinson's disease gene therapy: success by design meets failure by efficacy." *Mol Ther* 22 (3):487-97. doi: 10.1038/mt.2013.281.

Bartus, Raymond T., Christopher D. Herzog, Yaping Chu, Alistair Wilson, Lamar Brown, Joao Siffert, Eugene M. Johnson, C. Warren Olanow, Elliott J. Mufson, and Jeffrey H. Kordower. 2011. "Bioactivity of AAV2-neurturin gene therapy (CERE-120): Differences between Parkinson's disease and nonhuman primate brains." *Movement Disorders* 26 (1):27-36. doi: 10.1002/mds.23442.

Beck, M., P. Arn, R. Giugliani, J. Muenzer, T. Okuyama, J. Taylor, and S. Fallet. 2014. "The natural history of MPS I: global perspectives from the MPS I Registry." *Genet Med* 16 (10):759-65. doi: 10.1038/gim.2014.25.

Bell, Peter, Guangping Gao, Mark E Haskins, Lili Wang, Meg Sleeper, Huan Wang, Roberto Calcedo, Luk H Vandenberghe, Shu-Jen Chen, and Chick Weisse. 2011. "Evaluation of adeno-associated viral vectors for liver-directed gene transfer in dogs." *Human gene therapy* 22 (8):985-997.

Bevan, A. K., S. Duque, K. D. Foust, P. R. Morales, L. Braun, L. Schmelzer, C. M. Chan, M. McCrate, L. G. Chicoine, B. D. Coley, P. N. Porensky, S. J. Kolb, J. R. Mendell, A. H. M. Burghes, and B. K. Kaspar. 2011. "Systemic gene delivery in large species for targeting spinal cord, brain, and peripheral tissues for pediatric disorders." *Molecular Therapy* 19 (11):1971-1980. doi: 10.1038/mt.2011.157.

Billingham, R. E., L. Brent, and P. B. Medawar. 1953. "Actively acquired tolerance of foreign cells." *Nature* 172 (4379):603-6.

Björklund, A., D. Kirik, C. Rosenblad, B. Georgievska, C. Lundberg, and R. J. Mandel. 2000. "Towards a neuroprotective gene therapy for Parkinson's disease: use of adenovirus, AAV and lentivirus vectors for gene transfer of GDNF to the nigrostriatal system in the rat Parkinson model." *Brain Research* 886 (1–2):82-98. doi: http://dx.doi.org/10.1016/S0006-8993(00)02915-2.

Boelens, J. J., R. F. Wynn, A. O'Meara, P. Veys, Y. Bertrand, G. Souillet, J. E. Wraith, A. Fischer, M. Cavazzana-Calvo, K. W. Sykora, P. Sedlacek, A. Rovelli, Cspm Uiterwaal, and N. Wulffraat. 2007. "Outcomes of hematopoietic stem cell transplantation for Hurler's syndrome in Europe: a risk factor analysis for graft failure." *Bone Marrow Transplantation* 40 (3):225-233. doi: 10.1038/sj.bmt.1705718.

Bohn, M. C., D. L. Choi-Lundberg, B. L. Davidson, C. Leranth, D. A. Kozlowski, J. C. Smith, M. K. O'Banion, and D. E. Redmond, Jr. 1999. "Adenovirus-mediated transgene expression in nonhuman primate brain." *Hum Gene Ther* 10 (7):1175-84. doi: 10.1089/10430349950018166.

Braunlin, E. A., N. R. Stauffer, C. H. Peters, J. L. Bass, J. M. Berry, J. J. Hopwood, and W. Krivit. 2003. "Usefulness of bone marrow transplantation in the Hurler syndrome." *American Journal of Cardiology* 92 (7):882-886. doi: 10.1016/s0002-9149(03)00909-3.

Bryant, Laura M., Devin M. Christopher, April R. Giles, Christian Hinderer, Jesse L. Rodriguez, Jenessa B. Smith, Elizabeth A. Traxler, Josh Tycko, Adam P. Wojno, and James M. Wilson. 2013. "Lessons learned from the clinical development and market authorization of Glybera." *Human gene therapy. Clinical development* 24 (2):55-64. doi: 10.1089/humc.2013.087.

Bucher, T., L. Dubreil, M. A. Colle, M. Maquigneau, J. Deniaud, M. Ledevin, P. Moullier, and B. Joussemet. 2014a. "Intracisternal delivery of AAV9 results in oligodendrocyte and motor neuron transduction in the whole central nervous system of cats." *Gene Ther*. doi: 10.1038/gt.2014.16.

Bucher, Thomas, Laurence Dubreil, Marie-Anne Colle, M Maquigneau, Johan Deniaud, Mireille Ledevin, Philippe Moullier, and Béatrice Joussemet. 2014b. "Intracisternal delivery of AAV9 results in oligodendrocyte and motor neuron transduction in the whole central nervous system of cats." *Gene therapy* 21 (5):522-528.

Buchlis, G., G. M. Podsakoff, A. Radu, S. M. Hawk, A. W. Flake, F. Mingozzi, and K. A. High. 2012. "Factor IX expression in skeletal muscle of a severe hemophilia B patient 10 years after AAV-mediated gene transfer." *Blood* 119 (13):3038-41. doi: 10.1182/blood-2011-09-382317.

Burns, R S, C C Chiueh, S P Markey, M H Ebert, D M Jacobowitz, and I J Kopin. 1983. "A primate model of parkinsonism: selective destruction of dopaminergic neurons in the pars compacta of the substantia nigra by N-methyl-4-phenyl-1,2,3,6-tetrahydropyridine." *Proceedings of the National Academy of Sciences* 80 (14):4546-4550.

Calias, P., M. Papisov, J. Pan, N. Savioli, V. Belov, Y. Huang, J. Lotterhand, M. Alessandrini, N. Liu, A. J. Fischman, J. L. Powell, and M. W. Heartlein. 2012. "CNS penetration of intrathecal-lumbar idursulfase in the monkey, dog and mouse: implications for neurological outcomes of lysosomal storage disorder." *Plos One* 7 (1):13. doi: 10.1371/journal.pone.0030341.

Castle, M. J., E. Perlson, E. L. Holzbaur, and J. H. Wolfe. 2014. "Long-distance axonal transport of AAV9 is driven by dynein and kinesin-2 and is trafficked in a highly motile Rab7-positive compartment." *Mol Ther* 22 (3):554-66. doi: 10.1038/mt.2013.237.

Chen, A., C. Vogler, M. McEntee, S. Hanson, N. M. Ellinwood, J. Jens, E. Snella, M. Passage, S. Le, C. Guerra, and P. Dickson. 2011. "Glycosaminoglycan storage in neuroanatomical regions of mucopolysaccharidosis I dogs following intrathecal recombinant human iduronidase." *Apmis* 119 (8):513-521. doi: 10.1111/j.1600-0463.2011.02760.x.

Ciron, C., N. Desmaris, M. A. Colle, S. Raoul, B. Joussemet, L. Verot, J. Ausseil, R. Froissart, F. Roux, Y. Cherel, Y. Lajat, B. Schwartz, M. T. Vanier, I. Maire, M. Tardieu, P. Moullier, and J. M. Heard. 2006. "Gene therapy of the brain in the dog model of Hurler's syndrome." *Annals of Neurology* 60 (2):204-213. doi: 10.1002/ana.20870.

Clarke, L. A., J. E. Wraith, M. Beck, E. H. Kolodny, G. M. Pastores, J. Muenzer, D. M. Rapoport, K. I. Berger, M. Sidman, E. D. Kakkis, and G. F. Cox. 2009. "Long-term efficacy and safety of laronidase in the treatment of mucopolysaccharidosis I." *Pediatrics* 123 (1):229-40. doi: 10.1542/peds.2007-3847.

Constantopoulos, George, Khalid Iqbal, and Anatole S. Dekaban. 1980. "Mucopolysaccharidosis Types IH, IS, II and IIIA: Glycosaminoglycans and Lipids of Isolated Brain Cells and Other Fractions from Autopsied Tissues." *Journal of Neurochemistry* 34 (6):1399-1411. doi: 10.1111/j.1471-4159.1980.tb11220.x.

Crudele, J. M., J. D. Finn, J. I. Siner, N. B. Martin, G. P. Niemeyer, S. Zhou, F. Mingozzi, C. D. Lothrop, Jr., and V. R. Arruda. 2015. "AAV liver expression of FIX-Padua prevents and eradicates FIX inhibitor without increasing thrombogenicity in hemophilia B dogs and mice." *Blood*. doi: 10.1182/blood-2014-07-588194.

Dahms, N. M., P. Lobel, and S. Kornfeld. 1989. "Mannose 6-phosphate receptors and lysosomal-enzyme targeting." *Journal of Biological Chemistry* 264 (21):12115-12118.

de Ru, M. H., J. J. Boelens, A. M. Das, S. A. Jones, J. H. van der Lee, N. Mahlaoui, E. Mengel, M. Offringa, A. O'Meara, R. Parini, A. Rovelli, K. W. Sykora, V. Valayannopoulos, A. Vellodi, R. F. Wynn, and F. A. Wijburg. 2011. "Enzyme replacement therapy and/or hematopoietic stem cell transplantation at diagnosis in patients with mucopolysaccharidosis type I: results of a European consensus procedure." *Orphanet Journal of Rare Diseases* 6:9. doi: 10.1186/1750-1172-6-55.

Dickson, P., N. M. Ellinwood, A. Dierenfeld, K. Kline, J. Parkes, S. Hanson, C. Vite, A. Mlikotic, A. Chen, W. Gross, M. Haskins, K. Ponder, and S. Le. 2010. "Intrathecal enzyme replacement therapy treats meningeal storage and spinal cord

compression in MPS I dogs." *Molecular Genetics and Metabolism* 99 (2):S15-S15. doi: 10.1016/j.ymgme.2009.10.053.

Dickson, P. I., N. M. Ellinwood, S. Hanson, C. Vite, M. Passage, S. Le, and C. Guerra. 2009. "Intrathecal enzyme replacement therapy may stabilize or reverse signs of spinal cord compression in MPS I dogs." *Molecular Genetics and Metabolism* 98 (1-2):70-70.

Dickson, P. I., S. Hanson, M. F. McEntee, C. H. Vite, C. A. Vogler, A. Mlikotic, A. H. Chen, K. P. Ponder, M. E. Haskins, B. L. Tippin, S. Q. Le, M. B. Passage, C. Guerra, A. Dierenfeld, J. Jens, E. Snella, S. H. Kan, and N. M. Ellinwood. 2010. "Early versus late treatment of spinal cord compression with long-term intrathecal enzyme replacement therapy in canine mucopolysaccharidosis type I." *Molecular Genetics and Metabolism* 101 (2-3):115-122. doi: 10.1016/j.ymgme.2010.06.020.

Dickson, P. I., D. Naylor, A. Mlikotic, A. Victoroff, A. Chen, M. Passage, S. Le, and M. P. S. Intrathecal Res Collaborat. 2008. "Intrathecal recombinant human a-L-iduronidase alleviates spinal cord compression symptoms and is well-tolerated in attenuated MPS I patients." *Molecular Genetics and Metabolism* 93 (3):247-247.

Dickson, P., D. Naylor, A. Mlikotic, A. Victoroff, A. Chen, M. Passage, and S. Le. 2008. "Initial experience with intrathecal recombinant human alpha-L-iduronidase for spinal cord compression in two mucopolysaccharidosis I patients." *Molecular Genetics and Metabolism* 93 (2):S19-S19. doi: 10.1016/j.ymgine.2007.10.034.

Dickson, Patricia I., N. Matthew Ellinwood, Jillian R. Brown, Robert G. Witt, Steven Q. Le, Merry B. Passage, Moin U. Vera, and Brett E. Crawford. 2012. "Specific antibody titer alters the effectiveness of intrathecal enzyme replacement therapy in canine mucopolysaccharidosis I." *Molecular Genetics and Metabolism* 106 (1):68-72. doi: 10.1016/j.ymgme.2012.02.003.

Dickson, Patricia, Maryn Peinovich, Michael McEntee, Thomas Lester, Steven Le, Aimee Krieger, Hayden Manuel, Catherine Jabagat, Merry Passage, and Emil D. Kakkis. 2008. "Immune tolerance improves the efficacy of enzyme replacement therapy in canine mucopolysaccharidosis I." *Journal of Clinical Investigation* 118 (8):2868-2876. doi: 10.1172/jci34676.

Duque, Sandra I, W David Arnold, Philipp Odermatt, Xiaohui Li, Paul N Porensky, Leah Schmelzer, Kathrin Meyer, Stephen J Kolb, Daniel Schümperli, and Brian K Kaspar. 2015. "A large animal model of spinal muscular atrophy and correction of phenotype." *Annals of neurology* 77 (3):399-414.

Ellinwood, N. M., M. A. Colle, M. A. Well, M. L. Casal, C. H. Vite, S. Wiemelt, C. W. Hasson, T. M. O'Malley, X. X. He, U. Prociuk, L. Verot, J. R. Melniczek, A. Lannon, G. D. Aguirre, V. W. Knox, S. M. Evans, M. T. Vanier, E. H. Schuchman, S. U. Walkley, and M. E. Haskins. 2007. "Bone marrow transplantation for feline mucopolysaccharidosis I." *Molecular Genetics and Metabolism* 91 (3):239-250. doi: 10.1016/j.ymgme.2007.03.001.

Ellinwood, N. Matthew, Jerome Ausseil, Nathalie Desmaris, Stephanie Bigou, Song Liu, Jackie K. Jens, Elizabeth M. Snella, Eman E. A. Mohammed, Christopher B. Thomson, Sylvie Raoul, Beatrice Joussemet, Francoise Roux, Yan Cherel, Yaouen Lajat, Monique Piraud, Rachid Benchaouir, Stephan Hermening, Harald Petry, Roseline Froissart, Marc Tardieu, Carine Ciron, Philippe Moullier, Jennifer Parkes, Karen L. Kline, Irene Maire, Marie-Therese Vanier, Jean-Michel Heard, and Marie-Anne Colle. 2011. "Safe, Efficient, and Reproducible Gene Therapy of the Brain in the Dog Models of Sanfilippo and Hurler Syndromes." *Mol Ther* 19

(2):251-259. doi: http://www.nature.com/mt/journal/v19/n2/suppinfo/mt2010265s1.html.
Emborg, M. E., M. Carbon, J. E. Holden, M. J. During, Y. Ma, C. Tang, J. Moirano, H. Fitzsimons, B. Z. Roitberg, E. Tuccar, A. Roberts, M. G. Kaplitt, and D. Eidelberg. 2007. "Subthalamic glutamic acid decarboxylase gene therapy: changes in motor function and cortical metabolism." *J Cereb Blood Flow Metab* 27 (3):501-9. doi: 10.1038/sj.jcbfm.9600364.
Fan, X., A. Ang, S. M. Pollock-Barziv, A. I. Dipchand, P. Ruiz, G. Wilson, J. L. Platt, and L. J. West. 2004. "Donor-specific B-cell tolerance after ABO-incompatible infant heart transplantation." *Nat Med* 10 (11):1227-33. doi: 10.1038/nm1126.
Finn, Jonathan D., Margareth C. Ozelo, Denise E. Sabatino, Helen W. G. Franck, Elizabeth P. Merricks, Julie M. Crudele, Shangzhen Zhou, Haig H. Kazazian, David Lillicrap, Timothy C. Nichols, and Valder R. Arruda. 2010. "Eradication of neutralizing antibodies to factor VIII in canine hemophilia A after liver gene therapy." *Blood* 116 (26):5842-5848.
Fleming, D. R., P. J. Henslee-Downey, G. Ciocci, E. H. Romond, E. Marciniak, R. K. Munn, and J. S. Thompson. 1998. "The use of partially HLA-mismatched donors for allogeneic transplantation in patients with mucopolysaccharidosis-I." *Pediatr Transplant* 2 (4):299-304.
Foust, K. D., E. Nurre, C. L. Montgomery, A. Hernandez, C. M. Chan, and B. K. Kaspar. 2009. "Intravascular AAV9 preferentially targets neonatal neurons and adult astrocytes." *Nat Biotechnol* 27 (1):59-65. doi: 10.1038/nbt.1515.
Foust, Kevin D, Desirée L Salazar, Shibi Likhite, Laura Ferraiuolo, Dara Ditsworth, Hristelina Ilieva, Kathrin Meyer, Leah Schmelzer, Lyndsey Braun, and Don W Cleveland. 2013. "Therapeutic AAV9-mediated suppression of mutant SOD1 slows disease progression and extends survival in models of inherited ALS." *Molecular Therapy* 21 (12):2148-2159.
Foust, Kevin D, Xueyong Wang, Vicki L McGovern, Lyndsey Braun, Adam K Bevan, Amanda M Haidet, Thanh T Le, Pablo R Morales, Mark M Rich, and Arthur HM Burghes. 2010. "Rescue of the spinal muscular atrophy phenotype in a mouse model by early postnatal delivery of SMN." *Nature biotechnology* 28 (3):271-274.
Furukawa, Yutaka, Ayumi Hamaguchi, Ichiro Nozaki, Takashi Iizuka, Takeshi Sasagawa, Yosuke Shima, Satoru Demura, Hideki Murakami, Norio Kawahara, Torayuki Okuyama, Kazuo Iwasa, and Masahito Yamada. 2011. "Cervical pachymeningeal hypertrophy as the initial and cardinal manifestation of mucopolysaccharidosis type I in monozygotic twins with a novel mutation in the alpha-l-iduronidase gene." *Journal of the Neurological Sciences* 302 (1-2):121-125. doi: 10.1016/j.jns.2010.11.022.
Gao, G. P., M. R. Alvira, L. L. Wang, R. Calcedo, J. Johnston, and J. M. Wilson. 2002. "Novel adeno-associated viruses from rhesus monkeys as vectors for human gene therapy." *Proceedings of the National Academy of Sciences of the United States of America* 99 (18):11854-11859. doi: 10.1073/pnas.182412299.
Gao, G. P., Y. Lu, R. Calcedo, R. L. Grant, P. Bell, L. L. Wang, J. Figueredo, M. Lock, and J. M. Wilson. 2006. "Biology of AAV serotype vectors in liver-directed gene transfer to nonhuman primates." *Molecular Therapy* 13 (1):77-87. doi: 10.1016/j.ymthe.2005.08.017.
Gao, G. P., L. H. Vandenberghe, M. R. Alvira, Y. Lu, R. Calcedo, X. Y. Zhou, and J. A. Wilson. 2004. "Clades of Adeno-associated viruses are widely disseminated in

human tissues." *Journal of Virology* 78 (12):6381-6388. doi: 10.1128/jvi.78.12.6381-6388.2004.
Gray, S. J., S. N. Kalburgi, T. J. McCown, and R. J. Samulski. 2013. "Global CNS gene delivery and evasion of anti-AAV-neutralizing antibodies by intrathecal AAV administration in non-human primates." *Gene Therapy* 20 (4):450-459. doi: 10.1038/gt.2012.101.
Gray, S. J., V. Matagne, L. Bachaboina, S. Yadav, S. R. Ojeda, and R. J. Samulski. 2011. "Preclinical differences of intravascular AAV9 delivery to neurons and glia: A comparative study of adult mice and nonhuman primates." *Molecular Therapy* 19 (6):1058-1069. doi: 10.1038/mt.2011.72.
Hadaczek, Piotr, Jamie L. Eberling, Philip Pivirotto, John Bringas, John Forsayeth, and Krystof S. Bankiewicz. 2010. "Eight Years of Clinical Improvement in MPTP-Lesioned Primates After Gene Therapy With AAV2-hAADC." *Mol Ther* 18 (8):1458-1461.
Haskins, Mark. 2009. "Gene therapy for lysosomal storage diseases (LSDs) in large animal models." *ILAR journal* 50 (2):112-121.
Haskins, Mark E, Gustavo D Aguirre, Peter F Jezyk, Robert J Desnick, and Donald F Patterson. 1983. "The pathology of the feline model of mucopolysaccharidosis I." *The American journal of pathology* 112 (1):27.
Haskins, Mark E, Peter F Jezyk, Robert J Desnick, Susan K Mcdonough, and Donald F Patterson. 1979. "Alpha-L-iduronidase deficiency in a cat: a model of mucopolysaccharidosis I." *Pediatric research* 13 (11):1294-1297.
Haskins, ME, RJ Desnick, SK McDonough, and DF Patterson. 1979. "Mucopolysaccharidosis in a domestic short-haired cat--a disease distinct from that seen in the Siamese cat." *Journal of the American Veterinary Medical Association* 175 (4):384-387.
Haurigot, V., S. Marco, A. Ribera, M. Garcia, A. Ruzo, P. Villacampa, E. Ayuso, S. Anor, A. Andaluz, M. Pineda, G. Garcia-Fructuoso, M. Molas, L. Maggioni, S. Munoz, S. Motas, J. Ruberte, F. Mingozzi, M. Pumarola, and F. Bosch. 2013. "Whole body correction of mucopolysaccharidosis IIIA by intracerebrospinal fluid gene therapy." *Journal of Clinical Investigation* 123 (8):3254-3271. doi: 10.1172/jci66778.
He, X. X., C. M. Li, C. M. Simonaro, Q. Wan, M. E. Haskins, R. J. Desnick, and E. H. Schuchman. 1999. "Identification and characterization of the molecular lesion causing mucopolysaccharidosis type I in cats." *Molecular Genetics and Metabolism* 67 (2):106-112. doi: 10.1006/mgme.1999.2860.
Hinderer, C., P. Bell, B. L. Gurda, Q. Wang, J. P. Louboutin, Y. Zhu, J. Bagel, P. O'Donnell, T. Sikora, T. Ruane, P. Wang, M. E. Haskins, and J. M. Wilson. 2014a. "Intrathecal Gene Therapy Corrects CNS Pathology in a Feline Model of Mucopolysaccharidosis I." *Mol Ther*. doi: 10.1038/mt.2014.135.
Hinderer, C., P. Bell, B. L. Gurda, Q. Wang, J. P. Louboutin, Y. Zhu, J. Bagel, P. O'Donnell, T. Sikora, T. Ruane, P. Wang, M. E. Haskins, and J. M. Wilson. 2014b. "Liver-directed gene therapy corrects cardiovascular lesions in feline mucopolysaccharidosis type I." *Proc Natl Acad Sci U S A* 111 (41):14894-9. doi: 10.1073/pnas.1413645111.
Hinderer, C., P. Bell, J. P. Louboutin, Y. Zhu, H. Yu, G. Lin, R. Choa, B. L. Gurda, J. Bagel, P. O'Donnell, T. Sikora, T. Ruane, P. Wang, A. F. Tarantal, M. L. Casal, M. E. Haskins, and J. M. Wilson. 2015. "Neonatal Systemic AAV Induces

Tolerance to CNS Gene Therapy in MPS I Dogs and Nonhuman Primates." *Mol Ther* 23 (8):1298-307. doi: 10.1038/mt.2015.99.

Hinderer, Christian, Peter Bell, Brittney L. Gurda, Qiang Wang, Jean-Pierre Louboutin, Yanqing Zhu, Jessica Bagel, Patricia O'Donnell, Tracey Sikora, Therese Ruane, Ping Wang, Mark E. Haskins, and James M. Wilson. 2014c. "Intrathecal Gene Therapy Corrects CNS Pathology in a Feline Model of Mucopolysaccharidosis I." *Mol Ther* 22 (12):2018-2027. doi: 10.1038/mt.2014.135.

Hinderer, Christian, Peter Bell, Charles H. Vite, Jean-Pierre Louboutin, Rebecca Grant, Erin Bote, Hongwei Yu, Bryan Pukenas, Robert Hurst, and James M. Wilson. 2014. "Widespread gene transfer in the central nervous system of cynomolgus macaques following delivery of AAV9 into the cisterna magna." *Molecular Therapy — Methods & Clinical Development* 1. doi: 10.1038/mtm.2014.51

http://www.nature.com/articles/mtm201451#supplementary-information.

Hopkins, P. V., C. Campbell, T. Klug, S. Rogers, J. Raburn-Miller, and J. Kiesling. 2014. "Lysosomal Storage Disorder Screening Implementation: Findings from the First Six Months of Full Population Pilot Testing in Missouri." *J Pediatr* 166 (1):172-177. doi: 10.1016/j.jpeds.2014.09.023.

Hu, C., R. G. Cela, M. Suzuki, B. Lee, and G. S. Lipshutz. 2011. "Neonatal helper-dependent adenoviral vector gene therapy mediates correction of hemophilia A and tolerance to human factor VIII." *Proc Natl Acad Sci U S A* 108 (5):2082-7. doi: 10.1073/pnas.1015571108.

Hwu, Wuh-Liang, Shin-ichi Muramatsu, Sheng-Hong Tseng, Kai-Yuan Tzen, Ni-Chung Lee, Yin-Hsiu Chien, Richard O Snyder, Barry J Byrne, Chun-Hwei Tai, and Ruey-Meei Wu. 2012. "Gene therapy for aromatic L-amino acid decarboxylase deficiency." *Science translational medicine* 4 (134):134ra61-134ra61.

Iliff, J. J., M. Wang, Y. Liao, B. A. Plogg, W. Peng, G. A. Gundersen, H. Benveniste, G. E. Vates, R. Deane, S. A. Goldman, E. A. Nagelhus, and M. Nedergaard. 2012. "A paravascular pathway facilitates CSF flow through the brain parenchyma and the clearance of interstitial solutes, including amyloid beta." *Sci Transl Med* 4 (147):147ra111. doi: 10.1126/scitranslmed.3003748.

Iliff, Jeffrey J., Hedok Lee, Mei Yu, Tian Feng, Jean Logan, Maiken Nedergaard, and Helene Benveniste. 2013. "Brain-wide pathway for waste clearance captured by contrast-enhanced MRI." *The Journal of Clinical Investigation* 123 (3):1299-1309. doi: 10.1172/JCI67677.

Janson, C., S. McPhee, L. Bilaniuk, J. Haselgrove, M. Testaiuti, A. Freese, D. J. Wang, D. Shera, P. Hurh, J. Rupin, E. Saslow, O. Goldfarb, M. Goldberg, G. Larijani, W. Sharrar, L. Liouterman, A. Camp, E. Kolodny, J. Samulski, and P. Leone. 2002. "Clinical protocol. Gene therapy of Canavan disease: AAV-2 vector for neurosurgical delivery of aspartoacylase gene (ASPA) to the human brain." *Hum Gene Ther* 13 (11):1391-412. doi: 10.1089/104303402760128612.

Jarraya, B., S. Boulet, G. S. Ralph, C. Jan, G. Bonvento, M. Azzouz, J. E. Miskin, M. Shin, T. Delzescaux, X. Drouot, A. S. Herard, D. M. Day, E. Brouillet, S. M. Kingsman, P. Hantraye, K. A. Mitrophanous, N. D. Mazarakis, and S. Palfi. 2009. "Dopamine gene therapy for Parkinson's disease in a nonhuman primate without associated dyskinesia." *Sci Transl Med* 1 (2):2ra4. doi: 10.1126/scitranslmed.3000130.

Jortner, B. S. 2006. "The return of the dark neuron. A histological artifact complicating contemporary neurotoxicologic evaluation." *Neurotoxicology* 27 (4):628-634. doi: 10.1016/j.neuro.2006.03.002.

Kachur, E., and R. Del Maestro. 2000. "Mucopolysaccharidoses and spinal cord compression: Case report and review of the literature with implications of bone marrow transplantation." *Neurosurgery* 47 (1):223-228. doi: 10.1097/00006123-200007000-00046.

Kakavanos, R., C. T. Turner, J. J. Hopwood, E. D. Kakkis, and D. A. Brooks. 2003. "Immune tolerance after long-term enzyme-replacement therapy among patients who have mucopolysaccharidosis I." *Lancet* 361 (9369):1608-1613. doi: 10.1016/s0140-6736(03)13311-9.

Kakkis, E. D., A. Matynia, A. J. Jonas, and E. F. Neufeld. 1994. "Overexpression of the human lysosomal-enzyme alpha-l-iduronidase in chinese-hamster ovary cells." *Protein Expression and Purification* 5 (3):225-232. doi: 10.1006/prep.1994.1035.

Kakkis, E., T. Lester, R. Yang, C. Tanaka, V. Anand, J. Lemontt, M. Peinovich, and M. Passage. 2004. "Successful induction of immune tolerance to enzyme replacement therapy in canine mucopolysaccharidosis I." *Proc Natl Acad Sci U S A* 101 (3):829-34. doi: 10.1073/pnas.0305480101.

Kakkis, E., M. McEntee, C. Vogler, S. Le, B. Levy, P. Belichenko, W. Mobley, P. Dickson, S. Hanson, and M. Passage. 2004. "Intrathecal enzyme replacement therapy reduces lysosomal storage in the brain and meninges of the canine model of MPS I." *Molecular Genetics and Metabolism* 83 (1-2):163-174. doi: 10.1016/j.ymgme.2004.07.003.

Kaplitt, M. G., A. Feigin, C. Tang, H. L. Fitzsimons, P. Mattis, P. A. Lawlor, R. J. Bland, D. Young, K. Strybing, D. Eidelberg, and M. J. During. 2007. "Safety and tolerability of gene therapy with an adeno-associated virus (AAV) borne GAD gene for Parkinson's disease: an open label, phase I trial." *Lancet* 369 (9579):2097-2105. doi: 10.1016/s0140-6736(07)60982-9.

Keane, J. R. 1973. "Cisternal puncture complications. Treatment of coccidioidal meningitis with amphotericin B." *CALIF.MED.* 119 (3):10-15.

Kennedy, D. W., and J. L. Abkowitz. 1997. "Kinetics of central nervous system microglial and macrophage engraftment: analysis using a transgenic bone marrow transplantation model." *Blood* 90 (3):986-93.

Langereis, E. J., N. van Vlies, H. J. Church, R. B. Geskus, C. E. Hollak, S. A. Jones, W. Kulik, H. van Lenthe, J. Mercer, L. Schreider, K. L. Tylee, T. Wagemans, F. A. Wijburg, and B. W. Bigger. 2014. "Biomarker responses correlate with antibody status in mucopolysaccharidosis type I patients on long-term enzyme replacement therapy." *Mol Genet Metab*. doi: 10.1016/j.ymgme.2014.10.012.

Langford-Smith, K. J., J. Mercer, J. Petty, K. Tylee, H. Church, J. Roberts, G. Moss, S. Jones, R. Wynn, J. E. Wraith, and B. W. Bigger. 2011. "Heparin cofactor II-thrombin complex and dermatan sulphate:chondroitin sulphate ratio are biomarkers of short- and long-term treatment effects in mucopolysaccharide diseases." *Journal of Inherited Metabolic Disease* 34 (2):499-508. doi: 10.1007/s10545-010-9254-8.

Lawrence, R., J. R. Brown, K. Al-Mafraji, W. C. Lamanna, J. R. Beitel, G. J. Boons, J. D. Esko, and B. E. Crawford. 2012. "Disease-specific non-reducing end carbohydrate biomarkers for mucopolysaccharidoses." *Nat Chem Biol* 8 (2):197-204. doi: 10.1038/nchembio.766.

Leone, Paola, David Shera, Scott W.J. McPhee, Jeremy S. Francis, Edwin H. Kolodny, Larissa T. Bilaniuk, Dah-Jyuu Wang, Mitra Assadi, Olga Goldfarb, H. Warren Goldman, Andrew Freese, Deborah Young, Matthew J. During, R. Jude Samulski, and Christopher G. Janson. 2012. "Long-Term Follow-Up After Gene Therapy for Canavan Disease." *Science Translational Medicine* 4 (165):165ra163. doi: 10.1126/scitranslmed.3003454.

Liu, Q., and D. A. Muruve. 2003. "Molecular basis of the inflammatory response to adenovirus vectors." *Gene Ther* 10 (11):935-940.

LoDuca, P. A., B. E. Hoffman, and R. W. Herzog. 2009. "Hepatic Gene Transfer as a Means of Tolerance Induction to Transgene Products." *Current Gene Therapy* 9 (2):104-114.

Lund, Troy C., Weston Miller, Lynda Polgreen, Lisa Baso, Gerald Raymond, Jakub Tolar, and Paul Orchard. 2014. "Improvement in biomarkers after intrathecal iduronidase for children with MPS IH." *Molecular Genetics and Metabolism* 111 (2):S74. doi: http://dx.doi.org/10.1016/j.ymgme.2013.12.168.

Maguire, Albert M., Katherine A. High, Alberto Auricchio, J. Fraser Wright, Eric A. Pierce, Francesco Testa, Federico Mingozzi, Jeannette L. Bennicelli, Gui-shuang Ying, Settimio Rossi, Ann Fulton, Kathleen A. Marshall, Sandro Banfi, Daniel C. Chung, Jessica I. W. Morgan, Bernd Hauck, Olga Zelenaia, Xiaosong Zhu, Leslie Raffini, Frauke Coppieters, Elfride De Baere, Kenneth S. Shindler, Nicholas J. Volpe, Enrico M. Surace, Carmela Acerra, Arkady Lyubarsky, T. Michael Redmond, Edwin Stone, Junwei Sun, Jennifer Wellman McDonnell, Bart P. Leroy, Francesca Simonelli, and Jean Bennett. 2009. "Age-dependent effects of RPE65 gene therapy for Leber's congenital amaurosis: a phase 1 dose-escalation trial." *The Lancet* 374 (9701):1597-1605. doi: http://dx.doi.org/10.1016/S0140-6736(09)61836-5.

Maita, Nobuo, Takahiro Tsukimura, Takako Taniguchi, Seiji Saito, Kazuki Ohno, Hisaaki Taniguchi, and Hitoshi Sakuraba. 2013. "Human α-l-iduronidase uses its own N-glycan as a substrate-binding and catalytic module." *Proceedings of the National Academy of Sciences* 110 (36):14628-14633. doi: 10.1073/pnas.1306939110.

Mandel, R. J., and C. Burger. 2004. "Clinical trials in neurological disorders using AAV vectors: Promises and challenges." *Current Opinion in Molecular Therapeutics* 6 (5):482-490.

McCarthy, S. A., and F. H. Bach. 1983. "The cellular mechanism of maintenance of neonatally induced tolerance to H-2 class I antigens." *J Immunol* 131 (4):1676-82.

McCurdy, Victoria J., Aime K. Johnson, Heather L. Gray-Edwards, Ashley N. Randle, Brandon L. Brunson, Nancy E. Morrison, Nouha Salibi, Jacob A. Johnson, Misako Hwang, Ronald J. Beyers, Stanley G. Leroy, Stacy Maitland, Thomas S. Denney, Nancy R. Cox, Henry J. Baker, Miguel Sena-Esteves, and Douglas R. Martin. 2014. "Sustained normalization of neurological disease after intracranial gene therapy in a feline model." *Science Translational Medicine* 6 (231):231ra48. doi: 10.1126/scitranslmed.3007733.

McGlynn, R., K. Dobrenis, and S. U. Walkley. 2004. "Differential subcellular localization of cholesterol, gangliosides, and glycosaminoglycans in murine models of mucopolysaccharide storage disorders." *Journal of Comparative Neurology* 480 (4):415-426. doi: 10.1002/cne.20355.

McPhee, S. W. J., C. G. Janson, C. Li, R. J. Samulski, A. S. Camp, J. Francis, D. Shera, L. Lioutermann, M. Feely, A. Freese, and P. Leone. 2006. "Immune responses to

AAV in a phase I study for Canavan disease." *Journal of Gene Medicine* 8 (5):577-588. doi: 10.1002/jgm.885.

Menon, K. P., P. T. Tieu, and E. F. Neufeld. 1992. "Architecture of the canine IDUA gene and mutation underlying canine mucopolysaccharidosis I." *Genomics* 14 (3):763-8.

Meyer, K., L. Ferraiuolo, L. Schmelzer, L. Braun, V. McGovern, S. Likhite, O. Michels, A. Govoni, J. Fitzgerald, P. Morales, K. D. Foust, J. R. Mendell, A. H. Burghes, and B. K. Kaspar. 2014. "Improving Single Injection CSF Delivery of AAV9-mediated Gene Therapy for SMA: A Dose-response Study in Mice and Nonhuman Primates." *Mol Ther*. doi: 10.1038/mt.2014.210.

Mittermeyer, Gabriele, Chadwick W Christine, Kathryn H Rosenbluth, Suzanne L Baker, Philip Starr, Paul Larson, Paul L Kaplan, John Forsayeth, Michael J Aminoff, and Krystof S Bankiewicz. 2012. "Long-term evaluation of a phase 1 study of AADC gene therapy for Parkinson's disease." *Human gene therapy* 23 (4):377-381.

Moore, D., M. J. Connock, E. Wraith, and C. Lavery. 2008. "The prevalence of and survival in Mucopolysaccharidosis I: Hurler, Hurler-Scheie and Scheie syndromes in the UK." *Orphanet Journal of Rare Diseases* 3. doi: 10.1186/1750-1172-3-24.

Munoz-Rojas, M. V., T. Vieira, R. Costa, S. Fagondes, A. John, L. B. Jardim, L. M. Vedolin, M. Raymundo, P. I. Dickson, E. Kakkis, and R. Giugliani. 2008. "Intrathecal Enzyme Replacement Therapy in a Patient With Mucopolysaccharidosis Type I and Symptomatic Spinal Cord Compression." *American Journal of Medical Genetics Part A* 146A (19):2538-2544. doi: 10.1002/ajmg.a.32294.

Muramatsu, S., K. Fujimoto, K. Ikeguchi, N. Shizuma, K. Kawasaki, F. Ono, Y. Shen, L. Wang, H. Mizukami, A. Kume, M. Matsumura, I. Nagatsu, F. Urano, H. Ichinose, T. Nagatsu, K. Terao, I. Nakano, and K. Ozawa. 2002. "Behavioral recovery in a primate model of Parkinson's disease by triple transduction of striatal cells with adeno-associated viral vectors expressing dopamine-synthesizing enzymes." *Hum Gene Ther* 13 (3):345-54. doi: 10.1089/10430340252792486.

Nagahara, Alan H., David A. Merrill, Giovanni Coppola, Shingo Tsukada, Brock E. Schroeder, Gideon M. Shaked, Ling Wang, Armin Blesch, Albert Kim, James M. Conner, Edward Rockenstein, Moses V. Chao, Edward H. Koo, Daniel Geschwind, Eliezer Masliah, Andrea A. Chiba, and Mark H. Tuszynski. 2009. "Neuroprotective effects of brain-derived neurotrophic factor in rodent and primate models of Alzheimer's disease." *Nat Med* 15 (3):331-337. doi: http://www.nature.com/nm/journal/v15/n3/suppinfo/nm.1912_S1.html.

Nathwani, Amit C., Edward G. D. Tuddenham, Savita Rangarajan, Cecilia Rosales, Jenny McIntosh, David C. Linch, Pratima Chowdary, Anne Riddell, Arnulfo Jaquilmac Pie, Chris Harrington, James O'Beirne, Keith Smith, John Pasi, Bertil Glader, Pradip Rustagi, Catherine Y. C. Ng, Mark A. Kay, Junfang Zhou, Yunyu Spence, Christopher L. Morton, James Allay, John Coleman, Susan Sleep, John M. Cunningham, Deokumar Srivastava, Etiena Basner-Tschakarjan, Federico Mingozzi, Katherine A. High, John T. Gray, Ulrike M. Reiss, Arthur W. Nienhuis, and Andrew M. Davidoff. 2011. "Adenovirus-Associated Virus Vector-Mediated Gene Transfer in Hemophilia B." *New England Journal of Medicine* 365 (25):2357-2365. doi: 10.1056/NEJMoa1108046.

Nietupski, Jennifer B., Gregory D. Hurlbut, Robin J. Ziegler, Qiuming Chu, Bradley L. Hodges, Karen M. Ashe, Mark Bree, Seng H. Cheng, Richard J. Gregory, John

Marshall, and Ronald K. Scheule. 2011. "Systemic Administration of AAV8-[alpha]-galactosidase A Induces Humoral Tolerance in Nonhuman Primates Despite Low Hepatic Expression." *Mol Ther* 19 (11):1999-2011. doi: http://www.nature.com/mt/journal/v19/n11/suppinfo/mt2011119s1.html.

Papisov, Mikhail I., Vasily V. Belov, and Kimberley S. Gannon. 2013. "Physiology of the intrathecal bolus: the leptomeningeal route for macromolecule and particle delivery to CNS." *Molecular pharmaceutics* 10 (5):1522-1532. doi: 10.1021/mp300474m.

Passini, Marco A, Jie Bu, Amy M Richards, Christopher M Treleaven, Jennifer A Sullivan, Catherine R O'Riordan, Abraham Scaria, Adrian P Kells, Lluis Samaranch, and Waldy San Sebastian. 2014. "Translational Fidelity of Intrathecal Delivery of Self-Complementary AAV9–Survival Motor Neuron 1 for Spinal Muscular Atrophy." *Human gene therapy* 25 (7):619-630.

Pomerantz, S., Buchbinder, B., Hirsch, J. 2005. "Suboccipital puncture of the cisterna magna under CT-guidance with intravenous enhancement in order to circumvent anomalous course of posterior inferior cerebellar artery." *American Society of Spine Radiology* meeting abstract.

Pomerantz, Stuart, Bradley Buchbinder, and Joshua Hirsh. 2005. "Suboccipital Puncture of the Cisterna Magna under CT-Guidance with Intravenous Enhancement in order to Circumvent Anomalous Course of Posterior Inferior Cerebellar Artery." American Society of Spine Radiology.

Randall, Derrick R., Karen E. Colobong, Harmony Hemmelgarn, Graham B. Sinclair, Elly Hetty, Anita Thomas, Olaf A. Bodamer, Barbara Volkmar, Paul M. Fernhoff, Robin Casey, Alicia K. Chan, Grant Mitchell, Silvia Stockler, Serge Melancon, Tony Rupar, and Lorne A. Clarke. 2008. "Heparin cofactor II-thrombin complex: A biomarker of MPS disease." *Molecular Genetics and Metabolism* 94 (4):456-461. doi: 10.1016/j.ymgme.2008.05.001.

Samaranch, L., E. A. Salegio, W. San Sebastian, A. P. Kells, K. D. Foust, J. R. Bringas, C. Lamarre, J. Forsayeth, B. K. Kaspar, and K. S. Bankiewicz. 2012. "Adeno-associated virus serotype 9 transduction in the central nervous system of nonhuman primates." *Human Gene Therapy* 23 (4):382-389. doi: 10.1089/hum.2011.200.

Samaranch, L., E. A. Salegio, W. S. Sebastian, A. P. Kells, J. R. Bringas, J. Forsayeth, and K. S. Bankiewicz. 2013. "Strong cortical and spinal cord transduction after AAV7 and AAV9 delivery into the cerebrospinal fluid of nonhuman primates." *Human Gene Therapy* 24 (5):526-532. doi: 10.1089/hum.2013.005.

Samaranch, L., W. S. Sebastian, A. P. Kells, E. A. Salegio, G. Heller, J. R. Bringas, P. Pivirotto, S. DeArmond, J. Forsayeth, and K. S. Bankiewicz. 2014. "AAV9-mediated expression of a non-self protein in nonhuman primate central nervous system triggers widespread neuroinflammation driven by antigen-presenting cell transduction." *Molecular Therapy* 22 (2):329-337. doi: 10.1038/mt.2013.266.

Samaranch, Lluis, Waldy San Sebastian, Adrian P. Kells, John Bringas, Phillip Pivirotto, John Forsayeth, and Krystof S. Bankiewicz. 2013. "Immune Response Activation and Neurotoxicity after Intrathecal Infusion of AAV9 Vector Encoding a Non-Self Reporter Protein in the Non-Human Primate." *Molecular Therapy* 21:S227-S227.

Samulski, R J, L S Chang, and T Shenk. 1987. "A recombinant plasmid from which an infectious adeno-associated virus genome can be excised in vitro and its use to study viral replication." *Journal of Virology* 61 (10):3096-3101.

Samulski, R J, L S Chang, and T Shenk. 1989. "Helper-free stocks of recombinant adeno-associated viruses: normal integration does not require viral gene expression." *Journal of Virology* 63 (9):3822-3828.
Samulski, R. Jude, and Nicholas Muzyczka. 2014. "AAV-Mediated Gene Therapy for Research and Therapeutic Purposes." *Annual Review of Virology* 1 (1):427-451. doi: doi:10.1146/annurev-virology-031413-085355.
Sando, Gloria N., and Elizabeth F. Neufeld. 1977. "Recognition and receptor-mediated uptake of a lysosomal enzyme, α-l-iduronidase, by cultured human fibroblasts." *Cell* 12 (3):619-627. doi: http://dx.doi.org/10.1016/0092-8674(77)90262-8.
Saunders, Harry C., and Timothy J. Riordan. 1929. "Cisternal or suboccipital puncture." *New England Journal of Medicine* 201 (4):166-168. doi: doi:10.1056/NEJM192907252010406.
Shull, R. M., R. G. Helman, E. Spellacy, G. Constantopoulos, R. J. Munger, and E. F. Neufeld. 1984. "Morphologic and biochemical studies of canine mucopolysaccharidosis I." *Am J Pathol* 114 (3):487-95.
Shull, R. M., E. D. Kakkis, M. F. McEntee, S. A. Kania, A. J. Jonas, and E. F. Neufeld. 1994. "Enzyme replacement in a canine model of Hurler-syndrome." *Proceedings of the National Academy of Sciences of the United States of America* 91 (26):12937-12941. doi: 10.1073/pnas.91.26.12937.
Sifuentes, M., R. Doroshow, R. Hoft, G. Mason, I. Walot, M. Diament, S. Okazaki, K. Huff, G. F. Cox, S. J. Swiedler, and E. D. Kakkis. 2007. "A follow-up study of MPS I patients treated with laronidase enzyme replacement therapy for 6 years." *Molecular Genetics and Metabolism* 90 (2):171-180. doi: 10.1016/j.ymgme.2006.08.007.
Sonntag, Florian, Kristin Schmidt, and Jürgen A. Kleinschmidt. 2010. "A viral assembly factor promotes AAV2 capsid formation in the nucleolus." *Proceedings of the National Academy of Sciences* 107 (22):10220-10225. doi: 10.1073/pnas.1001673107.
Souillet, G., N. Guffon, I. Maire, M. Pujol, P. Taylor, F. Sevin, N. Bleyzac, C. Mulier, A. Durin, K. Kebaili, C. Galambrun, Y. Bertrand, R. Froissart, C. Dorche, L. Gebuhrer, C. Garin, J. Berard, and P. Guibaud. 2003. "Outcome of 27 patients with Hurler's syndrome transplanted from either related or unrelated haematopoietic stem cell sources." *Bone Marrow Transplantation* 31 (12):1105-1117. doi: 10.1038/sj.bmt.1704105.
Staba, Susan L., Maria L. Escolar, Michele Poe, Young Kim, Paul L. Martin, Paul Szabolcs, June Allison-Thacker, Susan Wood, David A. Wenger, Pablo Rubinstein, John J. Hopwood, William Krivit, and Joanne Kurtzberg. 2004. "Cord-Blood Transplants from Unrelated Donors in Patients with Hurler's Syndrome." *New England Journal of Medicine* 350 (19):1960-1969. doi: 10.1056/NEJMoa032613.
Sun, B., M. D. Kulis, S. P. Young, A. C. Hobeika, S. Li, A. Bird, H. Zhang, Y. Li, T. M. Clay, W. Burks, P. S. Kishnani, and D. D. Koeberl. 2010. "Immunomodulatory gene therapy prevents antibody formation and lethal hypersensitivity reactions in murine pompe disease." *Mol Ther* 18 (2):353-60. doi: 10.1038/mt.2009.195.
Taccone, A., P. T. Donati, A. Marzoli, A. Dellacqua, R. Gatti, and D. Leone. 1993. "Mucopolysaccharidosis - thickening of dura-mater at the craniocervical junction and other CT/MRI findings." *Pediatric Radiology* 23 (5):349-352. doi: 10.1007/bf02011954.

Tarantal, A. F. 2005. "Ultrasound Imaging in Rhesus (Macaca Mulatta) and Long-Tailed (Macaca fascicularis) Macaques: Reproductive and Research Applications." In *The Laboratory Primate*, edited by Wolfe-Coote S, 317-352. London: Academic Press.

Tarantal, A. F., R. J. McDonald, D. F. Jimenez, C. C. Lee, C. E. O'Shea, A. C. Leapley, R. H. Won, C. G. Plopper, C. Lutzko, and D. B. Kohn. 2005. "Intrapulmonary and intramyocardial gene transfer in rhesus monkeys (Macaca mulatta): safety and efficiency of HIV-1-derived lentiviral vectors for fetal gene delivery." *Mol Ther* 12 (1):87-98. doi: S1525-0016(05)00040-7 [pii]

10.1016/j.ymthe.2005.01.019.

Tardieu, M., M. Zerah, B. Husson, S. de Bournonville, K. Deiva, C. Adamsbaum, F. Vincent, M. Hocquemiller, C. Broissand, V. Furlan, R. G. Crystal, T. Baugnon, T. Roujeau, J. M. Heard, and O. Danos. 2013. "Intra cerebral administration of AAVrh.10 carrying human SGSH and SUMF1 cDNAs in children with MPSIIIA disease: result of a phase I/II trial." *Human Gene Therapy* 24 (12):A23-A24.

Terlato, N. J., and G. F. Cox. 2003. "Can mucopolysaccharidosis type I disease severity be predicted based on a patient's genotype? A comprehensive review of the literature." *Genet Med* 5 (4):286-94. doi: 10.1097/01.gim.0000078027.83236.49.

Traas, A. M., P. Wang, X. Ma, M. Tittiger, L. Schaller, P. O'Donnell, M. M. Sleeper, C. Vite, R. Herati, G. D. Aguirre, M. Haskins, and K. P. Ponder. 2007. "Correction of clinical manifestations of canine mucopolysaccharidosis I with neonatal retroviral vector gene therapy." *Mol Ther* 15 (8):1423-31. doi: 10.1038/sj.mt.6300201.

Vera, M., S. Le, S. H. Kan, H. Garban, D. Naylor, A. Mlikotic, I. Kaitila, P. Harmatz, A. Chen, and P. Dickson. 2013. "Immune response to intrathecal enzyme replacement therapy in mucopolysaccharidosis I patients." *Pediatric Research* 74 (6):712-720. doi: 10.1038/pr.2013.158.

Vijay, S., and J. E. Wraith. 2005. "Clinical presentation and follow-up of patients with the attenuated phenotype of mucopolysaccharidosis type I." *Acta Paediatrica* 94 (7):872-877. doi: 10.1080/08035250510031584.

Vite, C. H., J. C. McGowan, S. N. Niogi, M. A. Passini, K. J. Drobatz, M. E. Haskins, and J. H. Wolfe. 2005. "Effective gene therapy for an inherited CNS disease in a large animal model." *Annals of Neurology* 57 (3):355-364. doi: 10.1002/ana.20392.

Vite, Charles H., Igor Nestrasil, Anton Mlikotic, Jackie K. Jens, Elizabeth M. Snella, William Gross, Elsa G. Shapiro, Victor Kovac, James M. Provenzale, Steven Chen, Steven Q. Le, Shih-hsin Kan, Shida Banakar, Raymond Y. Wang, Mark E. Haskins, N. Matthew Ellinwood, and Patricia I. Dickson. 2013. "Features of Brain MRI in Dogs with Treated and Untreated Mucopolysaccharidosis Type I." *Comparative Medicine* 63 (2):163-173.

Vite, Charles H., Ping Wang, Reema T. Patel, Raquel M. Walton, Steven U. Walkley, Rani S. Sellers, N. Matthew Ellinwood, Alphonsus S. Cheng, Joleen T. White, Charles A. O'Neill, and Mark Haskins. 2011. "Biodistribution and pharmacodynamics of recombinant human alpha-L-iduronidase (rhIDU) in mucopolysaccharidosis type I-affected cats following multiple intrathecal administrations." *Molecular Genetics and Metabolism* 103 (3):268-274. doi: 10.1016/j.ymgme.2011.03.011.

Walkley, S. U., M. E. Haskins, and R. M. Shull. 1988. "Alterations in neuron morphology in mucopolysaccharidosis type I." *Acta Neuropathologica* 75 (6):611-620. doi: 10.1007/BF00686207.

Walkley, Steven U., and Marie T. Vanier. 2009. "Secondary lipid accumulation in lysosomal disease." *Biochimica et Biophysica Acta (BBA) - Molecular Cell Research* 1793 (4):726-736. doi: http://dx.doi.org/10.1016/j.bbamcr.2008.11.014.

Wang, G., Y. Miyahara, Z. Guo, M. Khattar, S. M. Stepkowski, and W. Chen. 2010. ""Default" generation of neonatal regulatory T cells." *J Immunol* 185 (1):71-8. doi: 10.4049/jimmunol.0903806.

Wang, L. L., R. Calcedo, P. Bell, J. P. Lin, R. L. Grant, D. L. Siegel, and J. M. Wilson. 2011. "Impact of Pre-Existing Immunity on Gene Transfer to Nonhuman Primate Liver with Adeno-Associated Virus 8 Vectors." *Human Gene Therapy* 22 (11):1389-1401. doi: 10.1089/hum.2011.031.

Wang, L., H. Wang, P. Bell, D. McMenamin, and J. M. Wilson. 2012. "Hepatic gene transfer in neonatal mice by adeno-associated virus serotype 8 vector." *Hum Gene Ther* 23 (5):533-9. doi: 10.1089/hum.2011.183.

Ward, E., W. W. Orrison, and C. B. Watridge. 1989. "Anatomic evaluation of cisternal puncture." *Neurosurgery* 25 (3):412-415.

Wendeler, Michaela, and Konrad Sandhoff. 2009. "Hexosaminidase assays." *Glycoconjugate Journal* 26 (8):945-952. doi: 10.1007/s10719-008-9137-5.

Whitley, C. B., K. G. Belani, P. N. Chang, C. G. Summers, B. R. Blazar, M. Y. Tsai, R. E. Latchaw, N. K. C. Ramsay, and J. H. Kersey. 1993. "Long-term outcome of hurler syndrome following bone-marrow transplantation." *American Journal of Medical Genetics* 46 (2):209-218. doi: 10.1002/ajmg.1320460222.

Whitney, N., H. Sun, J. M. Pollock, and D. A. Ross. 2013. "The human foramen magnum--normal anatomy of the cisterna magna in adults." *Neuroradiology* 55 (11):1333-9. doi: 10.1007/s00234-013-1269-z.

Wolf, Daniel A., Andrew W. Lenander, Zhenhong Nan, Lalitha R. Belur, Chester B. Whitley, Pankaj Gupta, Walter C. Low, and R. Scott McLvor. 2011. "Direct gene transfer to the CNS prevents emergence of neurologic disease in a murine model of mucopolysaccharidosis type I." *Neurobiology of Disease* 43 (1):123-133. doi: 10.1016/j.nbd.2011.02.015.

Wraith, J. E., M. Beck, R. Lane, A. van der Ploeg, E. Shapiro, Y. Xue, E. D. Kakkis, and N. Guffon. 2007. "Enzyme replacement therapy in patients who have mucopolysaccharidosis I and are younger than 5 years: Results of a multinational study of recombinant human alpha-L-iduronidase (Laronidase)." *Pediatrics* 120 (1):E37-E46. doi: 10.1542/peds.2006-2156.

Wraith, James E., Lorne A. Clarke, Michael Beck, Edwin H. Kolodny, Gregory M. Pastores, Joseph Muenzer, David M. Rapoport, Kenneth I. Berger, Stuart J. Swiedler, Emil D. Kakkis, Tanja Braakman, Elenie Chadbourne, Karen Walton-Bowen, and Gerald F. Cox. 2004. "Enzyme replacement therapy for mucopolysaccharidosis I: a randomized, double-blinded, placebo-controlled, multinational study of recombinant human α-L-iduronidase (laronidase)." *The Journal of Pediatrics* 144 (5):581-588. doi: http://dx.doi.org/10.1016/j.jpeds.2004.01.046.

Xiao, Weidong, Narendra Chirmule, Scott C Berta, Beth McCullough, Guangping Gao, and James M Wilson. 1999. "Gene therapy vectors based on adeno-associated virus type 1." *Journal of virology* 73 (5):3994-4003.

Xing, M., E. I. Parker, A. Moreno-De-Luca, E. Harmouche, and M. R. Terk. 2014. "Radiological and clinical characterization of the lysosomal storage disorders: non-lipid disorders." *British Journal of Radiology* 87 (1033):14. doi: 10.1259/bjr.20130467.

Xu, L., M. Mei, M. E. Haskins, T. C. Nichols, P. O'Donnell, K. Cullen, A. Dillow, D. Bellinger, and K. P. Ponder. 2007. "Immune response after neonatal transfer of a human factor IX-expressing retroviral vector in dogs, cats, and mice." *Thromb Res* 120 (2):269-80. doi: 10.1016/j.thromres.2006.09.010.

Zafeiriou, D. I., and S. P. Batzios. 2013. "Brain and Spinal MR Imaging Findings in Mucopolysaccharidoses: A Review." *American Journal of Neuroradiology* 34 (1):5-13. doi: 10.3174/ajnr.A2832.